DESIGN, ANALYSIS AND OPTIMIZATION OF NOZZLES IN A WASHING MACHINE

A THESIS SUBMITTED TO
THE GRADUATE SCHOOL OF NATURAL AND APPLIED SCIENCES
OF
MIDDLE EAST TECHNICAL UNIVERSITY

BY

MERT ÇİL

IN PARTIAL FULFILLMENT OF THE REQUIREMENTS
FOR
THE DEGREE OF MASTER OF SCIENCE
IN
MECHANICAL ENGINEERING

APRIL 2023

Approval of the thesis:

DESIGN, ANALYSIS AND OPTIMIZATION OF NOZZLES IN A WASHING MACHINE

submitted by **Mert Çil** in partial fulfillment of the requirements for the degree of **Master of Science** i**n Mechanical Engineering, Middle East Technical University** by,

Prof. Dr. Halil Kalıpçılar
Dean, Graduate School of **Natural and Applied Sciences** _____

Prof. Dr. M. A. Sahir Arıkan
Head of the Department, **Mechanical Engineering** _____

Prof. Dr. Mehmet Halûk Aksel
Supervisor, **Mechanical Engineering, METU** _____

Examining Committee Members:

Prof. Dr. Mehmet Metin Yavuz
Mechanical Engineering, METU _____

Prof. Dr. Mehmet Halûk Aksel
Mechanical Engineering, METU _____

Assist. Prof. Dr. Özgür Uğraş Baran
Mechanical Engineering, METU _____

Assist. Prof. Dr. Ali Karakuş
Mechanical Engineering, METU _____

Assist. Prof. Dr. Onur Baş
Mechanical Engineering, TEDU _____

Date: 26.04.2023

I hereby declare that all information in this document has been obtained and presented in accordance with academic rules and ethical conduct. I also declare that, as required by these rules and conduct, I have fully cited and referenced all material and results that are not original to this work.

Name Last name: Mert Çil

Signature:

ABSTRACT

DESIGN, ANALYSIS AND OPTIMIZATION OF NOZZLES IN A WASHING MACHINE

Çil, Mert
Master of Science, Mechanical Engineering
Supervisor: Prof. Dr. M. Halûk Aksel

April 2023, 97 pages

One of the most important issues in the washing machine is to provide a better washing performance with low energy consumption. In order to achieve better washing performance at low energy consumption, the stain needs to be removed quickly. Removal of the stain is increased through the circulation of the water and the directing of the water with the nozzle. With the existing nozzle designs, an additional part is required to spray water over a wider area, however with the new nozzle designs presented in this thesis, it is possible to spray water directly over a wider area. Fluidic oscillator nozzles are used in many industries, and this thesis examines of stain removal with these nozzles. For the design parameters, the ratios of the critical widths in the nozzle structure to the nozzle inlet width were studied. In order to understand the effect of the parameters on stain removal, analyzes were performed with Computational Fluid Dynamics (CFD) and velocity graphs at the nozzle outlet were investigated. An approximation method was determined to model the stain removal effect using the graph of the average velocity for one full sweep of the nozzles. For validation of the determined approach, nozzles with different flow movements of three different parameters were determined, then results of the numerical analyses and experimental tests were compared. These parameters were determined as the ratio of the inlet of the nozzle mixing chamber to the nozzle inlet

w1/w0, the ratio of the mixing chamber width to the nozzle inlet w2/w0 and the ratio of the nozzle outlet throat to the nozzle inlet w3/w0, respectively. The ratios of the reference nozzle were defined as w1/w0 = 2.0, w2/w0 = 4.06 and w3/w0 = 1.3. In order investigate the difference in flow analysis for the first parameter w1/w0, in addition to the reference ratio, ratios of 1.0 and 1.5 were also examined. In addition to the reference condition, the ratios of 3.2 and 4.8 were determined for the second parameter. As the final validation parameter, the ratios of 1.6 and 2.0 for w3/w0 were examined alongside the reference condition. The behavior of the stain removal curves is modeled using the nozzle output velocity graph obtained as a result of all validation tests. According to the determined model, the best ratios for w1/w0, w2/w0 and w3/w0 parameters were determined as 2.0, 5.02 and 0.75, respectively, using CFD analysis. Experimental studies were carried out for three different nozzles by changing only the specified parameter while keeping all other parameters constant. In addition, as a new parameter, the ratio of the backflow channels to the nozzle inlet w4/w0 was examined. CFD analyzes were performed with the determined model for w4/w0 and although w4/w0 = 1.47 was selected in the reference nozzle, the best nozzle design was determined as w4/w0 = 2.0 within the structural limits. It is seen that the experimental test results in all of the select ed nozzles are consistent with the determined method.

Keywords: Washing Machine, Nozzle Design, Fluidic Oscillator, Computational Fluid Dynamics, Stain Removal

ÖZ

ÇAMAŞIR MAKİNESİNDE NOZUL TASARIMI, ANALİZİ VE OPTİMİZASYONU

Çil, Mert
Yüksek Lisans, Makina Mühendisliği
Tez Yöneticisi: Prof. Dr. M. Halûk Aksel

Nisan 2023, 97 sayfa

Çamaşır makinesinde en önemli konulardan birisi düşük enerji tüketimiyle iyi bir yıkama performansı sağlamaktır. Düşük enerji tüketiminde iyi yıkama performansını sağlayabilmenin yolu ise suyun sirkülasyonunun sağlanması ve sirkülasyon hattından gelen suyun nozul ile yönlendirilmesi sayesinde lekenin kolayca çıkarılmasıdır. Mevcut nozul tasarımları ile geniş bir alana suyu ulaştırmak için ek parça gerekmesine karşılık bu tez kapsamında sunulan yeni nozul tasarımlarıyla suyu daha geniş bir alana ulaştırmak mümkündür. Akışkan osilatörler olarak da bilinen yeni tasarımlar birçok sektörde kullanılmakta olup, bu tezde ise leke çıkarmaya etkisi incelenmektedir. Tasarım parametreleri olarak nozul yapısındaki kritik genişliklerin nozul giriş genişliğine oranları incelenmiştir. Parametrelerin leke çıkarmaya etkisini görmek için Hesaplamalı Akışkanlar Dinamiği (HAD) ile analizler gerçekleştirilerek nozul çıkışındaki hız grafikleri incelenmiştir. Nozullerin bir salınımındaki ortalama hız grafiği ile leke çıkarma etkisini tahmin edebilmek için bir yaklaşım metodu belirlenmiştir. Belirlenen yaklaşımın doğrulanması için üç farklı parametrenin farklı akış hareketlerine sahip nozulleri belirlenmiş ve sayısal analiz sonuçları ile deneysel testler karşılaştırılmıştır. Üç parametre sırasıyla nozul karışım bölgesinin girişinin nozul girişine oranı w1/w0, karışım bölgesi genişliğinin nozul girişine oranı w2/w0

ve nozul çıkış boğazının nozul girişine oranı w3/w0 olarak belirlenmiştir. Referans nozul olarak belirlenen nozulun oranları w1/w0 = 2,0, w2/w0 = 4,06 ve w3/w0 = 1,3 olarak belirlenmiştir. Akış analizlerinin farkını inceleyebilmek için ilk olarak w1/w0 referans oranına ek olarak 1,0 ve 1,5 değerlerindeki durumlar incelenmiştir. İkinci parametre olan w2/w0 için referans değerine ek olarak 3,2 ve 4,8 oranları belirlenmiştir. Son doğrulama parametresi olarak w3/w0 için 1,6 ve 2,0 oranları referans koşulun yanı sıra incelenmiştir. Yapılan tüm doğrulama testleri sonucunda elde edilen nozul çıkışı hız grafiği sayesinde leke çıkarma eğrileri davranışı modellenmektedir. Belirlenen model sayesinde HAD analizleri kullanılarak w1/w0, w2/w0 ve w3/w0 parametreleri için en iyi oranlar sırasıyla 2,0, 5,02 ve 0,75 olarak belirlenmiştir. Diğer tüm parametreler sabit tutularak sadece belirlenen parametre değiştirilerek üç farklı nozul için deneysel çalışmalar gerçekleştirilmiştir. Ayrıca yeni bir parametre olarak geri akış kanallarının nozul girişe oranı w4/w0 incelenmiştir. Belirlenen modelle HAD analizleri yapılmış ve referans nozulde w4/w0 = 1,47 seçilmesine rağmen yapısal sınırlar içinde en iyi nozul tasarımı için w4/w0 = 2,0 olarak belirlenmiştir. Seçilen tüm nozullerde deneysel test sonuçlarının belirlenen yöntemle uyuştuğu görülmektedir.

Anahtar Kelimeler: Çamaşır Makinesi, Nozul Tasarımı, Akışkan Osilatör, Hesaplamalı Akışkan Dinamiği, Leke Çıkarımı

To My Family

ACKNOWLEDGMENTS

I would like to express my sincere appreciation to my supervisor, Prof. Dr. M. Halûk Aksel for his guidance and support.

I would also like to thank my manager Dr. Songül Bayraktar for her advice and support on the thesis. I also want to thank my colleagues Ehsan Tuzcuoğlu, Ekin Emek Saitoğlu, Aykut Efe, Ömer Ensar Durmuş, Tamer Alp Erendur, Rahmi Mert Akkülah and Samet Ilıca for their great supports.

Lastly, I would like to thank my family for their understanding, support, and encouragement.

TABLE OF CONTENTS

ABSTRACT v

ÖZ vii

ACKNOWLEDGMENTS x

TABLE OF CONTENTS xi

LIST OF TABLES xiii

LIST OF FIGURES xiv

CHAPTERS

1 INTRODUCTION 1

2 LITERATURE REVIEW 5

2.1 Circulation Systems in Washing Machine 5

2.2 Fluidic Oscillators 11

3 ANALYZES AND EXPERIMENTAL STUDIES FOR DETERMINATON OF A NEW METHOD 21

3.1 Experimental Setup 21

3.2 Analysis Method 24

3.3 Mesh Independency 28

3.4 Determination of Parameters and Method 31

3.5 First Validation 32

3.6 A New Method for Stain Removal Modelling 33

3.6.1 w1/w0 Parameter 33

3.6.2 w2/w0 Parameter 45

3.6.3 w3/w0 Parameter 55

3.7 Comparison of Fluidic Oscillator Nozzle and Original Nozzle 66
3.8 Oscillation Frequency Validation 67
4 ANALYZES OF NOZZLES FOR OPTIMUM DESIGNS WITH THE NEW METHOD 69
4.1 The Optimum Nozzle Design for w1/w0 Parameter 70
4.2 The Optimum Nozzle Design for w2/w0 Parameter 73
4.3 The Optimum Nozzle Design for w3/w0 Parameter 76
4.4 The Optimum Nozzle Design for w4/w0 Parameter 79
5 EXPERIMENTAL TESTS OF OPTIMUM DESIGNS 83
5.1 The Optimum Nozzle Results for w1/w0 Parameter 83
5.2 The Optimum Nozzle Results for w2/w0 Parameter 83
5.3 The Optimum Nozzle Results for w3/w0 Parameter 85
5.4 The Optimum Nozzle Results for w4/w0 Parameter 86
6 CONCLUSION 89
REFERENCES 93

LIST OF TABLES

TABLES

Table 3.1 The Validation of Analyzes with Mean Velocity 33
Table 3.2 The Maximum Angle of Nozzles for w1/w0 Parameter..... 37
Table 3.3 The Contacting Time and The Transition Time of Nozzles for w1/w0 Parameter 45
Table 3.4 The Maximum Angle of Nozzles for w2/w0 Parameter..... 48
Table 3.5 The Contacting Time and The Transition Time of Nozzles for w2/w0 Parameter 55
Table 3.6 The Maximum Angle of Nozzles for w1/w0 Parameter..... 59
Table 3.7 The Contacting Time and The Transition Time of Nozzles for w3/w0 Parameter 65
Table 3.8 Comparison of Area Under the Curve for FO & Current Nozzle..... 67
Table 3.9 Validation of Oscillation Time of Analysis and Experimental Results.. 68
Table 5.1 Areas Under the Curve for w2/w0..... 85
Table 5.2 Areas Under the Curve for w3/w0..... 86
Table 5.3 Areas Under the Curve for w4/w0..... 88

LIST OF FIGURES

FIGURES

Figure 1.1 Sinner Washing Cycle [1] 1
Figure 1.2 Circulation System of Washing Machine [3] 3
Figure 2.1 The spraying system from 6 or 8 points placed symmetrically on the gasket [4] 6
Figure 2.2 Spiral manner nozzle design [5] 6
Figure 2.3 Spraying device with a guiding part [6] 7
Figure 2.4 Micro-bubble nozzle design [7] 7
Figure 2.5 A nozzle design an inclined and spread form [8] 8
Figure 2.6 A small chamber design under the boiler [11] 9
Figure 2.7 A positioned drum with sensor and paddle design [12] 9
Figure 2.8 A flowthrough design for circulation system [13] 10
Figure 2.9 The Fluidic Oscillator Design and Parameters I [25] 12
Figure 2.10 The Fluidic Oscillator Design and Parameters II [26] 14
Figure 2.11 The Fluidic Oscillator Design and Parameters III [27] 15
Figure 2.12 The Fluidic Oscillator Design and Parameters in Detail [27] 16
Figure 2.13 The Fluidic Oscillator Design and Parameters IV [28] 17
Figure 2.14 The Fluidic Oscillator Design and Parameters V [29] 18
Figure 2.15 The Fluidic Oscillator Design and Parameters VI [30] 19
Figure 2.16 The Fluidic Oscillator Design and Parameters VII [31] 20
Figure 3.1 Front View of Experimental Setup 22
Figure 3.2 General View of Experimental Setup 22
Figure 3.3 Side View of Experimental Setup 23
Figure 3.4 Experimental Stained Textile 23
Figure 3.5 The Geometry and Boundaries of Analysis Model 25
Figure 3.6 The Geometry and Parameters of Nozzle Design Model 25
Figure 3.7 The General Mesh Structure of Analysis Model 26
Figure 3.8 The Mesh Structure of Nozzle in Analysis Model 27

Figure 3.9 Coarser Mesh Structure for Mesh Independency 28
Figure 3.10 Selecting Mesh Structure for Mesh Independency..... 29
Figure 3.11 Refiner Mesh Structure for Mesh Independency..... 29
Figure 3.12 Outlet Average Velocity Curves for Mesh Independency..... 30
Figure 3.13 Yplus Curve Along the Wall of Selected Nozzle 31
Figure 3.14 The Ratios of w1/w0 Parameter: (a) w1/w0 = 2.0, (b) w1/w0 = 1.0, (c) w1/w0 = 1.5 34
Figure 3.15 The Graph of Experimental Removal Stain Test Results of w1/w0 Parameter for Nozzle1, Nozzle2 and Nozzle5 35
Figure 3.16 The Graph of Mean Velocity Distribution Graph in One Full Oscillation for Nozzle1, Nozzle2 and Nozzle5 at Nozzle Outlet 36
Figure 3.17 The Graph of Shear Stress Distribution Graph in One Full Oscillation for Nozzle1, Nozzle2 and Nozzle5 at Wall Defined as Stained Textile 38
Figure 3.18 The Movement of Water in a Half of Oscillating Motion at t/12, t/6, t/4, t/3, 5t/12, and t/2 Instants at The Analysis for Nozzle1 39
Figure 3.19 The Movement of Water in a Half of Oscillating Motion at t/12, t/6, t/4, t/3, 5t/12, and t/2 Instants at The Experimental Setup for Nozzle1..... 40
Figure 3.20 The Movement of Water in a Half of Oscillating Motion at t/12, t/6, t/4, t/3, 5t/12, and t/2 Instants at The Analysis for Nozzle2 41
Figure 3.21 The Movement of Water in a Half of Oscillating Motion at t/12, t/6, t/4, t/3, 5t/12, and t/2 Instants at The Experimental Setup for Nozzle2..... 42
Figure 3.22 The Movement of Water in a Half of Oscillating Motion at t/12, t/6, t/4, t/3, 5t/12 and t/2 Instants at The Analysis for Nozzle5 43
Figure 3.23 The Movement of Water in a Half of Oscillating Motion at t/12, t/6, t/4, t/3, 5t/12, and t/2 Instants at The Experimental Setup for Nozzle5..... 44
Figure 3.24 The Ratios of w2/w0 Parameter: (a) w2/w0 = 4.06, (b) w2/w0 = 3.2, (c) w2/w0 = 4.8 46
Figure 3.25 The Graph of Experimental Removal Stain Test Results of w2/w0 Parameter for Nozzle1, Nozzle4 and Nozzle7 47

Figure 3.26 The Graph of Mean Velocity Distribution Graph in One Full Oscillation for Nozzle1, Nozzle4 and Nozzle7 at Nozzle Outlet 48
Figure 3.27 The Graph of Shear Stress Distribution Graph in One Full Oscillation for Nozzle1, Nozzle4 and Nozzle7 at Wall Defined as Stained Textile 49
Figure 3.28 The Graph of Shear Stress Distribution Graph in One Full Oscillation in Detail for Nozzle1 and Nozzle7 at Wall Defined as Stained Textile 50
Figure 3.29 The Movement of Water in a Half of Oscillating Motion at t/12, t/6, t/4, t/3, 5t/12, and t/2 Instants at The Analysis for Nozzle4 51
Figure 3.30 The Movement of Water in a Half of Oscillating Motion at t/12, t/6, t/4, t/3, 5t/12, and t/2 Instants at The Experimental Setup for Nozzle4 52
Figure 3.31 The Movement of Water in a Half of Oscillating Motion at t/12, t/6, t/4, t/3, 5t/12, and t/2 Instants at The Analysis for Nozzle7 53
Figure 3.32 The Movement of Water in a Half of Oscillating Motion at t/12, t/6, t/4, t/3, 5t/12, and t/2 Instants at The Experimental Setup for Nozzle7 54
Figure 3.33 The Ratios of w3/w0 Parameter: (a) w3/w0 = 1.3, (b) w3/w0 = 1.6, (c) w3/w0 = 2.0 56
Figure 3.34 The Graph of Experimental Removal Stain Test Results of w3/w0 Parameter for Nozzle1, Nozzle3 and Nozzle6 57
Figure 3.35 The Graph of Mean Velocity Distribution Graph in One Full Oscillation for Nozzle1, Nozzle3 and Nozzle6 at Nozzle Outlet 58
Figure 3.36 The Graph of Shear Stress Distribution Graph in One Full Oscillation for Nozzle1, Nozzle3 and Nozzle6 at Wall Defined as Stained Textile 60
Figure 3.37 The Graph of Shear Stress Distribution Graph in One Full Oscillation in Detail for Nozzle1 and Nozzle6 at Wall Defined as Stained Textile 61
Figure 3.38 The Movement of Water in A Half of Oscillating Motion at The Analysis for Nozzle3 62
Figure 3.39 The Movement of Water in A Half of Oscillating Motion at The Experimental Setup for Nozzle3 62
Figure 3.40 The Movement of Water in a Half of Oscillating Motion at t/12, t/6, t/4, t/3, 5t/12 and t/2 Instants at The Analysis for Nozzle6 63

Figure 3.41 The Movement of Water in a Half of Oscillating Motion at t/12, t/6, t/4, t/3, 5t/12, and t/2 Instants at The Experimental Setup for Nozzle6 64
Figure 3.42 Comparison of Fluidic Oscillator Nozzle and Original Nozzle 66
Figure 4.1 The Graph of Mean Velocity Distribution Graph in One Full Oscillation for Nozzle1, Nozzle2, Nozzle5 and w1/w0 = 2.1 Design at Nozzle Outlet 71
Figure 4.2 The Graph of Mean Velocity Distribution Depending on Changing Ratio of w1/w0 Parameter 72
Figure 4.3 The Graph of Homogeneous Distribution Depending on Changing Ratio of w1/w0 Parameter 73
Figure 4.4 The Graph of Mean Velocity Distribution Graph in One Full Oscillation for Nozzle1, Nozzle4, Nozzle7, w2/w0 = 5.02 And w2/w0 = 5.4 Design at Nozzle Outlet 74
Figure 4.5 The Graph of Mean Velocity Distribution Depending on Changing Ratio of w2/w0 Parameter 75
Figure 4.6 The Graph of Homogeneous Distribution Depending on Changing Ratio of w2/w0 Parameter 76
Figure 4.7 The Graph of Mean Velocity Distribution Graph in One Full Oscillation for Nozzle1, Nozzle3, Nozzle6, w3/w0 = 0.5, w3/w0 = 0.75, and w3/w0 = 1.0 Design at Nozzle Outlet 77
Figure 4.8 The Graph of Mean Velocity Distribution Depending on Changing Ratio of w3/w0 Parameter 78
Figure 4.9 The Graph of Homogeneous Distribution Depending on Changing Ratio of w3/w0 Parameter 79
Figure 4.10 The Graph of Mean Velocity Distribution Graph in One Full Oscillation for Nozzle1, w4/w0 = 0.5, w4/w0 = 1.0, w4/w0 = 2.0, and w4/w0 = 3.0 Design at Nozzle Outlet 80
Figure 4.11 The Graph of Mean Velocity Distribution Depending on Changing Ratio of w4/w0 Parameter 81
Figure 4.12 The Graph of Homogeneous Distribution Depending on Changing Ratio of w4/w0 Parameter 82

Figure 5.1 The Graph of Experimental Removal Stain Test Results of w2/w0 Parameter for Nozzle1, Nozzle4, Nozzle7 and Nozzle8 84
Figure 5.2 The Graph of Experimental Removal Stain Test Results of w3/w0 Parameter for Nozzle1, Nozzle3, Nozzle6 and Nozzle9 85
Figure 5.3 The Graph of Experimental Removal Stain Test Results of w4/w0 Parameter for Nozzle1 and Nozzle10 87

CHAPTER 1

INTRODUCTION

Washing machines have long been utilized to enhance the convenience and efficiency of our daily lives. Within this sector, competition has been steadily increasing across various domains. The efficient removal of stains has been a crucial aspect in the development of washing machines. For this purpose, extensive research has been conducted on the four fundamental parameters of the Sinner Cycle, namely time, mechanical force, chemistry, and temperature, which are considered critical in achieving optimal stain removal results. [1]. The Sinner washing cycle is shown in Figure 1.1.



Figure 1.1 Sinner Washing Cycle [1]

The Sinner cycle offers a valuable design framework by utilizing four essential parameters effectively. In response to customer preferences, the time, temperature,

and mechanical effects of these parameters are minimized. In the light of this concern, the objective is to enhance the washing efficiency by improving the chemical impact. Numerous methods have been developed for this purpose, including the spraying of the water under the tub into the drum with the circulation system [2]. This technique facilitates the continuous application of detergent water onto the stained textile, resulting in shortened stain removal times. With this technology, environmentally friendly results such as reduced energy consumption and decreased detergent use are achieved. To understand the circulation system in washing machine, an example model is shown in Figure 1.2.

In circulation systems, at least one nozzle is required for spraying detergent water into the drum and different nozzle designs are available for this purpose [2]. The most important issue in nozzle designs used in washing machines is that the detergent water should penetrate all the stained laundry by scanning a wide area [2]. In all existing versions, the water is directed by an obstacle at exit of nozzle to spray the water into drum directly. However, in this method, using different types of nozzles does not make a difference.

A new nozzle design known as fluidic oscillator nozzle is designed to scan at a wide angle without any structural requirements. In this thesis, the structure of fluidic oscillator nozzle will be examined due to its wide area scanning. After the introduction in the first part, patent and literature reviews will be examined in the second part. In the third chapter, the newly developed method will be explained using analyzes and experimental studies. In the fourth and fifth chapters, analysis studies and experimental studies for the optimum nozzle will be shown respectively. In the last section, the results will be summarized.

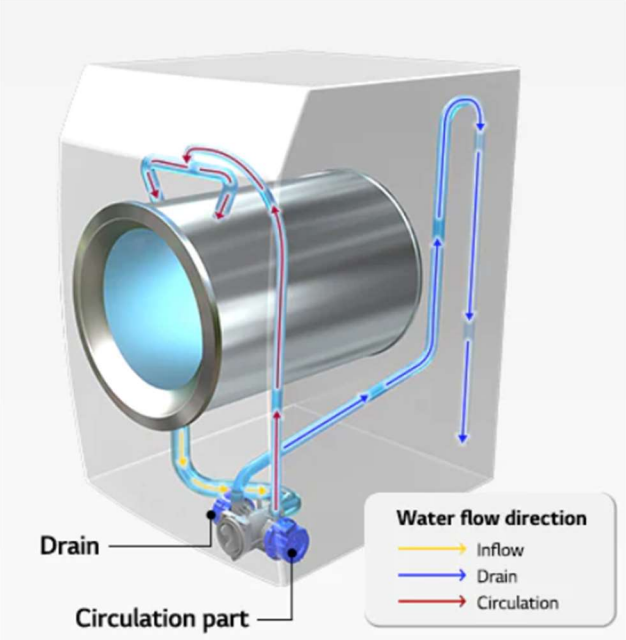


Figure 1.2 Circulation System of Washing Machine [3]

CHAPTER 2

LITERATURE REVIEW

In washing machines, circulation system and nozzle designs were found in different patents. Under this title, important and inspiring patents will be investigated briefly. Then, important articles about fluidic oscillator will be examined in detail.

2.1 Circulation Systems in Washing Machine

In different categories related to the circulation systems used in the washing machines, many patents have been published. According to the patent titles, the most important topic addressed in the patents is to control the spraying system with different nozzle designs and different number of nozzles. Lyu et al. aimed to spray detergent water to every point of the laundry by using the spraying system with 6 or 8 nozzles placed symmetrically on the gasket, as shown in Figure 2.1 [4]. Although this system aims to remove the stain better by spraying water from many different nozzles on the laundry, it consumes more water during washing by spraying from by all nozzles [4].

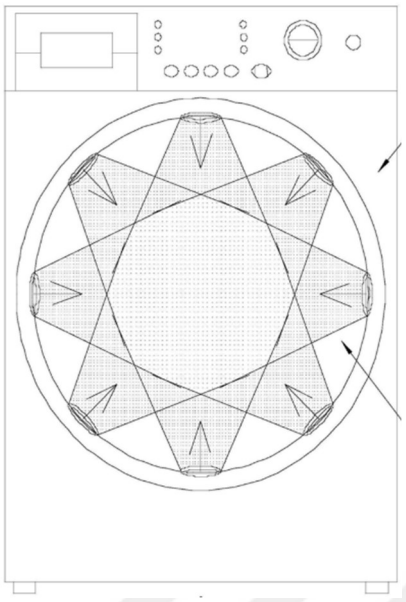


Figure 2.1 The spraying system from 6 or 8 points placed symmetrically on the gasket [4]

Zhao et al. adjusted the flow direction of the water in a spiral manner which is intended to ensure that water is sprayed to every point of the laundry by opening a hole (Figure 2.2) [5].

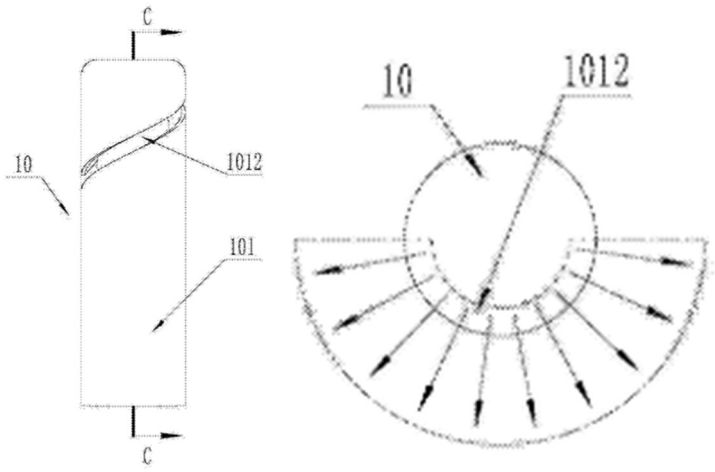


Figure 2.2 Spiral manner nozzle design [5]

Wang et al. designed a new nozzle, and this nozzle increases the velocity of the water with a structure that narrows towards the nozzle outlet, as illustrated Figure 2.3. In addition, it provides the nozzle outlet to be directed towards the inside of the drum

as desired with a guiding part. Although this nozzle structure directs the water to the laundry, it covers a limited area [6].

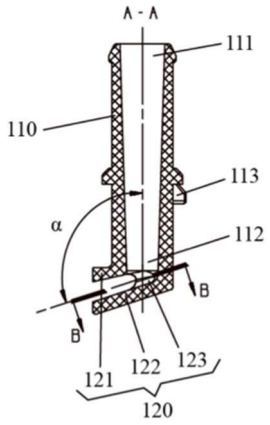


Figure 2.3 Spraying device with a guiding part [6]

Zhao et al., as shown in Figure 2.4, used Venturi effect in their design, so that there is a suction due to the negative pressure and micro-bubble can be obtained. Micro-bubble increases the washing performance by separating the stain from the laundry better [7]. Tartuferi et al. designed the nozzle outlet as an inclined and spread form, providing water to reach a wider area in the drum, as illustrated in Figure 2.5 [8]. Although there have been improvements in nozzle structures, they still have restrictions in terms of the surface area that they can effectively cover during the dispersion of the detergent water [8].

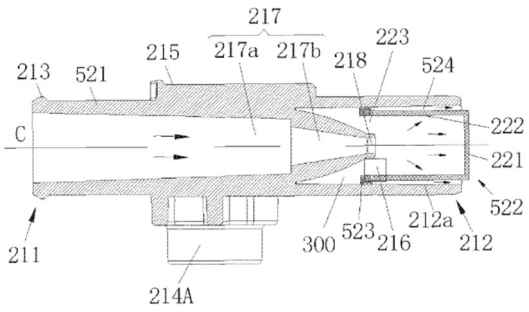


Figure 2.4 Micro-bubble nozzle design [7]

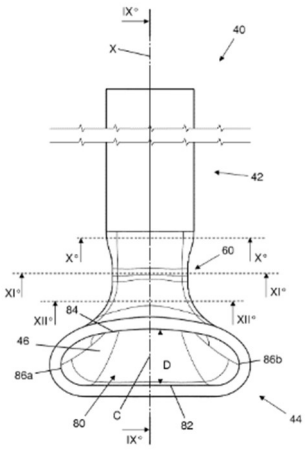


Figure 2.5 A nozzle design an inclined and spread form [8]

Another popular topic is to use spraying in different ways by controlling the rotation speed and direction of the drum. Im et al. designed a system that sprays from 4 different points using a circulation pump that can operate at different rotation speeds, as shown in Figure 2.6 [9]. While this system is believed to have a significant impact on washing performance by allowing for controlled circulation of water with different pump rotation speeds through the use of variable drum motor rotation speeds, it should be noted that it is an expensive system [9]. Jung et al. described a system similar to the previous one [10]. Differently, they defined pump control at different rpm values with new washing movements [10]. There are many patents written on this subject.

Instead of the nozzles used in the existing systems, there are different technologies that enable the circulation of detergent water into the drum from different points without spraying.

Yang et al., at the beginning of washing, described a method to dissolve the detergent quickly by placing the detergent water under the drum without reaching the laundry. Detergent water is mixed quickly in a small chamber under the boiler and taken into the drum. Dissolving the detergent at the beginning of the wash increases the washing performance, but the disadvantage of this system is that the system can only be used at the beginning of the wash [11].

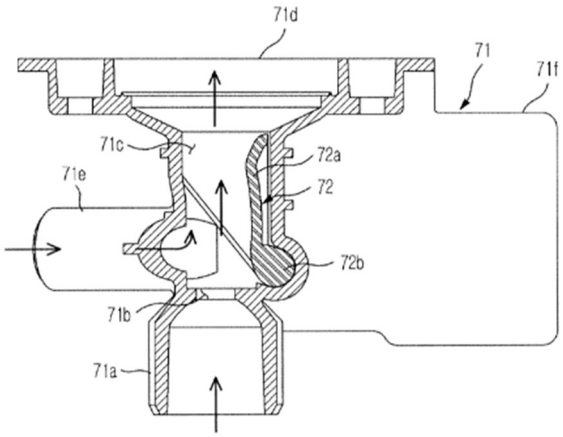


Figure 2.6 A small chamber design under the boiler [11]

Kasap et al. carried out a design in which a paddle in the drum is positioned at the upper point with the help of a sensor (Figure 2.7). In this system, the drum is positioned in certain steps of the washing, and the water is taken upwards thanks to the circulation pump and the detergent water is carried into the determined paddle. Detergent water is fall into the drum through the holes in the paddle. The system is designed to increase the washing performance in delicate washes by avoiding the high-speed spraying of water onto the laundry [12].

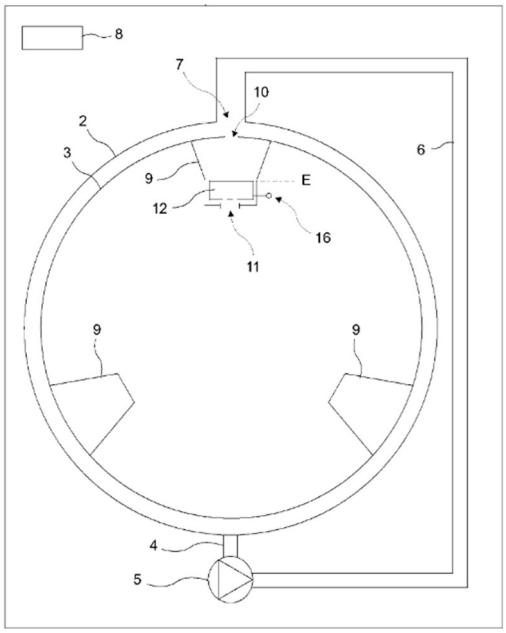


Figure 2.7 A positioned drum with sensor and paddle design [12]

There are new structural solutions to increase the washing performance during the circulation of detergent water. Demir et al. has developed a flowthrough solution that increases the water temperature during the way of water in the circulation line, as illustrated in Figure 2.8 [13]. The induction coil in this system heats the water passing through the line with magnetic energy, allowing hot water to be sprayed onto the laundry [13]. Although the system is costly, it is aimed to increase the washing performance [13].

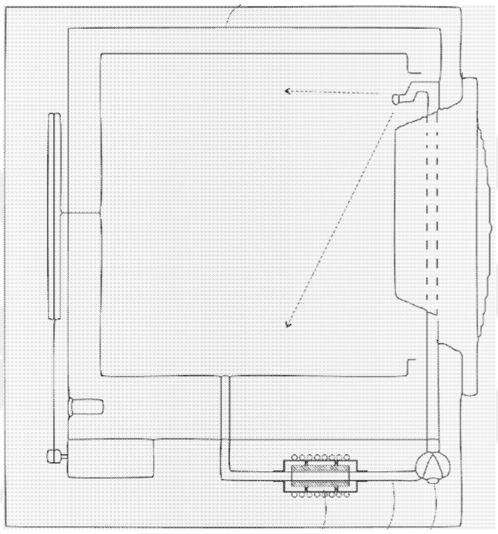


Figure 2.8 A flowthrough design for circulation system [13]

Lastly, Oh et al., in washing machine, spraying system including nozzle and pump is used to spray steam, which is generated by steam generator [14]. There are a lot of patents about steam generator or spraying steam, however this topic is not related directly with this thesis.

When all these systems were examined, it was decided that the most effective solution in terms of cost and performance is an effective nozzle design. In this context, it is decided to examine fluidic oscillator nozzles used in other sectors as a different nozzle design. The effect of these nozzles on the washing performance and optimum nozzle design will be examined in this thesis.

2.2 Fluidic Oscillators

Fluidic oscillators are helpful devices that can create an oscillating jet by only using the fluid dynamics principles, without any moving parts. Both compressible and incompressible flows have a wide variety of nozzle types described in the literature. Fluidic oscillators can be used to scan a wider area and boost chemical interaction. The first fluidic oscillator with feedback loop channels was designed by Warren [15]. Since then, a variety of applications have made by the use of fluidic oscillators. The use of fluidic oscillators as windshield washer nozzles on automobiles is their most well-known application [16]. These devices' ability to distribute their oscillating jet allows windshield washer fluid to be sprayed over a larger area while using a minimal amount of fluid. Since the oscillation frequency of a fluidic oscillator is only determined by the supply flow rate, the flow rate metering is another important application for fluidic oscillators [17, 18]. According to the thorough studies that can be found in the literature, fluidic oscillators have been employed for reducing noise, control of combustion, and control of separation [19, 20, 21, 22]. In aerospace applications, fluidic oscillators have been used to lower drag [23].

Results on the impact of seven geometrical parameters on the flow-switching frequencies generated in a 3D printed single feedback loop were reported by McDonough et al. in 2017. They discovered that the splitter distance between the power nozzle and two outlet streams was the most important factor influencing oscillations. It was realized that the angle between the outlet channels was also crucial, with wider angles yielding marginally higher frequencies. Wider feedback loops and shorter inlet zones were found to prevent flow switching [24].

An experimental investigation is made to determine how the internal geometry of a fluidic oscillator—specifically, the widths of the inlet wedge W1, mixing chamber W2, and exit throat W3—affects the operation of the device, which is shown in Figure 2.9. The flow dynamics both within and outside of the oscillator are measured simultaneously using time-resolved particle image velocimetry. In order to compute

the pressure fields, suitable orthogonal decomposition analysis is used to acquire the phase-averaged flow fields [25].

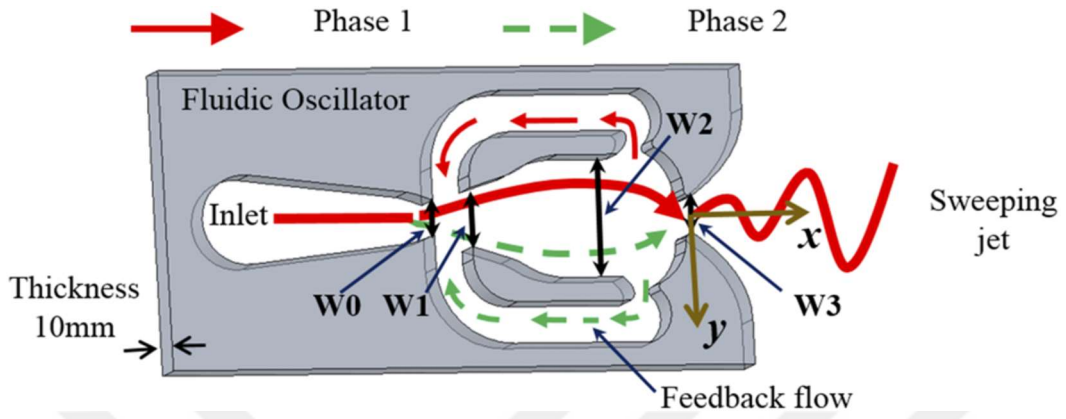


Figure 2.9 The Fluidic Oscillator Design and Parameters I [25]

The width of the inlet wedge is shown to be inversely proportional to the external jet spreading angle and oscillation frequency from W1/W0 = 0,8 to 2. This relationship is attributed to the effect of the inlet wedge on the feedback flow, which controls the recirculation bubble in the mixing chamber. With a stable external sweeping jet, there is no feedback flow at a crucial lower value of W1/W0 = 0.8. The inlet throat width is then achieved by increasing the inlet wedge width to W1/W0 = 1. As a result, the mixing chamber displays obvious recirculation bubbles together with a significantly enhanced spreading angle of the outside jet. Consequently, the forward flows in the feedback channels are drastically reduced and can be cancelled by an increase in the feedback flow. The flow separated from the main jet is decreased close to the inlet throat by expanding the inlet wedge to W1/W0 = 1.5. Due to the great velocity magnitude of the feedback flow, which dominates the feedback channel, noticeable jet sweeping occurs. The feedback flow is highest in all four situations when W1/W0 is increased to 2. In contrast to that at W1/W0 = 1.5, the exterior jet spreading angle exhibits little depression [25].

The size of the recirculation bubble is significantly proportionally controlled by the mixing chamber width W2/W0, which also controls the spreading angle. The mixing chamber ratio W2/W0 has considerable control over just the size of the recirculation

bubble, in contrast to the input wedge width ratio W1/W0. A larger recirculation bubble and an improvement in the jet spreading angle from 30 to 100 degrees can be obtained by raising W2/W0 from 2.9 to 4.2. Due to the mixing chamber's small size, there is not much of a recirculation bubble inside it at W2/W0 = 2.9, but the oscillator's strong feedback flow can nevertheless provide a stable exterior sweeping jet motion [25].

The issued jet width and the growth of the recirculation bubble are both affected by the exit throat width ratio W3/W0. The oscillation frequency and the external jet influenced area do not have a monotonous relationship. Three alternative values of W3/W0 are used to assess the throat width: 0.6, 1.4, and 4.2. At W3/W0 = 1.4, the external jet has a maximum influenced region and a minimum frequency. It is important to note that even when the exit throat width ratio (W3/W0) is equal to the mixing chamber width ratio (W2/W0), the fluidic oscillator may produce intense periodic external sweeping jets [25].

These findings have influenced the studies and produced some very significant outcomes for this thesis.

Next study focuses on the major geometric properties of fluidic oscillators of different lengths with constant depth. The frequency and sweeping properties of the fluidic oscillators are impacted by changes in the length of these nozzles [26].

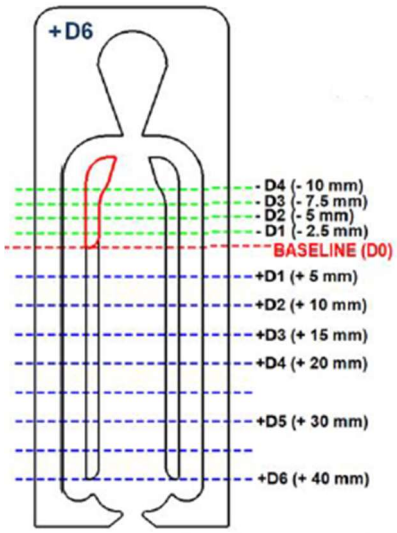


Figure 2.10 The Fluidic Oscillator Design and Parameters II [26]

D0 is the reference design, while the smallest and longest designs that were taken into consideration are -D4 (10 mm shorter than reference line) and +D6 (40 mm longer than reference line). Figure 2.10 displays all 11 designs over the longest +D6 design. The oscillation frequency and the sweep angle are the two key factors that determine the properties of a fluidic oscillator [26].

As a first observation, the nozzle does not function as an oscillator because -D4 and -D3 produced zero oscillations. Nevertheless with +D2, this trend changes, and the oscillator begins to produce an oscillating jet. Oscillation frequencies begin to fall as the oscillator length increases, and the trend of frequency change for a oscillator design becomes more linear. For instance, the design +D6 that is taken into consideration in this work could achieve an oscillation frequency of 126 Hz while the design -D2 can reach 1371 Hz [26].

As a second observation, the sweeping motion is undetectable for -D4 and -D3. On the other hand, design -D2's visualizations make the sweeping action visible and quantifiable. Following this design, the baseline D0 design's sweep angle rises to 41 degrees and then starts to fall. The longest +D6 design has a sweep angle of 20 degrees [26].

The next thesis focuses on various parameters of fluidic oscillators such as outlet region shape, mixing chamber inlet geometry, outlet nozzle geometry and feedback channel geometry. In the outlet region, it was discovered that removing a flow diverter downstream of the nozzle and removing the diverging nozzle walls have no influence on the oscillation frequency or deflection angle of the jet. As the mixing chamber inflow edges, second parameter in this paper, are separated, the oscillation frequency rises as shown in Figure 2.11. Larger inlet wedges significantly lower the reversed flow (i.e., negative mass flow) in the feedback channels. When the jet is attached to one side, the volume of the recirculation bubble in the mixing chamber is reduced for a larger area between the mixing chamber inlet wedges [27].

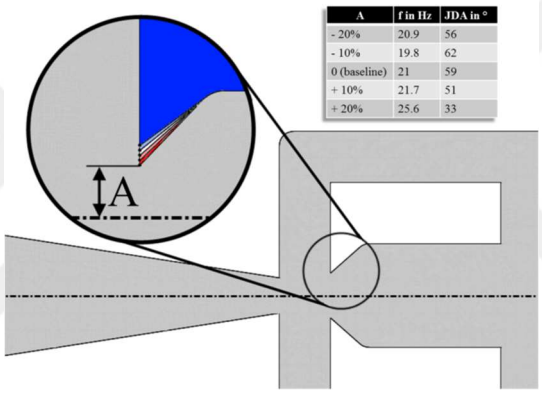


Figure 2.11 The Fluidic Oscillator Design and Parameters III [27]

The next parameter is the outlet geometry which includes angle and length of the converging part, which is shown in Figure 2.12. Firstly, in order to keep the open surface constant, the angle was first altered from -1 to +1 mm. Second, by altering the actuator's outlet region, the length of the converging component was altered from -20% to +50%. Surprisingly, with the exception of the outlet width being raised by 50%, the frequency is nearly constant for both designs. The pressure surrounding the stagnation point near the feedback channel inlet is the main cause of the reduced frequency at +50% for outlet width [27].

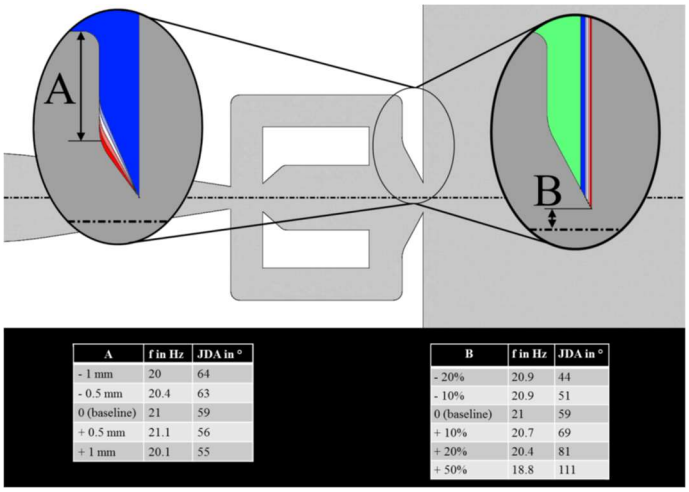


Figure 2.12 The Fluidic Oscillator Design and Parameters in Detail [27]

Last parameter is feedback channel geometry which is the most significant factor impacting the oscillation frequency of the jet. Three parameters are investigated under this parameter: the shape of the channel, the length of the channel and changes of feedback channel volume. Round shaped feedback channel type oscillator causes less frequency compared to reference oscillator. The frequency of the fluidic oscillator further decreases with lengthening of the feedback channels; however, frequency decreases drastically when feedback channel becomes too large (e.g., an additional length of +12mm). The same non-monotonic behavior is seen as the volume of the feedback channel increases. The pressure drop throughout the feedback channels increases and the frequency decreases for volume changes up to +50%. The pressure loss is again decreasing for a volume increase of +100%, resulting a higher frequency [27].

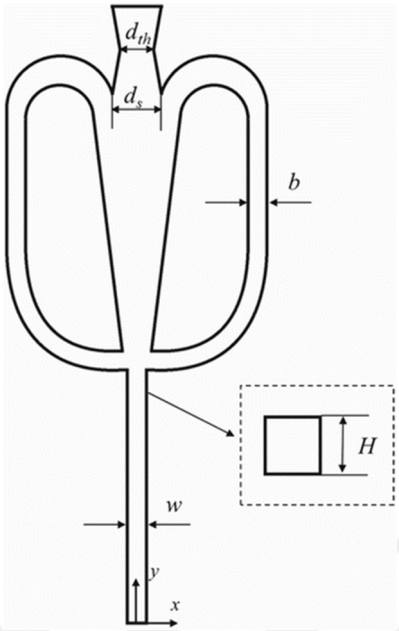


Figure 2.13 The Fluidic Oscillator Design and Parameters IV [28]

In the design, for which fluidic oscillator's geometrical parameters are shown in Figure 2.13 and the attention is focused on the changing ratio of the throat width (d_{th}) to hydraulic diameter of the throat (D_h). Based on the three-dimensional unsteady Reynolds-averaged Navier-Stokes analysis, a fluidic oscillator is optimized in this study to improve peak jet velocity at the outlet and at the same time decrease pressure drop. Water is the working liquid. The inlet of the input nozzle is considered to have a consistent velocity, so that the input is chosen as flow rate and the turbulence modal is determined as k-ε model [28].

A new optimization method is determined to obtain optimum fluidic oscillator nozzle design. Using the two design variables w/d_{th} and ds/d_{th}, respectively, numerical optimization of the fluidic oscillator was done to minimize the two objective functions, the negative of the peak jet velocity ratio at the outlet (F_{VR}) and the friction factor through the fluidic oscillator (F_f). As a result of the optimization, 4 different design points, defined as Pareto-optimal designs (POD) A, B, C and D, are determined, and analyzed. The designs suggested that decreases in d_s/d_{th} values with essentially unchanged w/d_{th} values when switching to a forward POD A nozzle with a greater velocity ratio. The widest zone of high local velocity ratio from the splitters

to the outlet surface is represented by the jet velocity-oriented design, or POD A, which does not have a throat in the outlet nozzle ($d_s/d_{th} < 1$). As a result, a smaller value of ds/dth improved F_{VR} whereas a larger value of d_s/d_{th} decreased F_f. Compared to the friction factor-oriented design, which is POD D, the jet velocity-oriented design enhanced F_{VR} and F_f by 11.18% and 16.82%, respectively. The frequency decreased to its lowest value at POD C with variations in the ratio of d_s to d_{th} which approaches 1,2 [28].

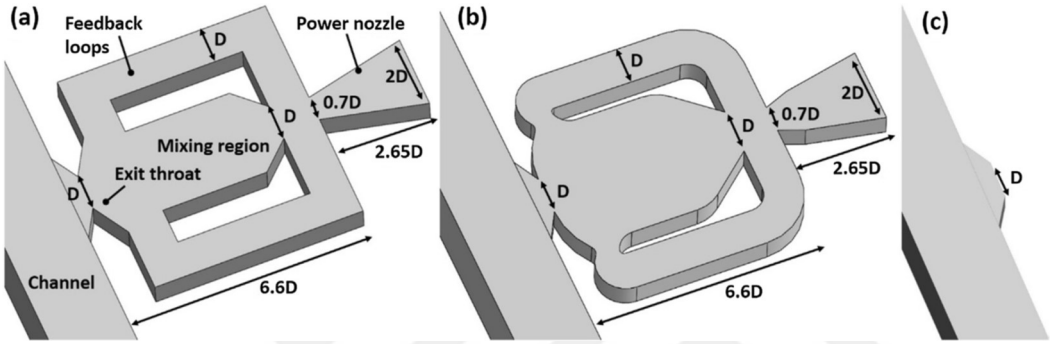


Figure 2.14 The Fluidic Oscillator Design and Parameters V [29]

In another paper, heat transfer enhancement is the main aim however two different types of fluidic oscillator nozzle shown in Figure 2.14 are investigated for their frequency values. The performance of heat transfer of two fluid was compared using numerical simulations with unsteady Reynolds-averaged Navier-Stokes (RANS) and large eddy simulation (LES) turbulence models. The k-w SST model is used to all regions with the exception of the exit throat in order to reduce computational costs. The dynamic Smagorinsky model is utilized to get more precise fluid dynamics and heat transfer results in the exit throat and the regions of the sweeping jet. With SST method, curved nozzle design has higher frequency than angled fluidic oscillator nozzle design at the same Reynolds number [29].

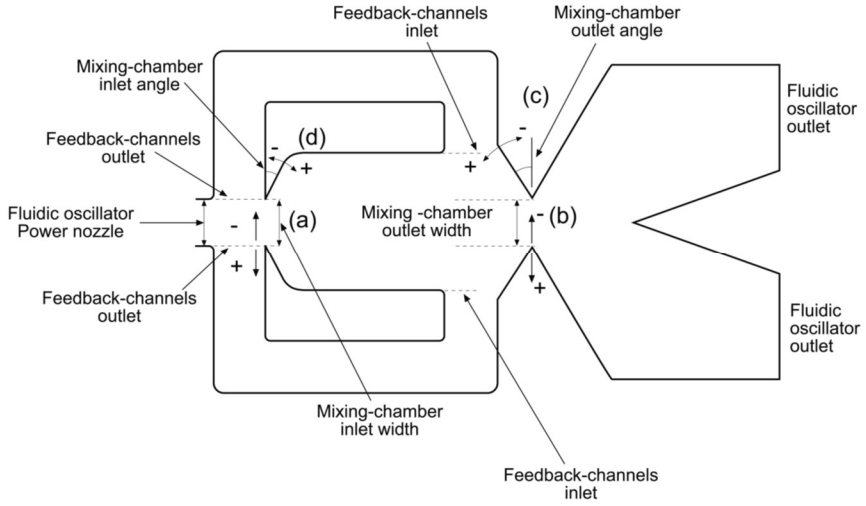


Figure 2.15 The Fluidic Oscillator Design and Parameters VI [30]

As in another paper, a fluidic oscillator under turbulent conditions has been analyzed a thorough 3D-CFD analysis. The investigation enables to determine the most important dimensional factor among the inlet width, the outlet width, the mixing chamber inlet angle, and the outlet wall inclination angle, are more important in relation to changing the frequency and output amplitude of the fluidic actuator. This design and related parameters are shown in Figure 2.15. The flow stops to oscillate, and the amplitude decreases to zero for inlet widths that exceeds a limit in either direction, whether they are too large or too small. The output frequency and amplitude decrease as the outlet width or angle is increased. When there is backward flow at the outlets, the maximum outlet mass flow amplitude is always reached, the greater the reverse flow value, the greater the outlet mass flow amplitude. In contrast to the baseline situation, which has an outlet mass flow amplitude of less than 2%, the inlet angle increased by almost twice. As shown in all preceding situations, the frequency and amplitude variations become increasingly significant as the Reynolds number increases. The outlet mass flow oscillation frequency only marginally increases with the increase in the inlet angle [30].

At the end of the paper, a linear relationship between the Reynolds number and frequency is shown in almost all cases. When compared to the reference conditions, the highest inlet width situation yields the maximum frequency for the higher

Reynolds number while highest outlet angle case produces the lowest frequency [30].

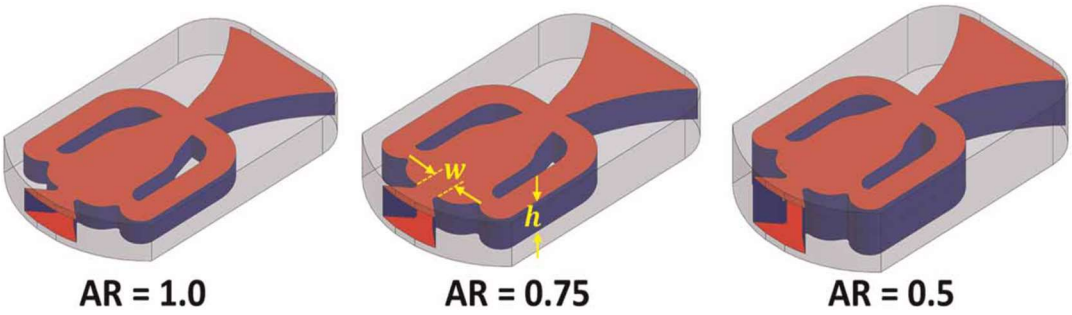


Figure 2.16 The Fluidic Oscillator Design and Parameters VII [31]

Hossain et al. [31] investigated the mechanism of heat transfer for a sweeping jet and a steady jet. For sweeping jet part, the ratio throat width to throat height is analyzed as 1.0, 0.75, and 0.5, which shown in detail in Figure 2.16. At the same mass flow rate, the frequency increases when the aspect ratio increases.

After an extensive review of the relevant literature, it was determined that a novel approach was needed to investigate the impact of fluidic oscillator designs on stain removal. Critical parameters have been determined for the purpose of conducting parametric studies and comprehensive studies have been conducted under the following headings to identify optimal designs.

CHAPTER 3

ANALYZES AND EXPERIMENTAL STUDIES FOR DETERMINATON OF A NEW METHOD

In this section, the results of stain removal tests obtained by experimental studies are compared with the results of the numerical analyzes. It is decided how the results obtained from the analyzes will be evaluated in deciding on the optimum nozzle design.

3.1 Experimental Setup

The experimental setup designed for tests performed outside the washing machine is shown in Figure 3.1, Figure 3.2, and Figure 3.3. The setup is designed to have the same distance between the pump and the nozzle used in the washing machine. The distance between the nozzle and the stained textile was taken as 115 mm to simulate the washing machine. The stain on the target textile used to evaluate stain removal is the sebum stain, which is the most common stain in daily life. This sebum-stained textile is shown in Figure 3.4.

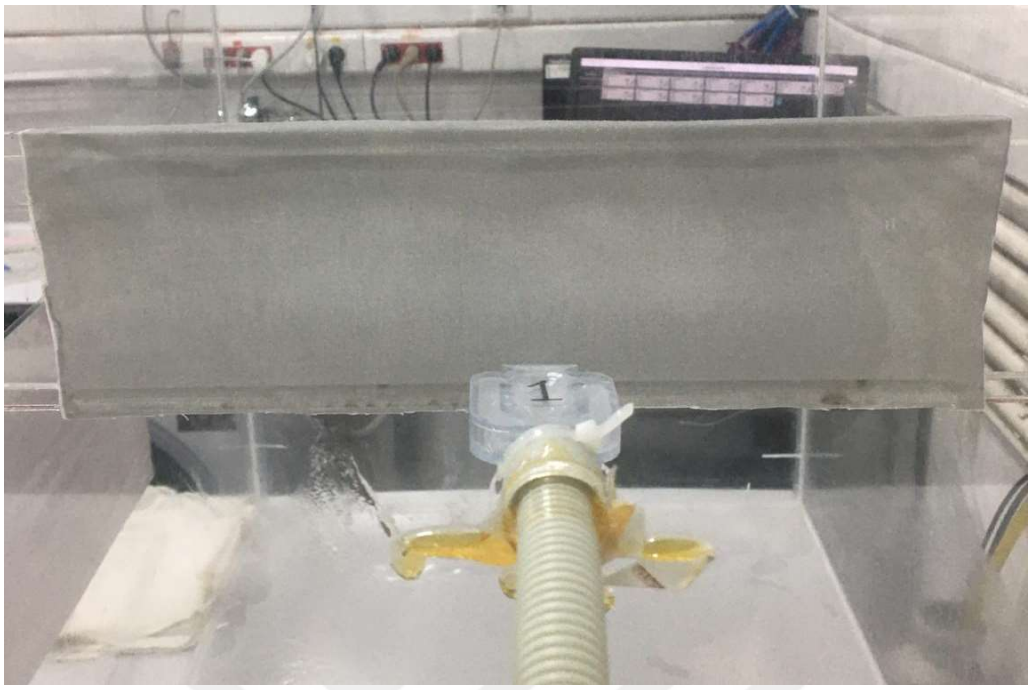


Figure 3.1 Front View of Experimental Setup

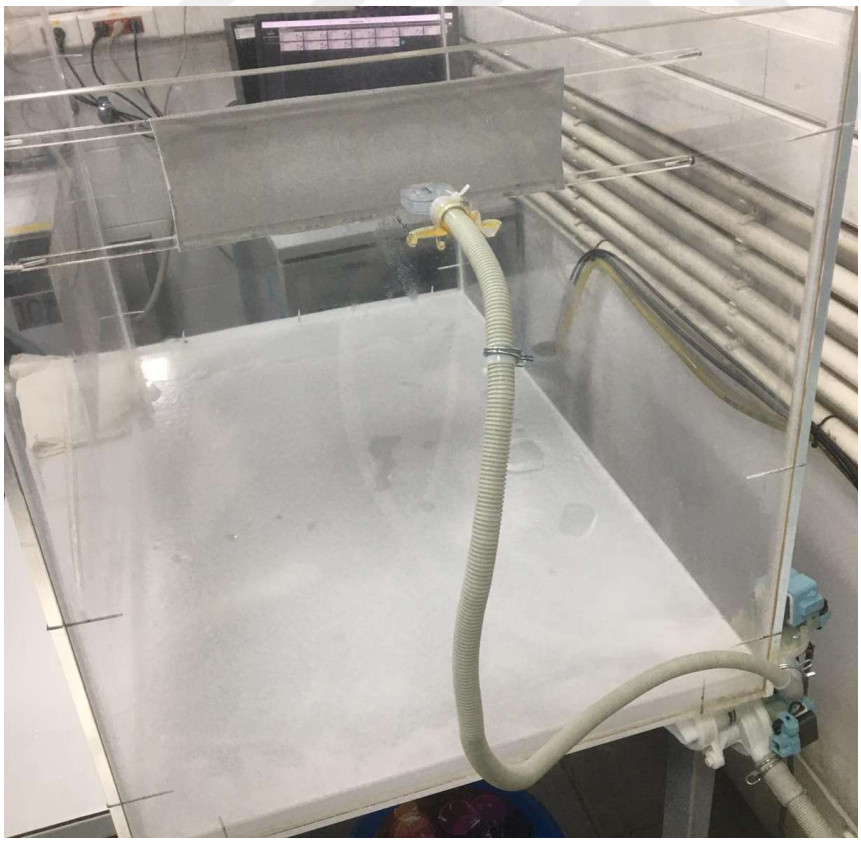


Figure 3.2 General View of Experimental Setup



Figure 3.3 Side View of Experimental Setup

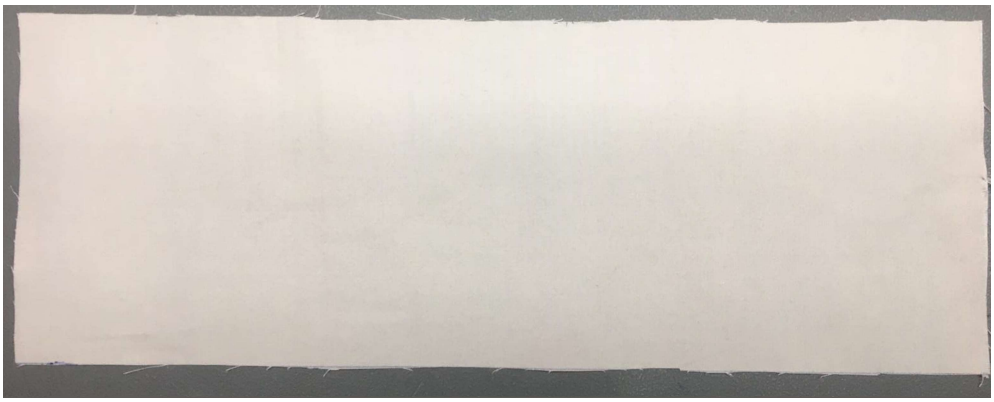


Figure 3.4 Experimental Stained Textile

DataColor device, which measures the Y value and works depending on the transmittance rate of the light, was used to measure the stain removal. Y value represents the whiteness or reflection value of textile and Y value's range is between

0 and 100. If Y value is equal to 0, textile is completely black and there is not reflection. When Y value is measured as 100, textile has not been stained. 21 points were determined on stained textile having a length of 30 cm and measurements were taken at 1.5 cm intervals. Since the diameter of the measuring device is 3 cm, the entire area was covered in detail. These fluidic oscillator nozzle designs remove the stain as line, thus analyzes were performed as 2D and experimental measurements were taken as line.

3.2 **Analysis Method**

Analysis studies were carried out in Ansys Fluent to validate the results obtained from experimental studies with Computational Fluid Dynamics (CFD) analyzes. Analysis studies were conducted as transient, and gravity was not included because gravity is in the z direction. The flow is modelled by using Reynolds Averaged Navier-Stokes (RANS) equations. Different turbulence methods have been used in the literature, the Eulerian method and the k-w SST viscous model were chosen for the approach to be used in this thesis. The inlet boundary is defined as pressure inlet with a pressure of 11300 Pa since there are two backflow channels causing losses. Y+ values are less than 80 for each nozzle design, these values are accepted sufficient in literature for this viscous model [32]. The 2D geometry and critical parameters determined for the analysis are shown in Figure 3.5.

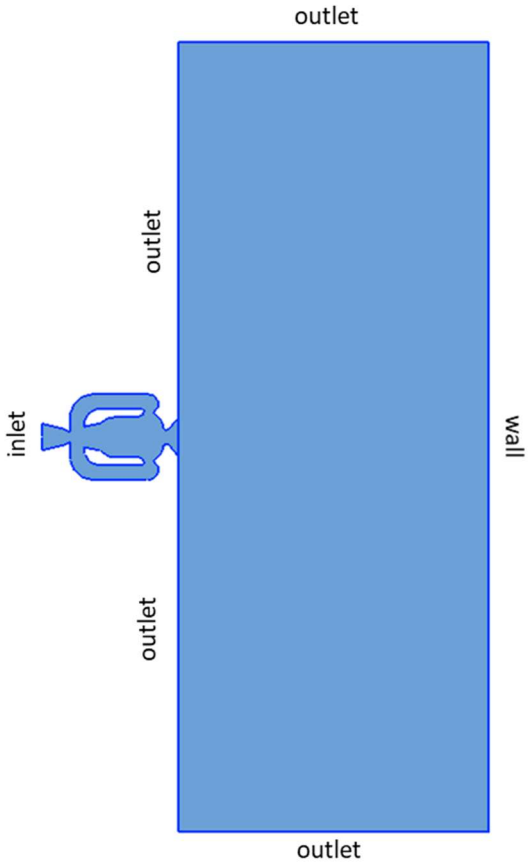


Figure 3.5 The Geometry and Boundaries of Analysis Model

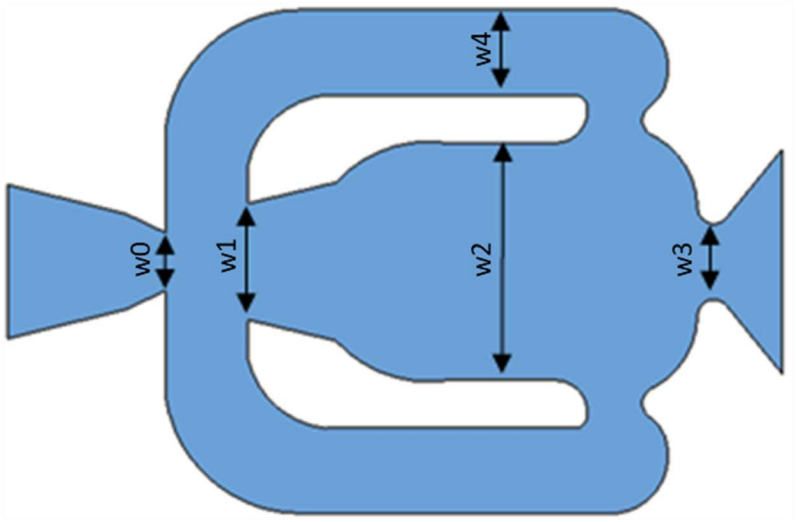


Figure 3.6 The Geometry and Parameters of Nozzle Design Model

Figure 3.6 shows the reference nozzle used for analysis. The most important reason for choosing this nozzle as a reference nozzle is that ratios are chosen close to the ones in the literature. The w0 length shown in Figure 3.6 was determined as the reference width and the ratios of the other widths to the w0 were examined in this study.

Mesh structure of the reference nozzle is shown in Figure 3.7 and the details of nozzle mesh structure is given in Figure 3.8. Mesh elements are generated is too small thanks to 2D analysis, therefore the boundary layer thickness is convenient for analysis.

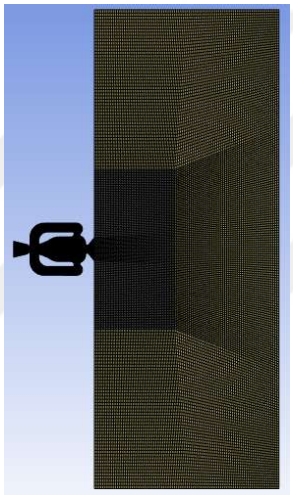


Figure 3.7 The General Mesh Structure of Analysis Model

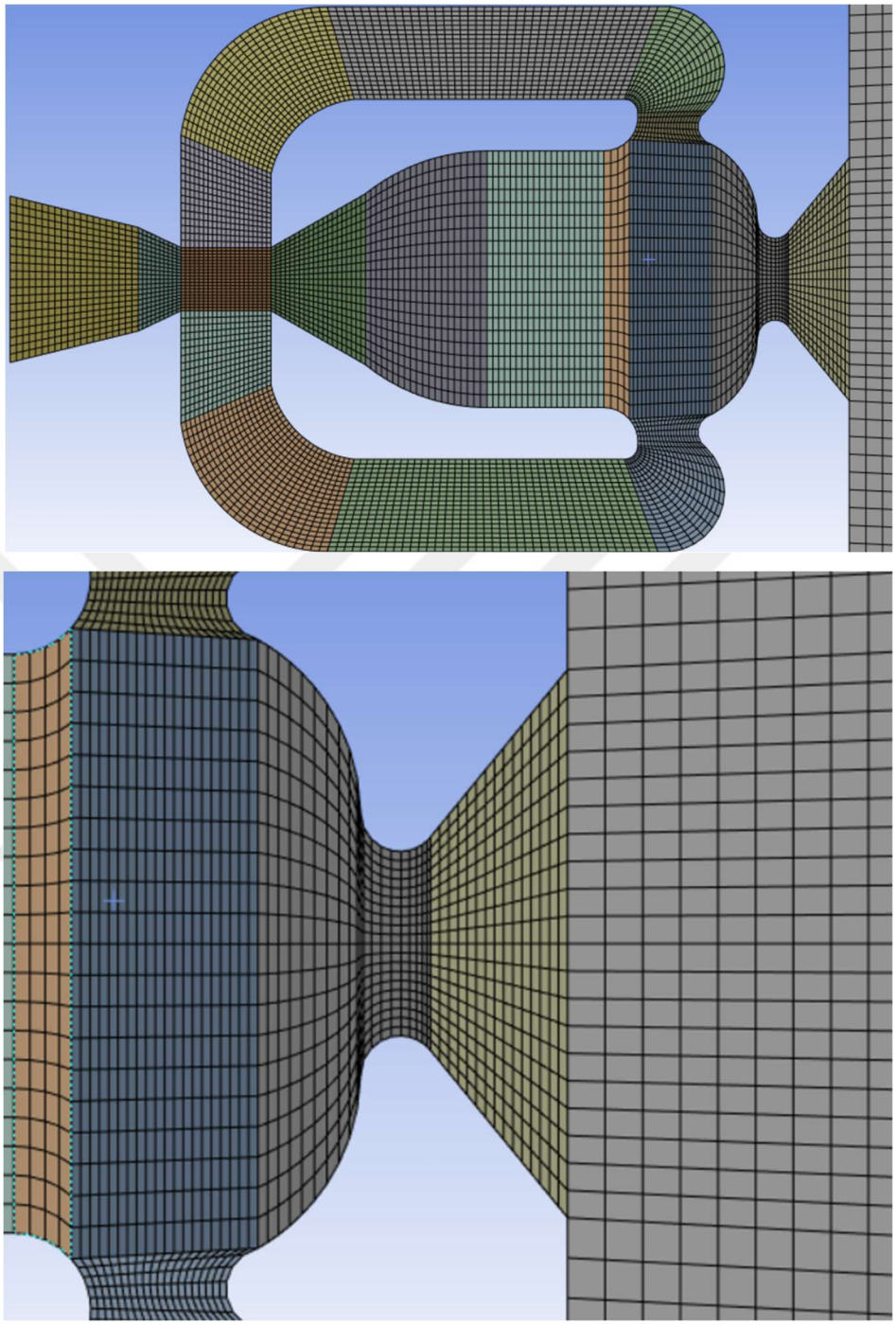


Figure 3.8 The Mesh Structure of Nozzle in Analysis Model

3.3 **Mesh Independency**

In order to show that the selected element number and element sizes are sufficient, analyzes were made with a nozzle with coarser and refiner elements according to the element sizes selected one. The courser one, selected one and refiner element at the nozzle outlet are shown in Figures 3.9 and 3.11. In the numerical results, the average velocity graphs in an oscillation at the nozzle outlet were examined. The reason for examining the velocity curve is that it is the most critical value to be used in this thesis. Velocity curves were examined in Figure 3.12, the coarse mesh has very different curve from other cases because it has only 10 elements at the output. Comparing selecting and refiner element size or number, the element number and size of determining one are sufficient to be investigated.

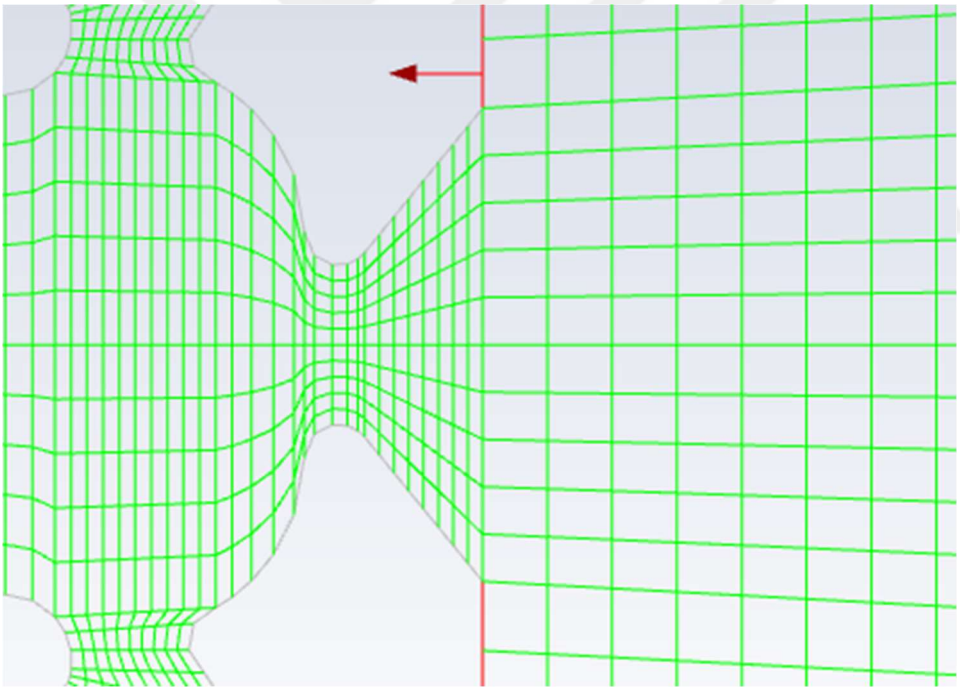


Figure 3.9 Coarser Mesh Structure for Mesh Independency

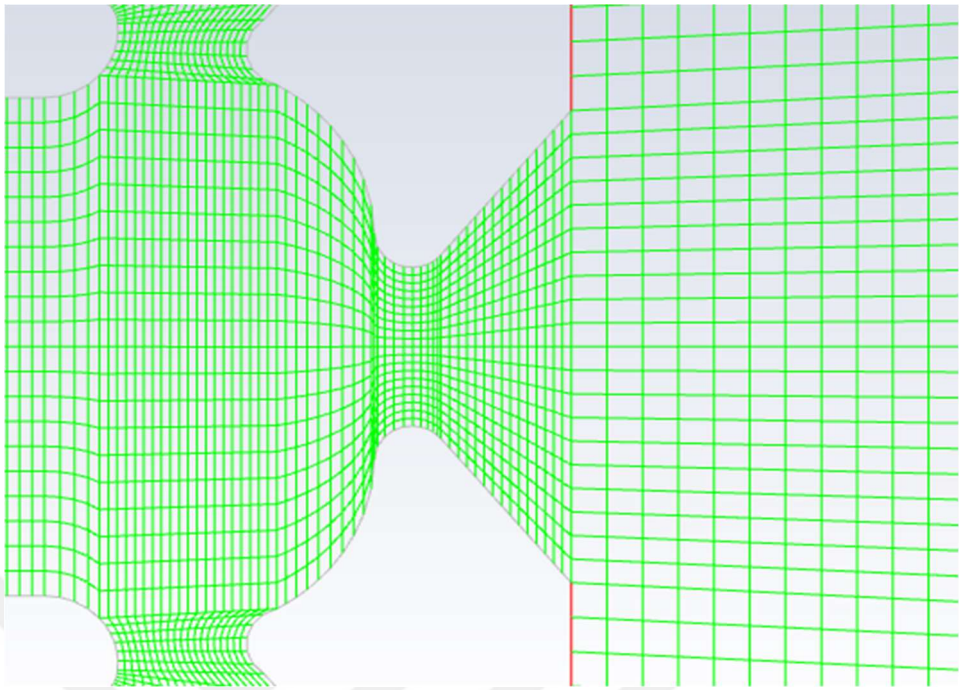


Figure 3.10 Selecting Mesh Structure for Mesh Independency

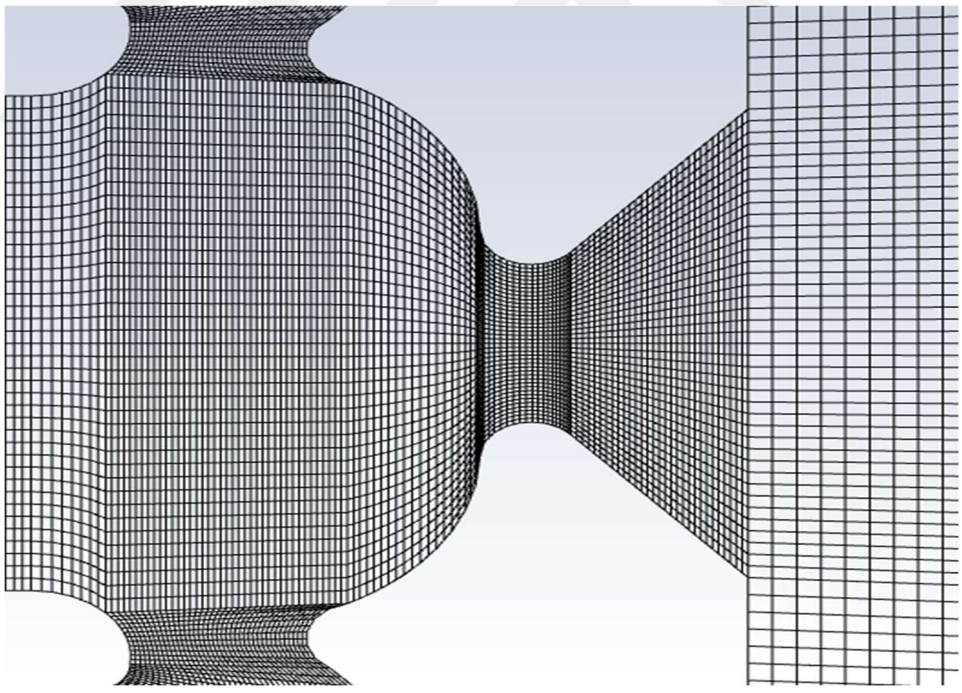


Figure 3.11 Refiner Mesh Structure for Mesh Independency

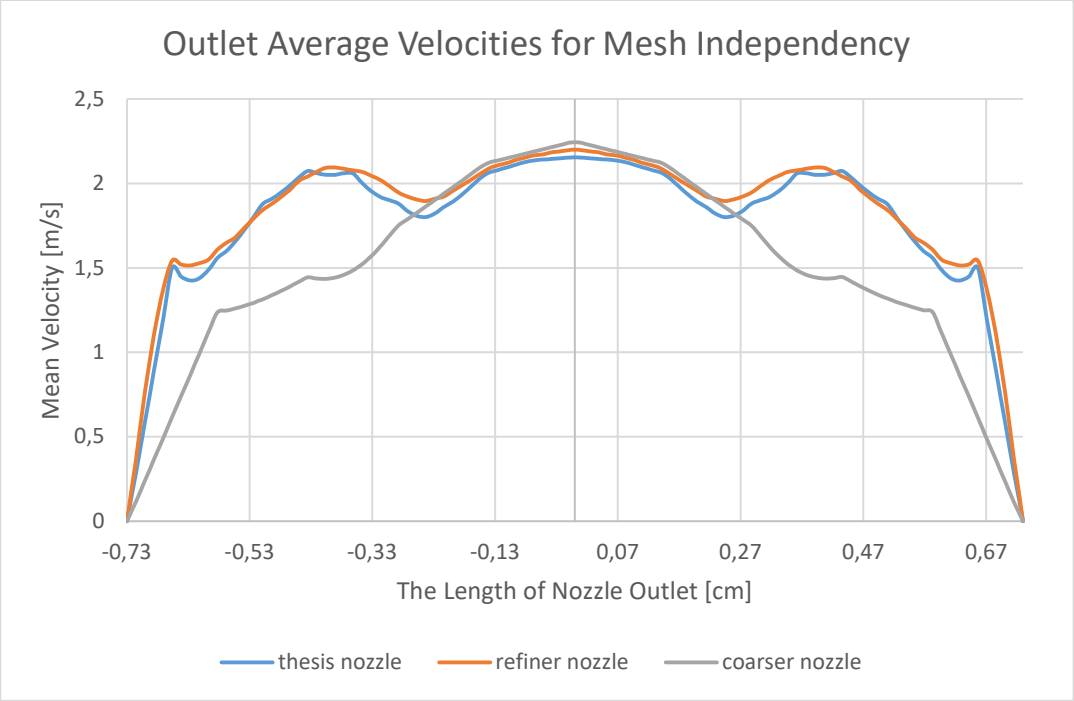


Figure 3.12 Outlet Average Velocity Curves for Mesh Independency

Y+ value of selected nozzle's wall which has the maximum Y+ value at selected time and point. Y+ curve along the upper wall of throat area of selected nozzle is shown in Figure 3.13. Y+ value is about 70 and it is sufficient for this turbulence analysis method [32].

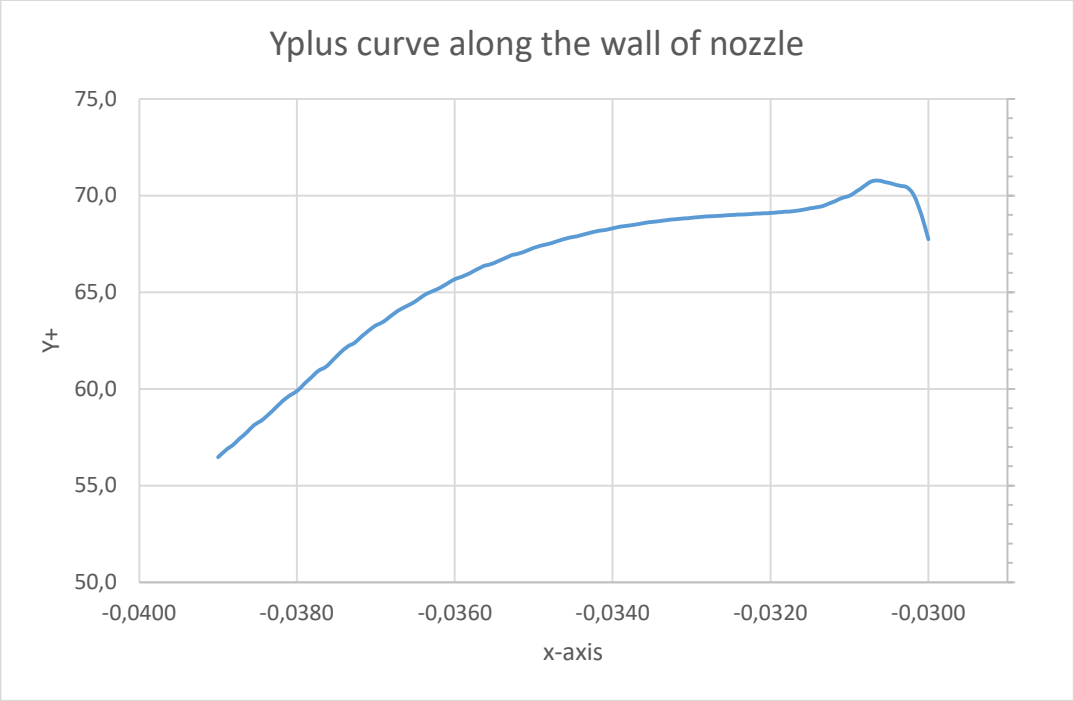


Figure 3.13 Yplus Curve Along the Wall of Selected Nozzle

3.4 **Determination of Parameters and Method**

In line with the information obtained from the literature, the ratios of different widths in the nozzle to the inlet width were examined. The ratios shown in detail in Figure 3.6 are w1/w0, w2/w0, and w3/w0.

For each case, 3 different conditions are determined based on the literature. As a reference, Nozzle1 with w1/w0 = 2, w2/w0 = 4.06, and w3/w0 = 1.3 is chosen. First, analyzes are made with the cases where the w1/w0 ratios are 1.0, 1.5, and 2.0, and validations are carried out with experimental studies. Then, analyzes are made with the cases where the w2/w0 ratios are 3.2, 4.06 and 4.8, and validation is carried out with experimental studies. The final analysis results, which are confirmed by experimental studies, are completed with the cases where the w3/w0 ratios are 1.3, 1.6, and 2.0. Briefly, there are 7 nozzles including 2 more nozzles for each parameter in addition to reference nozzle. For 2 more nozzles for each parameter, other parameters' values are equal to reference nozzle values.

In order to find out which parameters are effective, velocity distributions at the nozzle exit or in the region where the stained textile is observed were examined in the analysis studies. The stained textile is defined as a wall, and for this reason, obtaining velocity graph at the wall has led to misleading and complex results. Due to this problem, the average velocity distribution in an oscillation period at the nozzle outlet was investigated. In order to explain the velocity distributions at the nozzle outlet, the maximum angles instantaneously formed by each nozzle were determined from the values of the velocities along the x and y axis. Finally, the shear stresses on the wall, defined as the stain strip, are examined to explain that the velocity graph and the actual stain removal curves are consistent.

After the experimental studies, it was seen that the areas under the curve in the velocity graphs showed parallelism with the area under the curve in the stain removal graph. Therefore, velocity graphs at the nozzle outlet were primarily examined to analyze optimum nozzles.

3.5 **First Validation**

The first validation is carried out to compare the mean velocity results as experimental just for one nozzle which is the reference nozzle design. After this validation, validation was carried out by comparing the average velocities of the 7 nozzles determined for validation at the inlet with the average velocities at the inlet in the analysis results. In the velocity comparison results shown in all results were below the 4% error rate.

Table 3.1 The Validation of Analyzes with Mean Velocity

Type of Nozzle	*Experimental Mean Velocity*	*Analysis Mean Velocity*	*Error*
Nozzle1	1,341	1,352	0,84%
Nozzle2	1,242	1,235	-0,56%
Nozzle3	1,601	1,612	0,69%
Nozzle4	1,467	1,498	2,08%
Nozzle5	1,280	1,284	0,33%
Nozzle6	1,488	1,437	-3,54%
Nozzle7	1,308	1,362	3,96%

After the first validation studies, each parametric group was examined within itself for the optimum nozzle and the optimum ratios were determined separately.

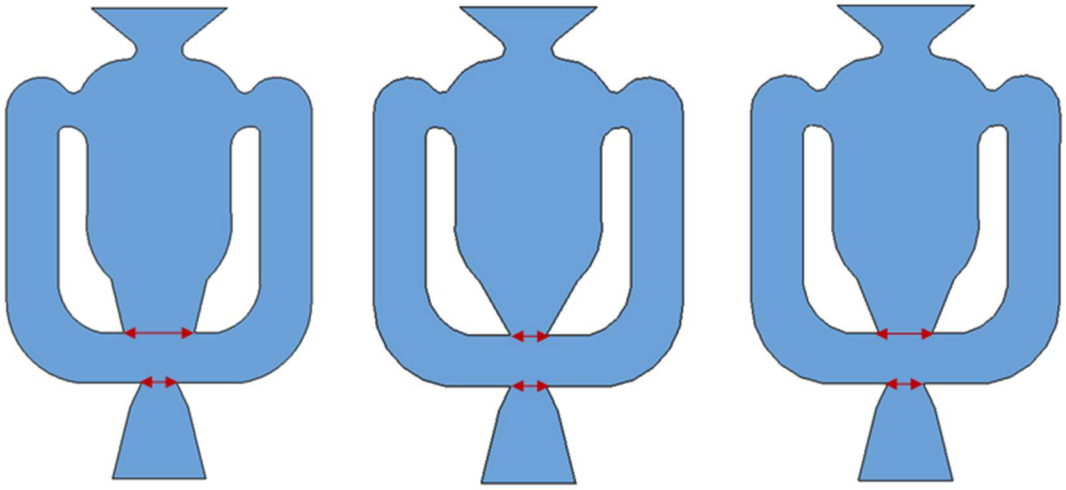
As a result of all these studies, additionally, it is seen that the analyzes are confirmed with the experimental studies, and the optimum ratio is determined for ratio of w4/w0 parameter.

3.6 **A New Method for Stain Removal Modelling**

3.6.1 w1/w0 Parameter

The ratio of w1/w0 is determined as 2.0 in the reference nozzle design, because the ratios close to this value are usually given in the literature. In addition, it has been stated that if this ratio increases above 2.0, oscillations cannot be seen. In order to understand the behavior of w1/w0 ratio and determine its optimum value, numerical analyzes and tests were carried for w1/w0 ratios of was 1.0 and 1,5.

Nozzles, which are labeled as nozzle1, nozzle2, and nozzle5 having, w1/w0 ratios of 2.0, 1.0, and 1.5 respectively are shown in Figure 3.14.



(a) (b) (c)

Figure 3.14 The Ratios of w1/w0 Parameter: (a) w1/w0 = 2.0, (b) w1/w0 = 1.0, (c) w1/w0 = 1.5

Firstly, the stain removal curves of nozzle1, nozzle2 and nozzle5 were examined to understand the effect of w1/w0 ratio, as shown in Figure 3.15. In this figure, ΔY represents the difference between the reflection values before and after washing. In this graph, the areas under the stain removal curve are examined to stain removal capacity of nozzles. Stain removal capacity represents the washing performance for each nozzle. Then, two peaks on the curve are investigated to determine the homogeneity of the distribution. Homogeneous distribution of curves is important to reach more area on the stained textile. Nozzle1 is disadvantageous in terms of homogeneous distribution since it creates two peaks with a smaller angle difference between them. However, this small difference in the angle can be neglected because of its higher stain removal amount. In order to find the best solution for this parameter, the analysis studies were carried out in the light of the information obtained from the experimental studies and these analyzes will be examined in the next section.

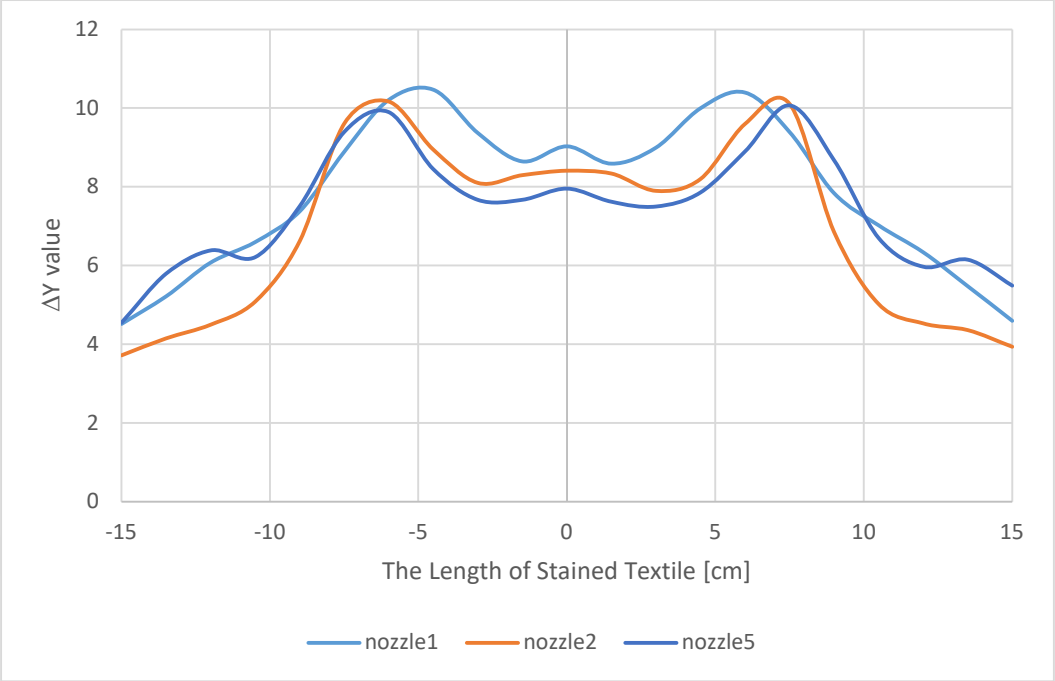


Figure 3.15 The Graph of Experimental Removal Stain Test Results of w1/w0 Parameter for Nozzle1, Nozzle2 and Nozzle5

In the analysis phase, first of all, a line was determined at the nozzle outlet and the variation of the velocity was plotted along this line. Velocity graphs for nozzle1, nozzle2, and nozzle5 are shown in Figure 3.16. In the nozzle1 velocity graph, which was determined as the reference nozzle, it was observed that the peaks occurred within a narrower distance, and this is consistent with the experimental observations. In addition, the area under nozzle1 velocity curve has a higher value than the other two nozzles.

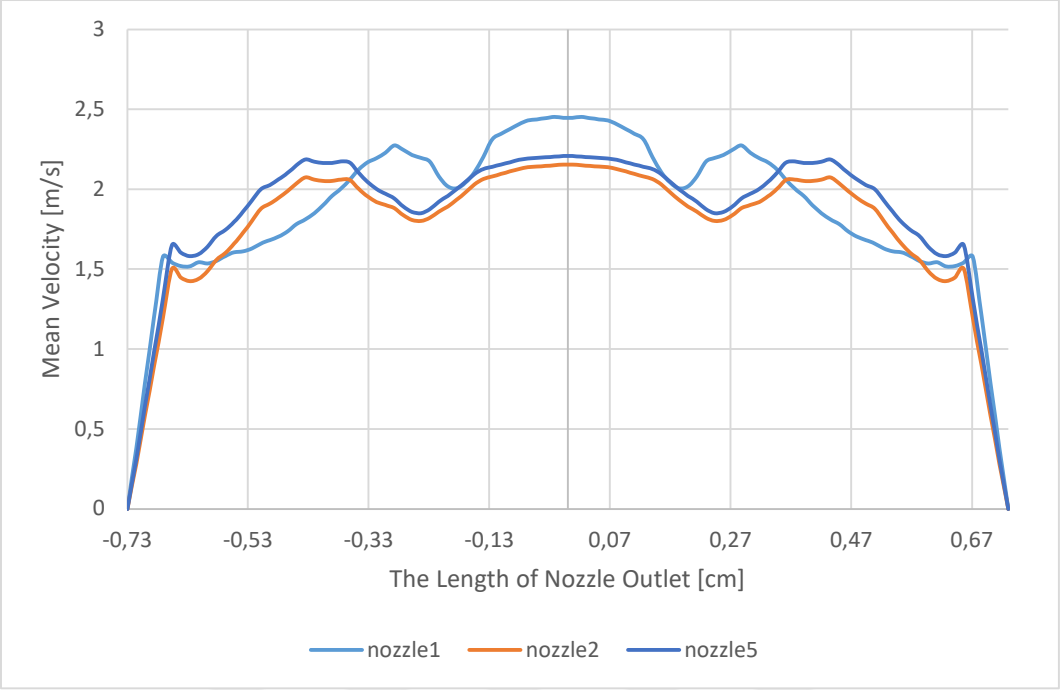


Figure 3.16 The Graph of Mean Velocity Distribution Graph in One Full Oscillation for Nozzle1, Nozzle2 and Nozzle5 at Nozzle Outlet

In order to understand the reason for these behaviors on the velocity graph and to understand how to remove the stain more, the moment and point at which the ratio of the velocity in the y axis to the velocity in the x axis is the maximum at the nozzle exit was determined. Firstly, maximum y-direction velocity is found at the exit of nozzle, then x-direction velocity is obtained at same moment and point. After that, the maximum angle is calculated with these velocities. For each nozzle, the maximum velocities, and these rates on analyzes are shown in

Table 3.2. Looking at this table, it is seen that nozzle2 and nozzle5 nozzles can reach a wider angle with a similar angle. The maximum angle of nozzle1 is smaller, which explains the difference in the velocity graph.

Table 3.2 The Maximum Angle of Nozzles for w1/w0 Parameter

Type of Nozzle	*Maximum Velocity in the y direction*	*The Velocity in the x direction at this time & point*	*Angle of The Velocity*
Nozzle1	2.07 m/s	2.02 m/s	45.7
Nozzle2	2.42 m/s	2.00 m/s	50.2
Nozzle5	2.38 m/s	2.00 m/s	50.05

There are two main differences between the velocity graphs in the analysis studies and the stain removal graphs in the experimental study. The first of these, the peaks formed in the velocity graphs were formed with a wider angle, and the second, the peaks formed in the middle of the velocity graph were not formed in the stain removal curves. The first difference does not pose a problem for the approach to be used in this thesis, and the second difference is explained by shear stress. Stain removal behavior is also directly affected by shear stress since water does not pass through the textile, therefore stained textile can be imagined as rigid plate and stain can be removed with this force. Shear stress plots are shown in Figure 3.17 for nozzle1, nozzle2, and nozzle5. Although the shear stress values do not directly affect the stain removal, when the shear stress graphs are examined, it is seen that the shear stress drops abruptly around the midpoint, and this explains the reason why no peak occurs at the midpoint of the stain removal graph.

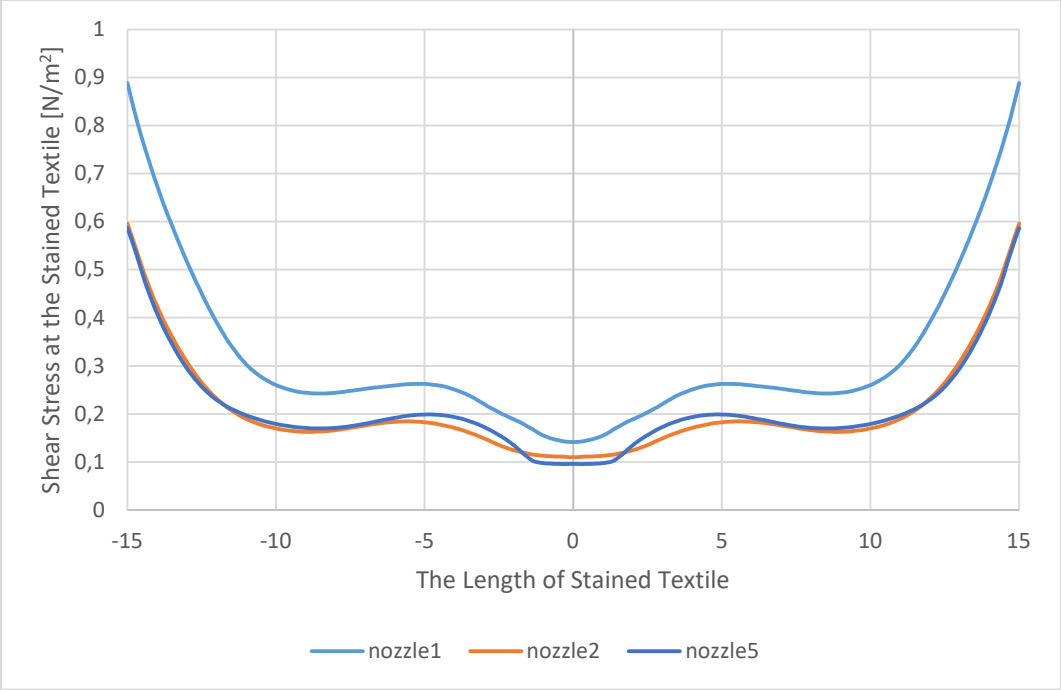


Figure 3.17 The Graph of Shear Stress Distribution Graph in One Full Oscillation for Nozzle1, Nozzle2 and Nozzle5 at Wall Defined as Stained Textile

In order to examine the effect of the w1/w0 ratio, the movement of water within the half period of the oscillating motion at instants of t/12, t/6, t/4, t/3, 5t/12 and t/2 for the numerical analysis and experimental study in Figure 3.18 toFigure 3.23.

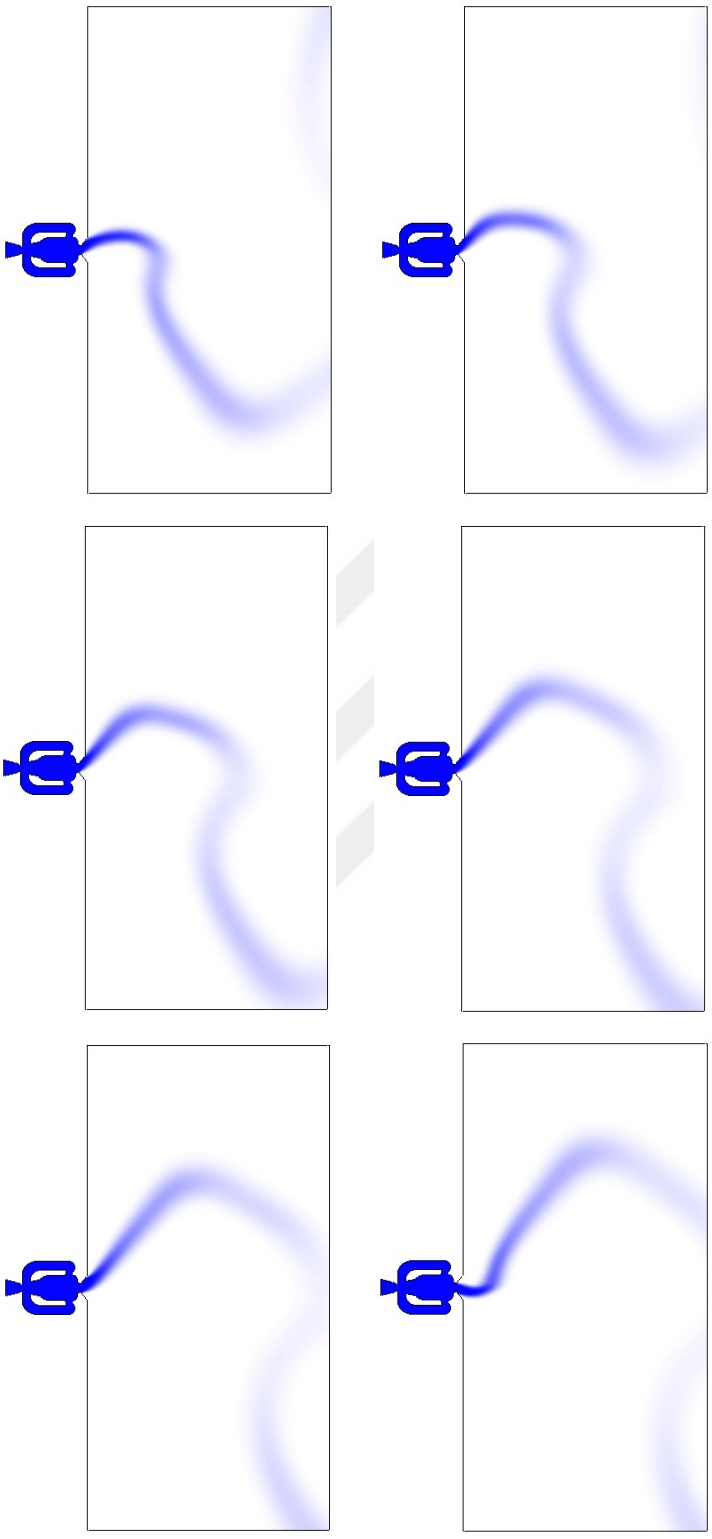


Figure 3.18 The Movement of Water in a Half of Oscillating Motion at t/12, t/6, t/4, t/3, 5t/12, and t/2 Instants at The Analysis for Nozzle1

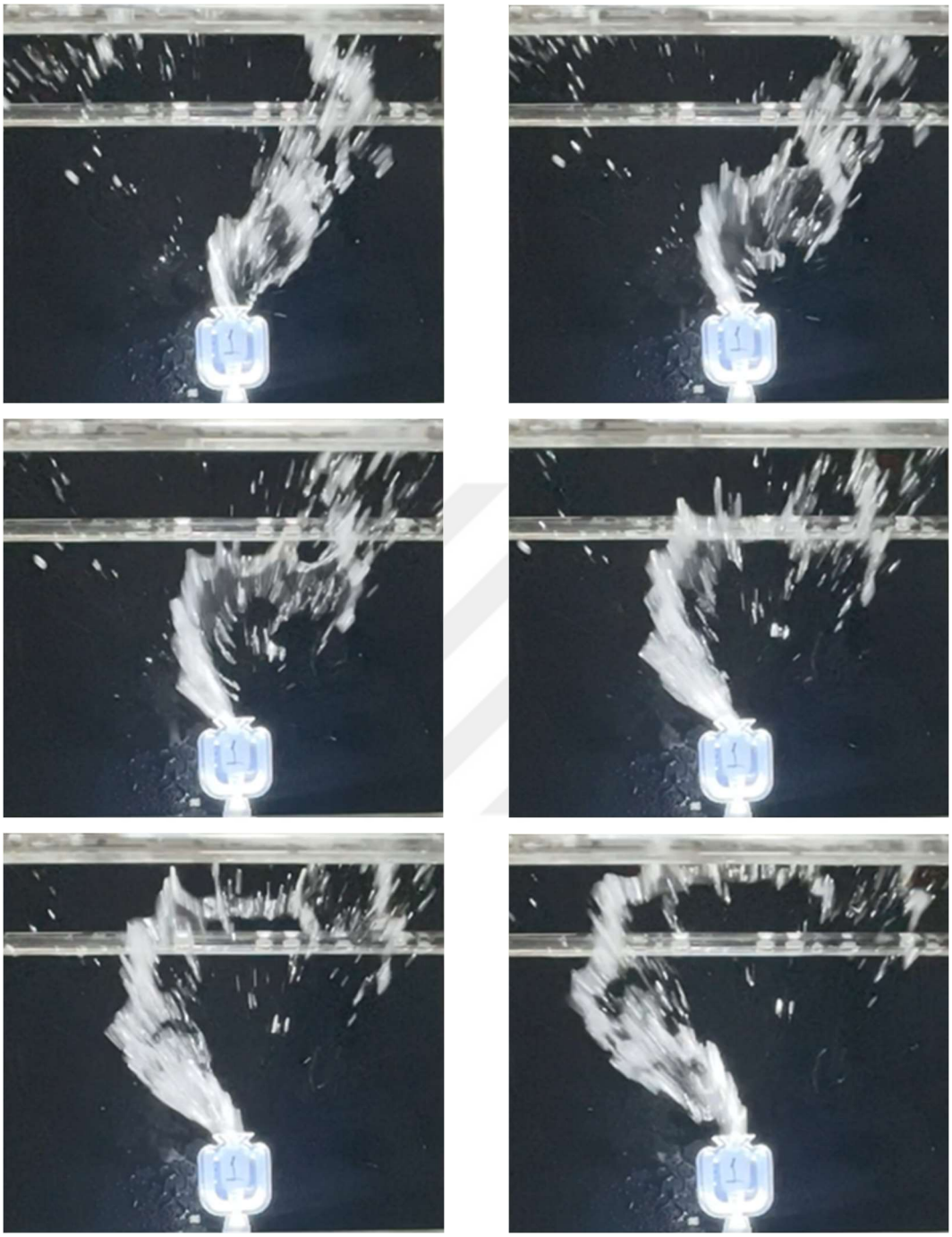


Figure 3.19 The Movement of Water in a Half of Oscillating Motion at t/12, t/6, t/4, t/3, 5t/12, and t/2 Instants at The Experimental Setup for Nozzle1

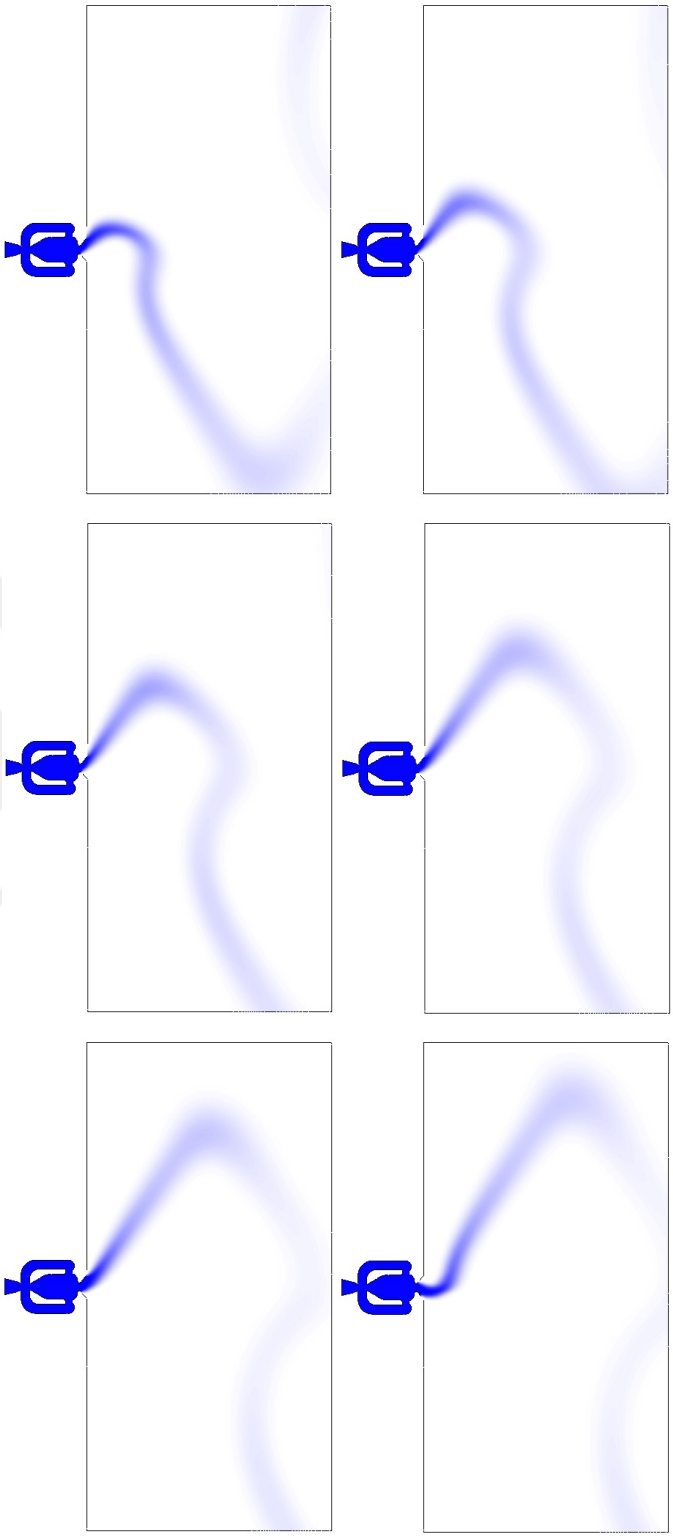


Figure 3.20 The Movement of Water in a Half of Oscillating Motion at t/12, t/6, t/4, t/3, 5t/12, and t/2 Instants at The Analysis for Nozzle2

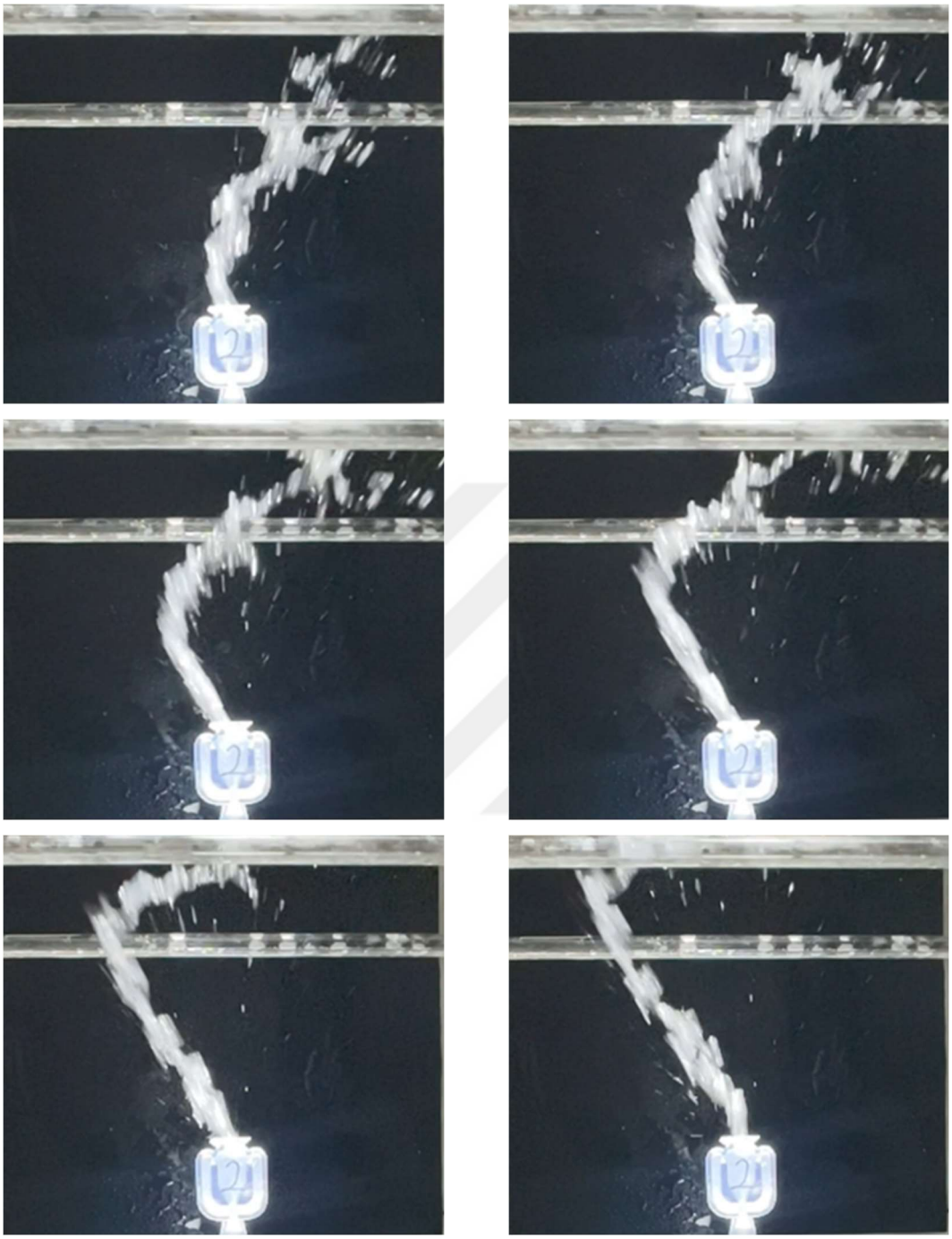


Figure 3.21 The Movement of Water in a Half of Oscillating Motion at t/12, t/6, t/4, t/3, 5t/12, and t/2 Instants at The Experimental Setup for Nozzle2

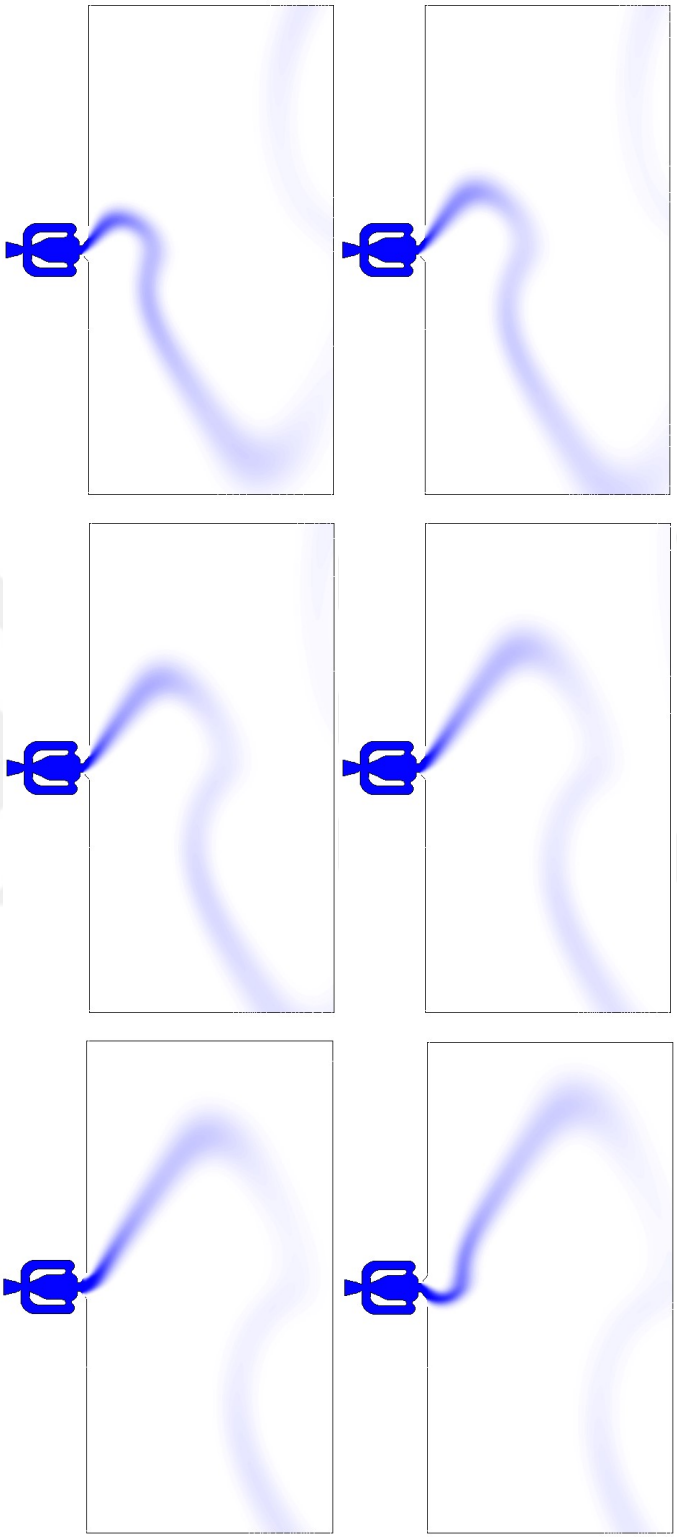


Figure 3.22 The Movement of Water in a Half of Oscillating Motion at t/12, t/6, t/4, t/3, 5t/12 and t/2 Instants at The Analysis for Nozzle5

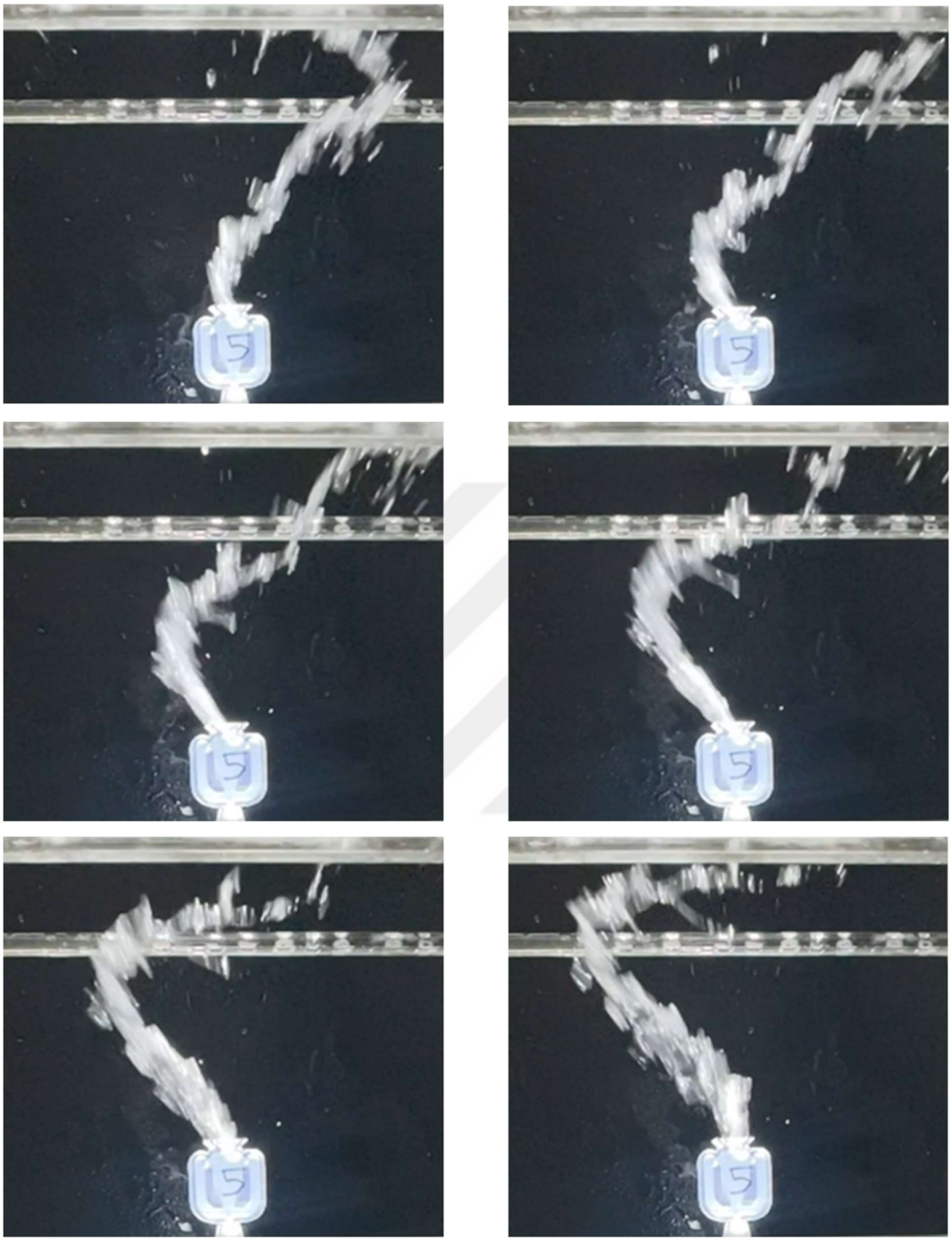


Figure 3.23 The Movement of Water in a Half of Oscillating Motion at t/12, t/6, t/4, t/3, 5t/12, and t/2 Instants at The Experimental Setup for Nozzle5

Finally, as shown in Table 3.3, the residence time of the water on the side wall at the nozzle exit and the total time spent at transition zone for all nozzles were compared in numerical studies. When the three nozzles are examined, it is seen that the results

of the experimental and analysis studies are in close agreement with each other. In addition, the higher peak in the nozzle1 velocity graph can be explained by the longer time spent in the transition. While the time spent by nozzle1 in transition is 38%, it is seen that is 30% in nozzle2 and 24% in nozzle5.

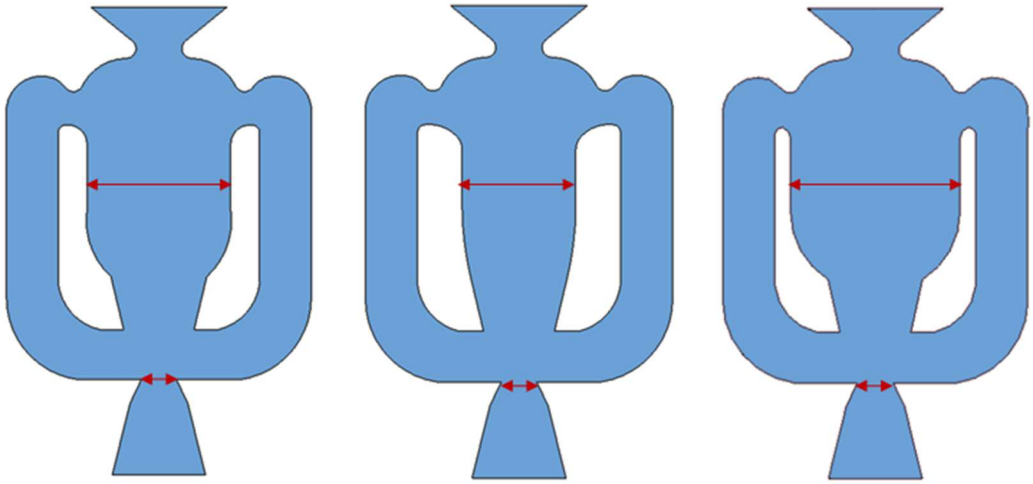
Table 3.3 The Contacting Time and The Transition Time of Nozzles for w1/w0 Parameter

Type of Nozzle	*Half of Total Duration of One Period of Oscillating*	*Time of Contacting the Wall of Water*	*Transition Time*
Nozzle1	0.064 s	62%	38%
Nozzle2	0.087 s	70%	30%
Nozzle5	0.062 s	76%	24%

3.6.2 w2/w0 Parameter

The w2/w0 ratio is determined as 4.06 in the reference nozzle design, because the ratios close to this value are usually given in the literature. In order to determine the optimum value of this ratio, numerical analyzes and tests were carried out when the ratio w2/w0 was 3.2 and 4.8.

Figure 3.24 displays the nozzle1, nozzle4, and nozzle7, which have w2/w0 ratios of 4.06, 3.2, and 4.8, respectively.



(a) (b) (c)

Figure 3.24 The Ratios of w2/w0 Parameter: (a) w2/w0 = 4.06, (b) w2/w0 = 3.2, (c) w2/w0 = 4.8

The first step was to examine the w2/w0 ratio's impact on the stain removal curves of nozzles 1, 4, and 7, which are displayed in Figure 3.25. The areas under the stain removal curve in the graph in Figure 3.25 are investigated, as well as their homogeneous distribution. Nozzle1 and nozzle7 showed similar stain removal plots, with peaks formed at similar angles. Although these nozzles are similar in terms of uniformity, the nozzle7 is more advantageous in terms of the area under the stain removal curve. In nozzle4 the oscillation feature starts to diminish so that it oscillates through a very small angle. The optimum solution was found in nozzle7, for which the w2/w0 ratio was 4.8.

The analysis studies were conducted in light of the results from the experimental studies in order to find the best solution for this parameter, and these analyses will be discussed in the following section.

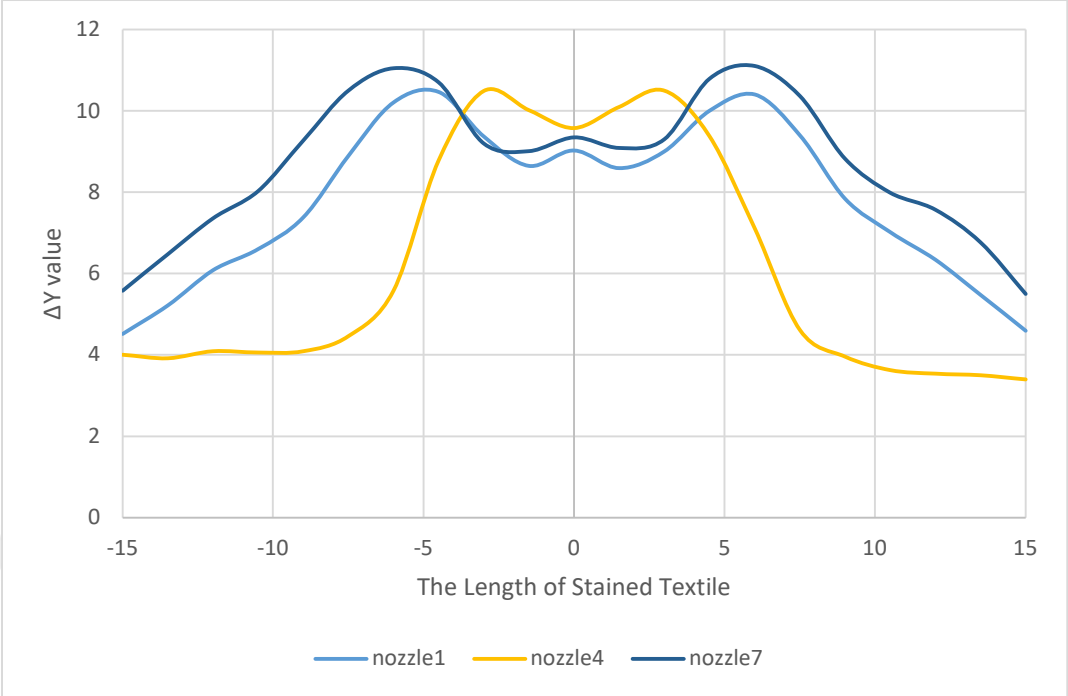


Figure 3.25 The Graph of Experimental Removal Stain Test Results of w2/w0 Parameter for Nozzle1, Nozzle4 and Nozzle7

During the analysis phase, a line was first drawn at the nozzle outlet, and graphs of velocity curves were plotted along this line for each nozzle. Figure 3.26 displays the variation of velocity for the nozzle1, nozzle4, and nozzle7. The peaks were seen to occur at a similar location on the nozzle1 and nozzle7 velocity curves. On the other hand, there is a single high peak at the midpoint on the velocity curve of nozzle4, and the total area under it is less than the ones in the other nozzles. Although the velocity graphs of nozzle1 and nozzle7 are similar, the area under the velocity curve of nozzle7 is the largest.

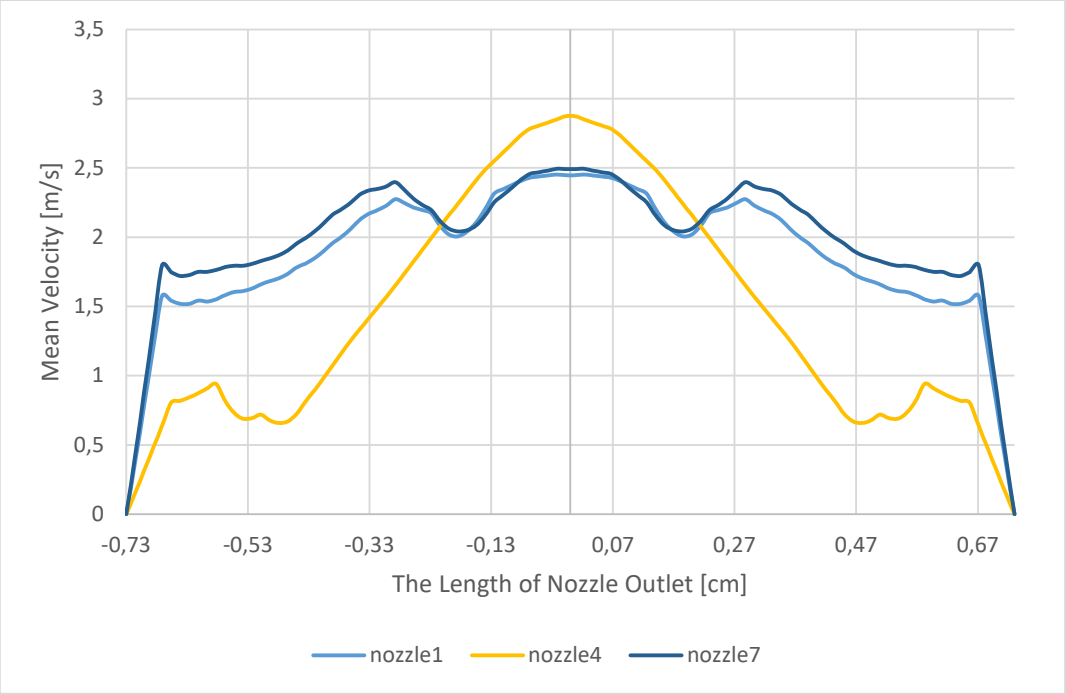


Figure 3.26 The Graph of Mean Velocity Distribution Graph in One Full Oscillation for Nozzle1, Nozzle4 and Nozzle7 at Nozzle Outlet

The moment and location at which the ratio of the velocity in the y axis to the velocity in the x axis is highest at the nozzle exit was identified in order to better understand the cause of this behavior on the velocity graph and how to remove the stain. Table 3.4 displays the maximum velocities for each nozzle as well as these rates from the analyzes. The table shows that nozzles 1 and 7 can reach a wider angle at a similar angle. The difference in the velocity graph is explained by the fact that maximum angle of nozzle4 is so much smaller.

Table 3.4 The Maximum Angle of Nozzles for w2/w0 Parameter

Type of Nozzle	*Maximum Velocity in the y direction*	*The Velocity in the x direction at this time & point*	*Angle of The Velocity*
Nozzle1	2.07 m/s	2.02 m/s	45.7
Nozzle4	0.81 m/s	2.87 m/s	15.6
Nozzle7	2.22 m/s	2.00 m/s	47.9

There is a difference between the velocity curves in the numerical studies and the stain removal graphs in the experimental study. The peaks that were formed in the middle region of the velocity curves were not observed in the stain removal curves. The difference can be explained by shear stress. Stain removal behavior is also directly affected by shear stress since water does not pass through the textile. Shear stress plots are shown in Figure 3.27 for nozzle1, nozzle4, and nozzle7. In Nozzle4, the shear stress is much higher than the shear stress of other nozzles. Based on these results, when a homogeneous distribution is not obtained in the velocity graph or if a single large peak occurs in the middle, then the shear stress values are quite high. However, it has been decided that the velocity graph is a much more effective approach since the total amount of stain removal in nozzle4 is minimum. On the wall defined for stained textile, the shear stress values of nozzle4 decrease towards the ends of the wall, while the shear stresses of nozzle1 and nozzle7 increase. The reason for this is that the water is directed towards the midpoint region in nozzle4.

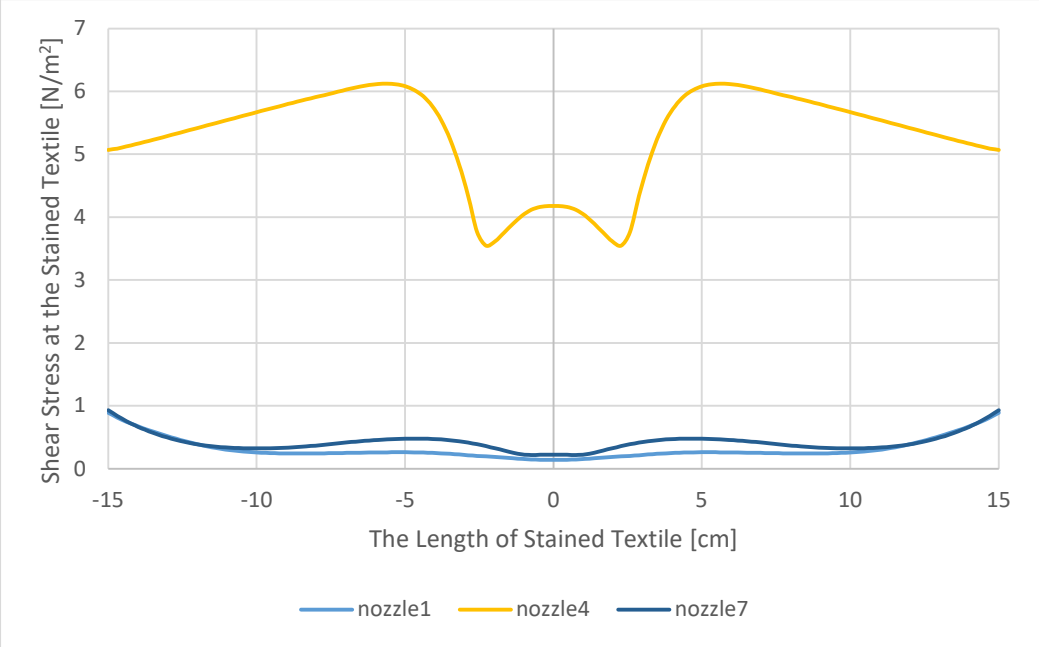


Figure 3.27 The Graph of Shear Stress Distribution Graph in One Full Oscillation for Nozzle1, Nozzle4 and Nozzle7 at Wall Defined as Stained Textile

Nozzle1 and nozzle7 shear stresses are also examined in Figure 3.28. Shear stress is higher in nozzle7, similar to the velocity graph, but the difference in shear stress results is greater. Considering the stain removal curve graph, it is a more accurate approach to look at the velocity curve again. However, the reason for the peak not appearing in the middle of the stain removal graph is the shear stress.

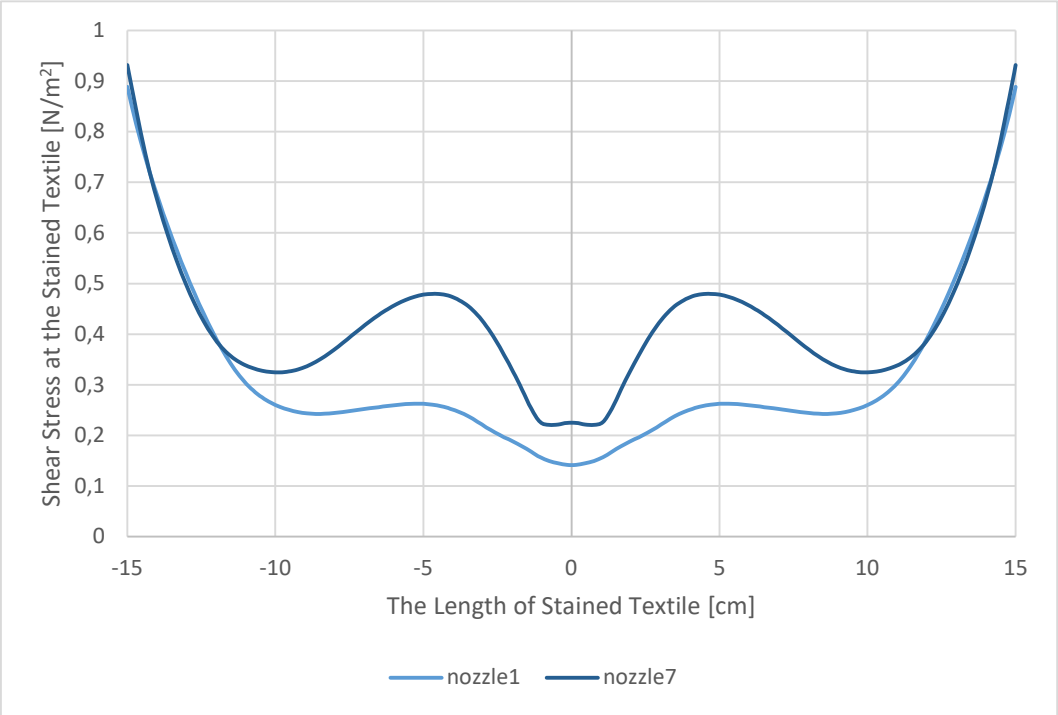


Figure 3.28 The Graph of Shear Stress Distribution Graph in One Full Oscillation in Detail for Nozzle1 and Nozzle7 at Wall Defined as Stained Textile

In order to examine the effect of the w2/w0 ratio, the movement of water within the half period of the oscillating motion at instants of t/12, t/6, t/4, t/3, 5t/12 and t/2 for the numerical analysis and experimental study in Figure 3.29 to Figure 3.32.

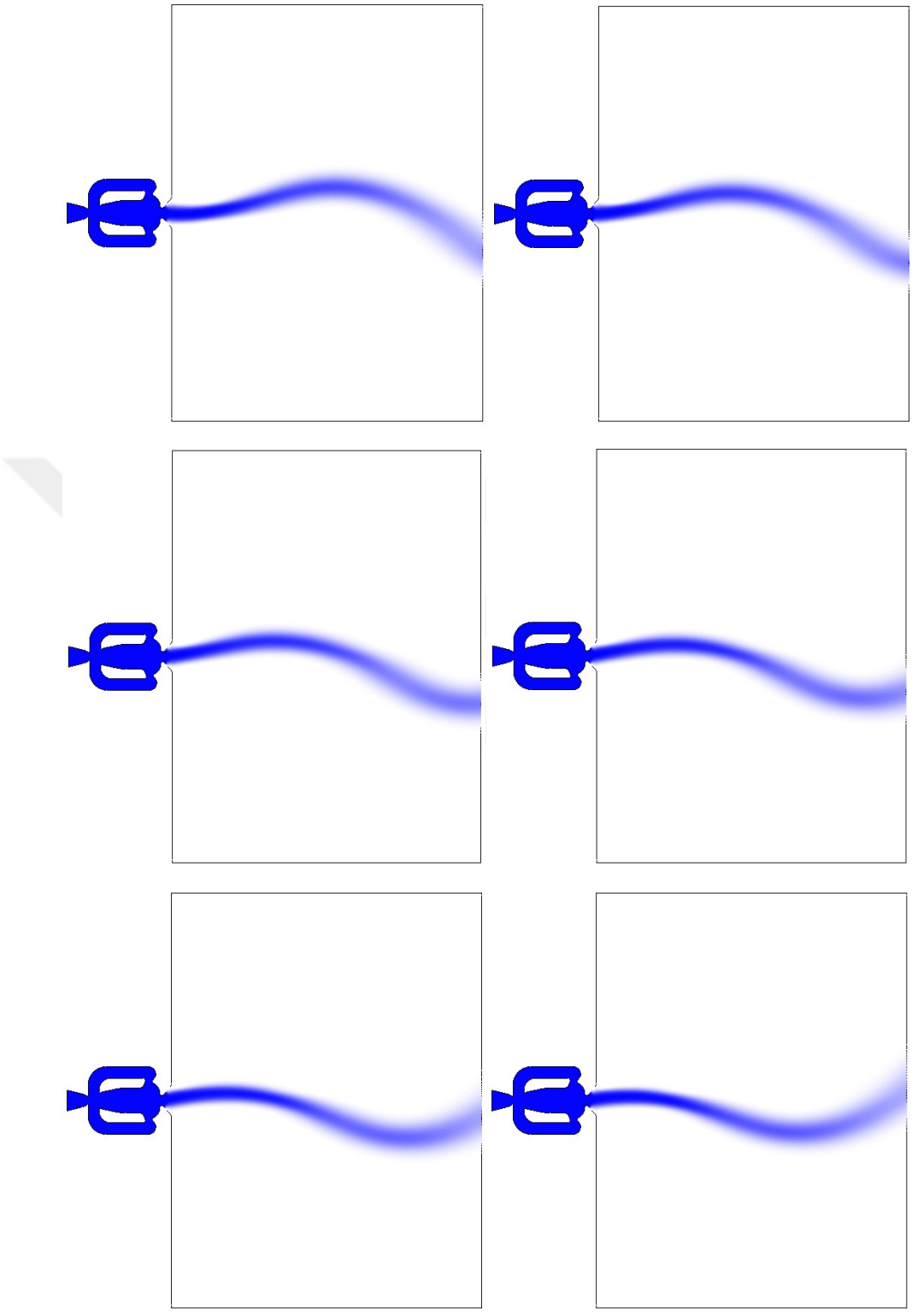


Figure 3.29 The Movement of Water in a Half of Oscillating Motion at t/12, t/6, t/4, t/3, 5t/12, and t/2 Instants at The Analysis for Nozzle4

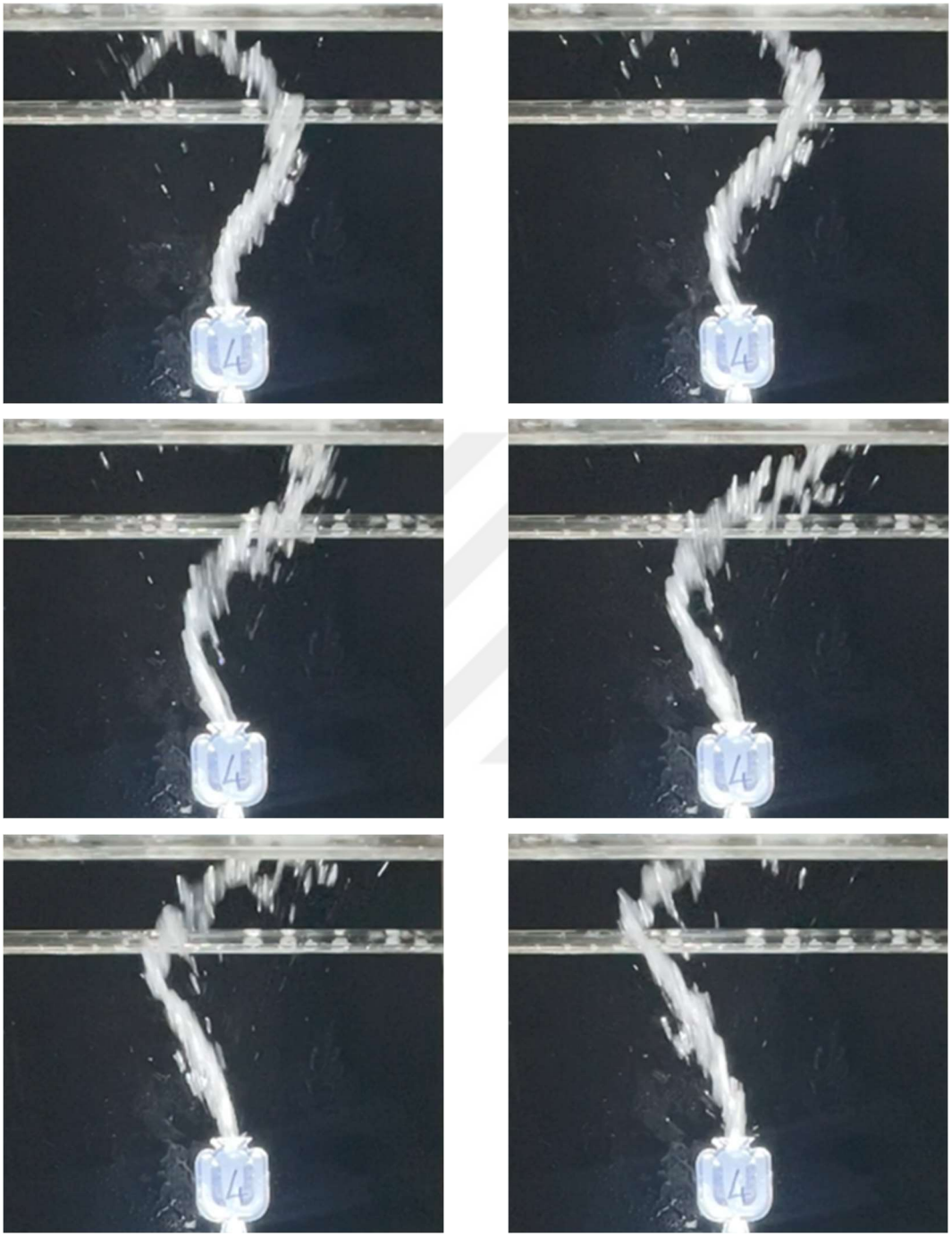


Figure 3.30 The Movement of Water in a Half of Oscillating Motion at t/12, t/6, t/4, t/3, 5t/12, and t/2 Instants at The Experimental Setup for Nozzle4

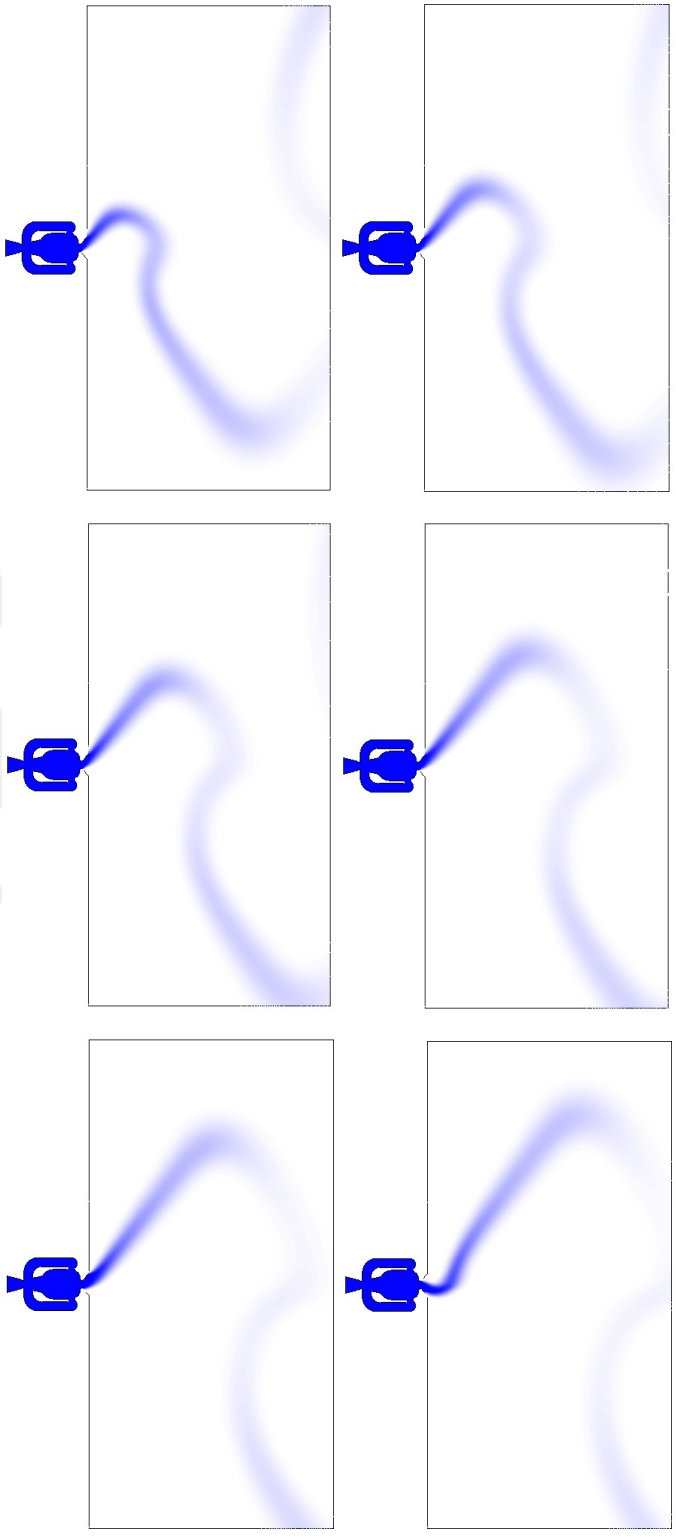


Figure 3.31 The Movement of Water in a Half of Oscillating Motion at t/12, t/6, t/4, t/3, 5t/12, and t/2 Instants at The Analysis for Nozzle7

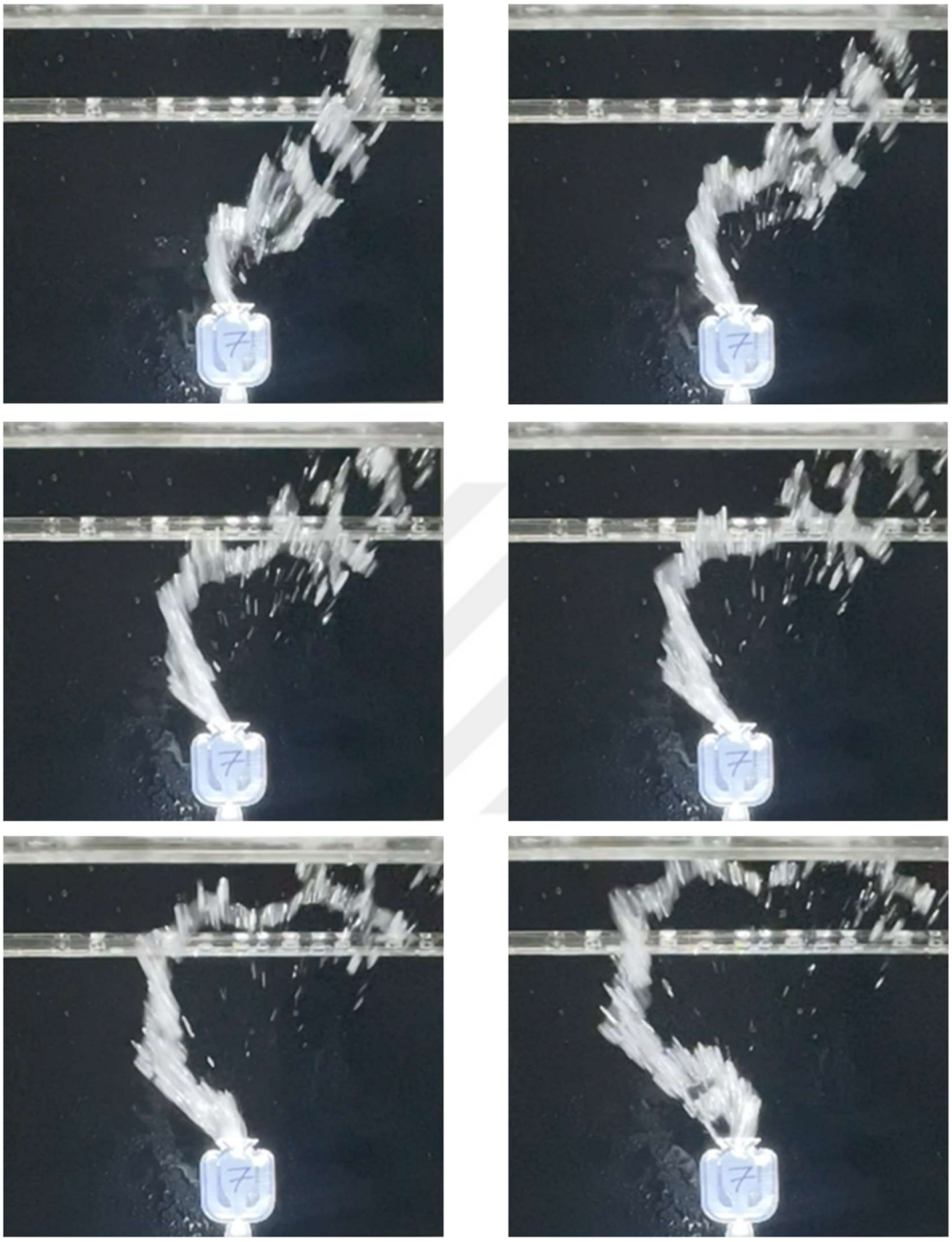


Figure 3.32 The Movement of Water in a Half of Oscillating Motion at t/12, t/6, t/4, t/3, 5t/12, and t/2 Instants at The Experimental Setup for Nozzle7

In Table 3.5, the residence time of the water on the side wall at the nozzle exit and the total time spent at transition zone in all nozzles were compared in the experimental and analysis studies. When the three nozzles are examined, it is seen

that the results of the experimental and analysis studies are in close agreement with each other. While the peak at the midpoint of the nozzle1 velocity curve is approximately the same as the peak in the nozzle7 velocity curve, the two peaks on the sides are lower, because the time spent in the transition for nozzle1 is 38% of the total time, while this value is 33% in nozzle7.

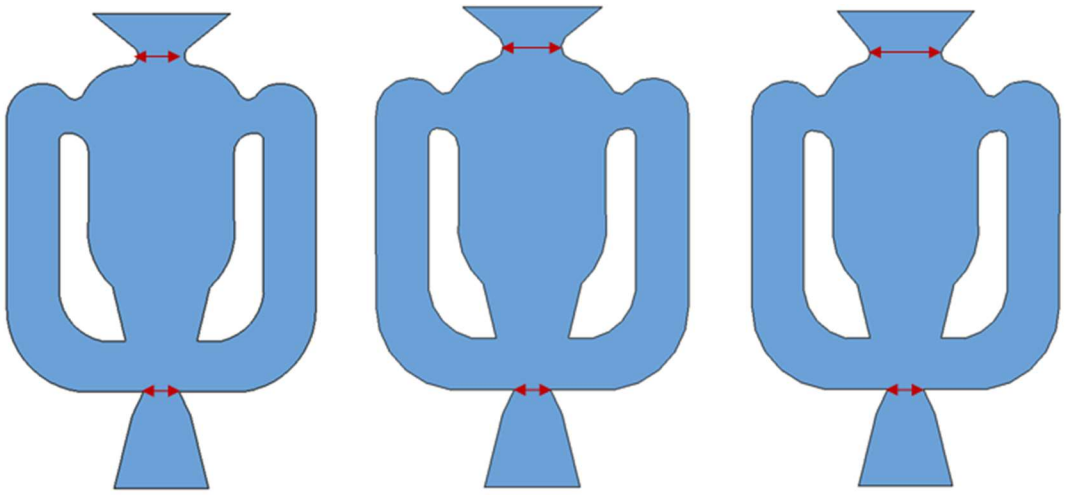
Table 3.5 The Contacting Time and The Transition Time of Nozzles for w2/w0 Parameter

Type of Nozzle	*Half of Total Duration of One Period of Oscillating*	*Time of Contacting the Wall of Water*	*Transition Time*
Nozzle1	0.064 s	62%	38%
Nozzle4	0.055 s	0	100%
Nozzle7	0.064 s	67%	33%

3.6.3 w3/w0 Parameter

The w3/w0 ratio is determined as 1.3 for the reference nozzle design, because the ratios close to this value are usually given in the literature. In order to determine the optimum value of this ratio, numerical analyzes and tests were carried out when the ratio w3/w0 was 1.6 and 2.0.

Nozzles, which are nozzle1, nozzle6, and nozzle3, with w3/w0 ratios of 1.3, 1.6, and 2.0, respectively, are shown in Figure 3.33.



(a) (b) (c)

Figure 3.33 The Ratios of w3/w0 Parameter: (a) w3/w0 = 1.3, (b) w3/w0 = 1.6, (c) w3/w0 = 2.0

Figure 3.34 presents the stain removal curves for nozzles 1, 3, and 6 that were obtained to investigate the impact of the w3/w0 ratio. The areas under the stain removal curve are examined to determine the homogeneity and whether they are homogeneously distributed are examined. Although the best homogeneous distribution was obtained for Nozzle6, this nozzle has a lower stain removal amount than the result of nozzle1. Nozzle3, on the other hand, does not always show a stable oscillating motion when tested experimentally. It has been observed that this nozzle does not oscillating for most of the times and when it starts to oscillate at certain times, it loses this oscillation after a while. Depending on this situation, the mass flow rate or inlet velocity changes. Therefore, 2.0 seems to be the upper limit for w3/w0. When the stain removal graph is examined, it is seen that it creates a peak at a single point, and therefore the area under the curve is minimum. The tests with different values of w3/w0 ratio indicated, that the variation of this ratio causes very different results. In summary, as a result of the tests, nozzle1 was found to be the most effective of the three nozzles, although it was not the most homogeneous distribution. In order to find the best solution for this parameter, the analysis studies were carried out in the light of the information obtained from the experimental studies and these analyzes will be examined in the next section.

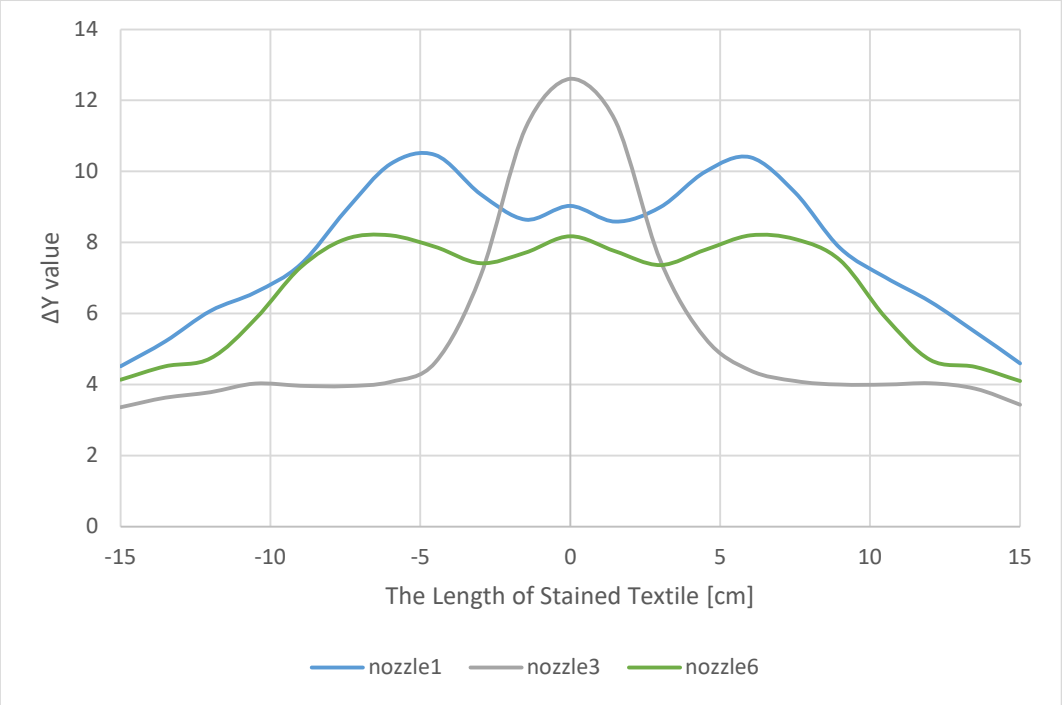


Figure 3.34 The Graph of Experimental Removal Stain Test Results of w3/w0 Parameter for Nozzle1, Nozzle3 and Nozzle6

In the analysis phase, first, a line was determined at the nozzle outlet and velocity distributions were plotted along this line for each nozzle. Velocity graphs for nozzle1, nozzle3, and nozzle6 are shown in Figure 3.35. Three peaks, which were close to each other, were observed in the velocity distribution for nozzle1. Nozzle6 created three peaks far apart, however the maximum values of the side peaks are smaller than the middle one. When this graph and the stain removal graph in the experimental tests are examined, it is seen that the distribution behavior of nozzle6 causes a homogeneous oscillation but lower washing results. The velocity distribution in nozzle3 has a large peak in the middle, while the magnitude of the peaks on the two sides are small and do not affect the flow in the y-direction. When the areas under the velocity graphs are analyzed, the area under the velocity curve of nozzle1 has a larger value than the ones for the other two nozzles.

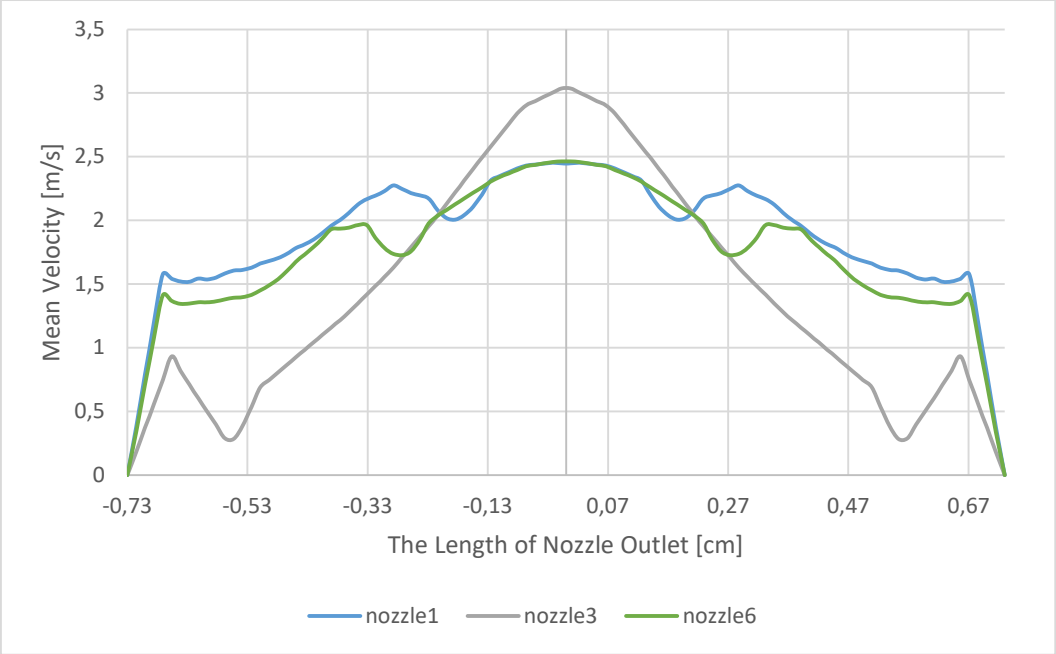


Figure 3.35 The Graph of Mean Velocity Distribution Graph in One Full Oscillation for Nozzle1, Nozzle3 and Nozzle6 at Nozzle Outlet

In order to understand the reason for this behavior on the velocity graph and to understand how to remove the stain more, the moment and location at which the ratio of the velocity in the y direction to the velocity in the x direction is the maximum at the nozzle exit was determined. For each nozzle, the maximum velocities, and the corresponding velocity at the same time and location are presented in Table 3.6. This table indicates that, nozzle3 has a flow pattern which do not create oscillations. The maximum velocity in the y-direction for nozzle6 is less than the maximum velocity in the y-direction for nozzle1. Although the angles formed are similar, there is a difference between the velocity curves due to the low velocities' values in nozzle6.

Table 3.6 The Maximum Angle of Nozzles for w1/w0 Parameter

Type of Nozzle	*Maximum Velocity in the y direction*	*The Velocity on the x direction at this time & at the same point*	*Angle of The Velocity*
Nozzle1	2.07 m/s	2.02 m/s	45.7
Nozzle3	0 m/s	3.07 m/s	0
Nozzle6	1.86 m/s	1.90 m/s	44.39

There is a difference between the velocity curves in the numerical analyses and the stain removal graphs in the experimental study. The peaks formed in the middle of the velocity graph were not formed in the stain removal curves. The difference can be explained by shear stress. Stain removal behavior is also directly affected by shear stress since water does not pass through the textile. Shear stress plots are shown in Figure 3.36 for nozzle1, nozzle3, and nozzle6. The shear stress in nozzle6 is much higher than the shear stress of the other nozzles similar to the nozzle4 in the previous shear stress graph. As seen in nozzle4, although the shear stress values were very high in the nozzle6, the stain removal effect was only seen at the midpoint. In the velocity graphs, the shear stress of the nozzles that form a single peak at the midpoint is high, and this information does not have an effect on stain removal.

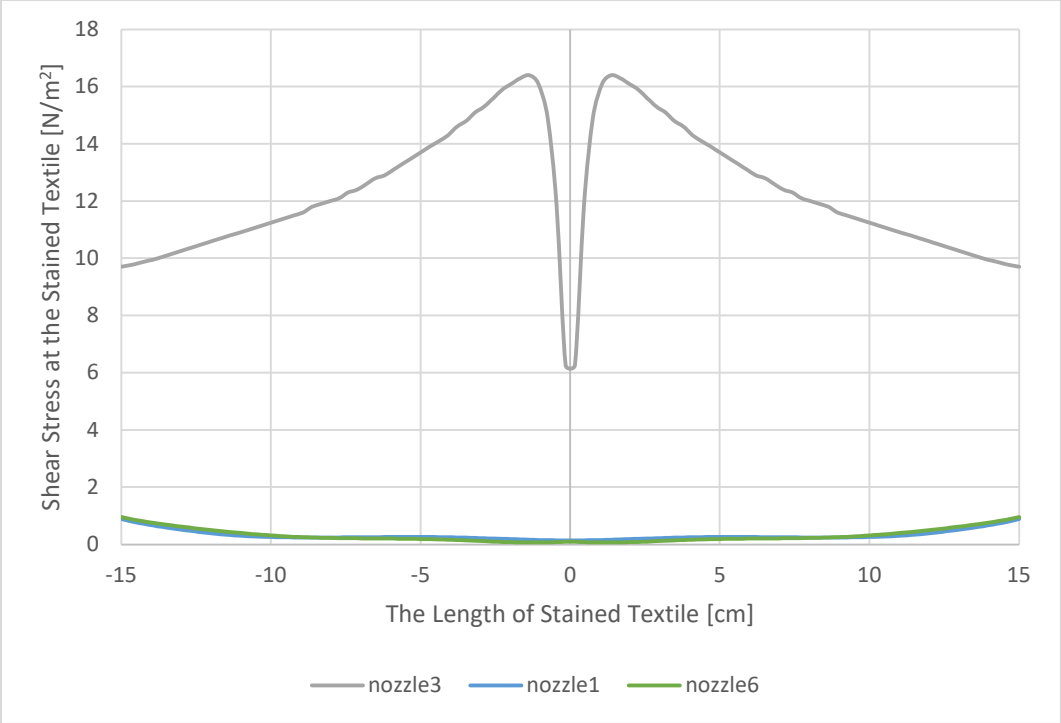


Figure 3.36 The Graph of Shear Stress Distribution Graph in One Full Oscillation for Nozzle1, Nozzle3 and Nozzle6 at Wall Defined as Stained Textile

The shear stress distributions in nozzle1 and nozzle6 are re-examined in Figure 3.37. Although the nozzle6 shear stress curve rises locally at the midpoint, it tends to decrease towards the middle. This graph is also the reason why the high velocity at the midpoint has less effect on the stain removal.

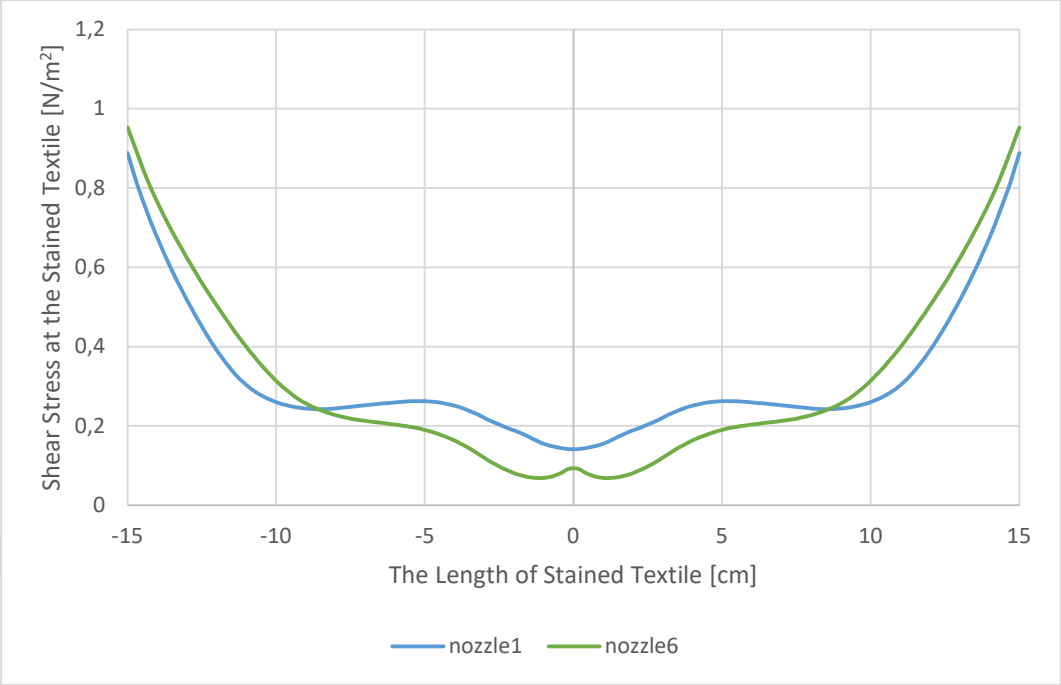


Figure 3.37 The Graph of Shear Stress Distribution Graph in One Full Oscillation in Detail for Nozzle1 and Nozzle6 at Wall Defined as Stained Textile

In order to examine the effect of the w3/w0 ratio, the movement of water within the half period of oscillating motion at instants of t/12, t/6, t/4, t/3, 5t/12 and t/2 for the numerical analysis and experimental study in from Figure 3.38 Figure 3.41.

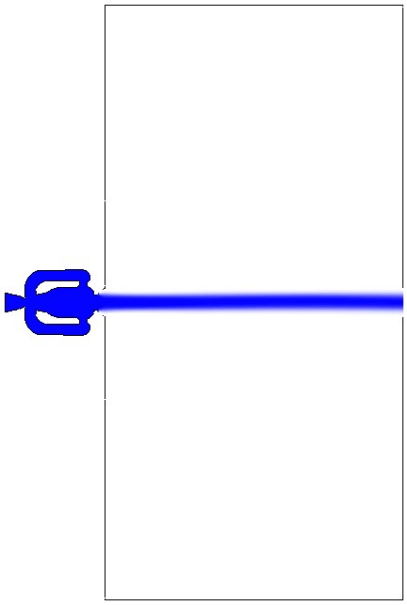


Figure 3.38 The Movement of Water in A Half of Oscillating Motion at The Analysis for Nozzle3

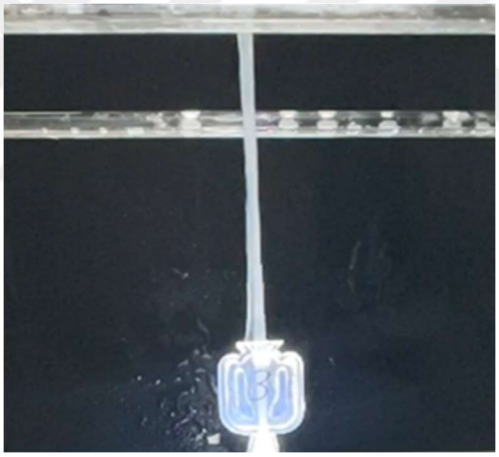


Figure 3.39 The Movement of Water in A Half of Oscillating Motion at The Experimental Setup for Nozzle3

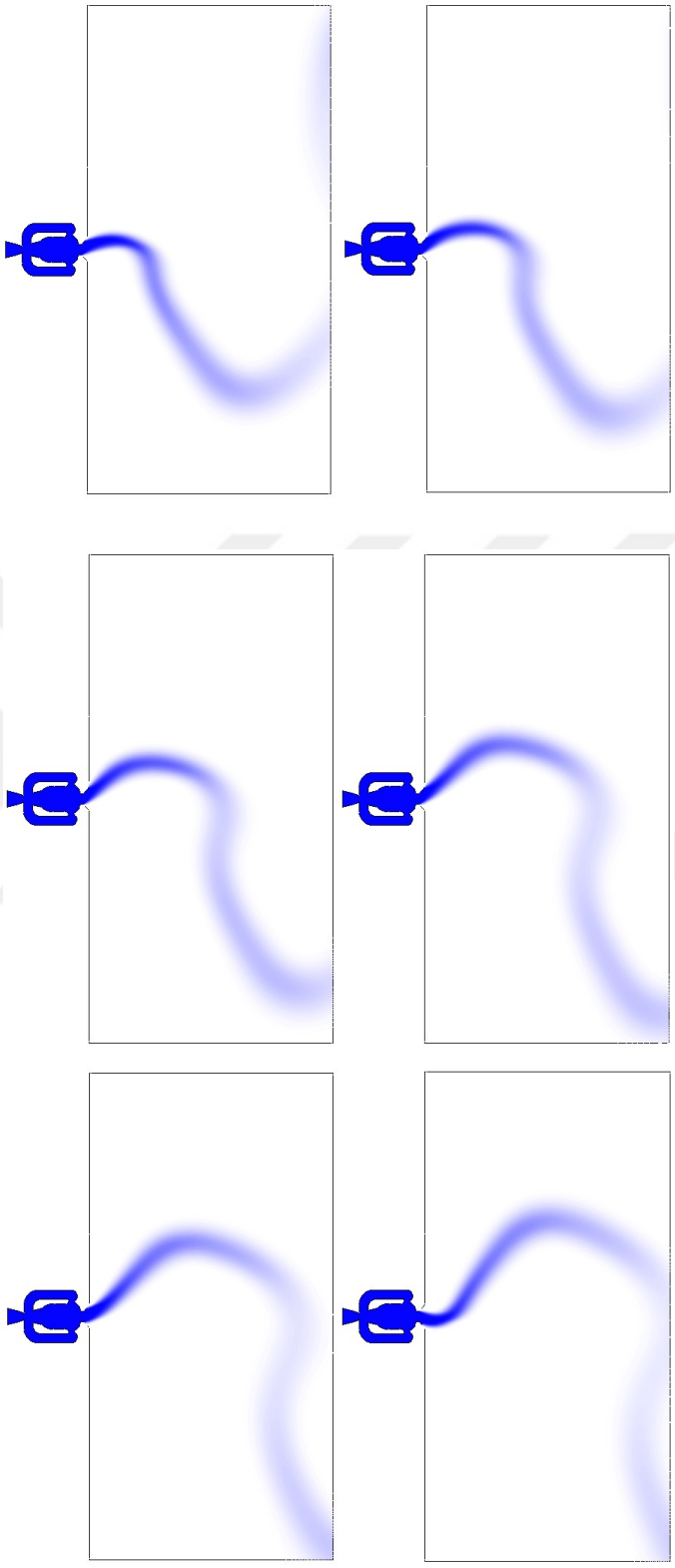


Figure 3.40 The Movement of Water in a Half of Oscillating Motion at t/12, t/6, t/4, t/3, 5t/12 and t/2 Instants at The Analysis for Nozzle6

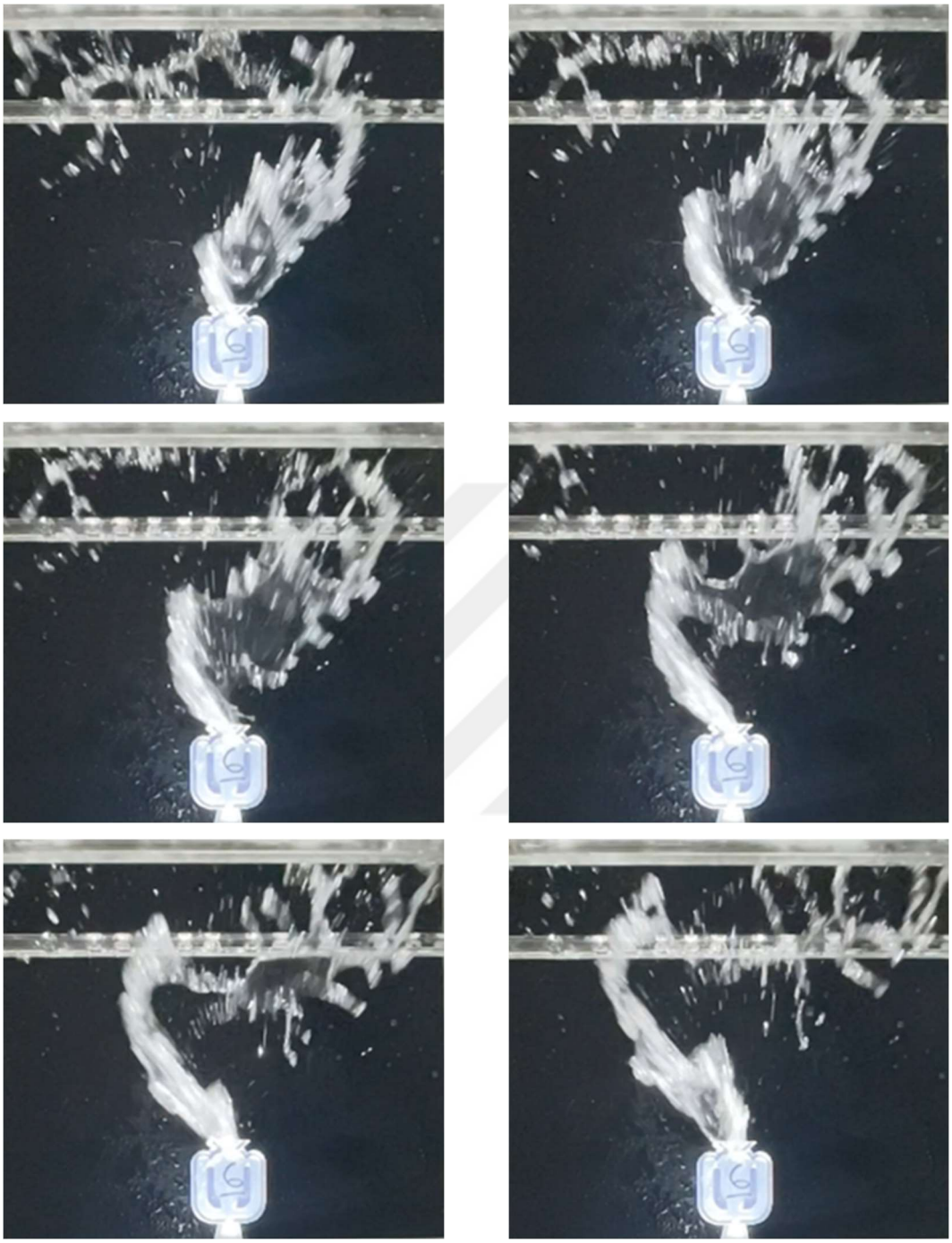


Figure 3.41 The Movement of Water in a Half of Oscillating Motion at t/12, t/6, t/4, t/3, 5t/12, and t/2 Instants at The Experimental Setup for Nozzle6

Finally, as shown in Table 3.7, the residence time of the water on the side wall at the nozzle exit and the total time spent at transition zone in all nozzles were compared in the experimental and numerical studies. When the three nozzles are examined, it

is seen that the results of the experimental and analysis studies have close agreement with each other. While the time spent by nozzle1 in transition is 38%, it is seen that it is 40% in nozzle6.

Table 3.7 The Contacting Time and The Transition Time of Nozzles for w3/w0 Parameter

Type of Nozzle	*Half of Total Duration of One Period of Oscillating*	*Time of Contacting the Wall of Water*	*Transition Time*
Nozzle1	0.064 s	62%	38%
Nozzle3	0.0 s	0	No sweeping
Nozzle6	0.062 s	60%	40%

3.7 Comparison of Fluidic Oscillator Nozzle and Original Nozzle

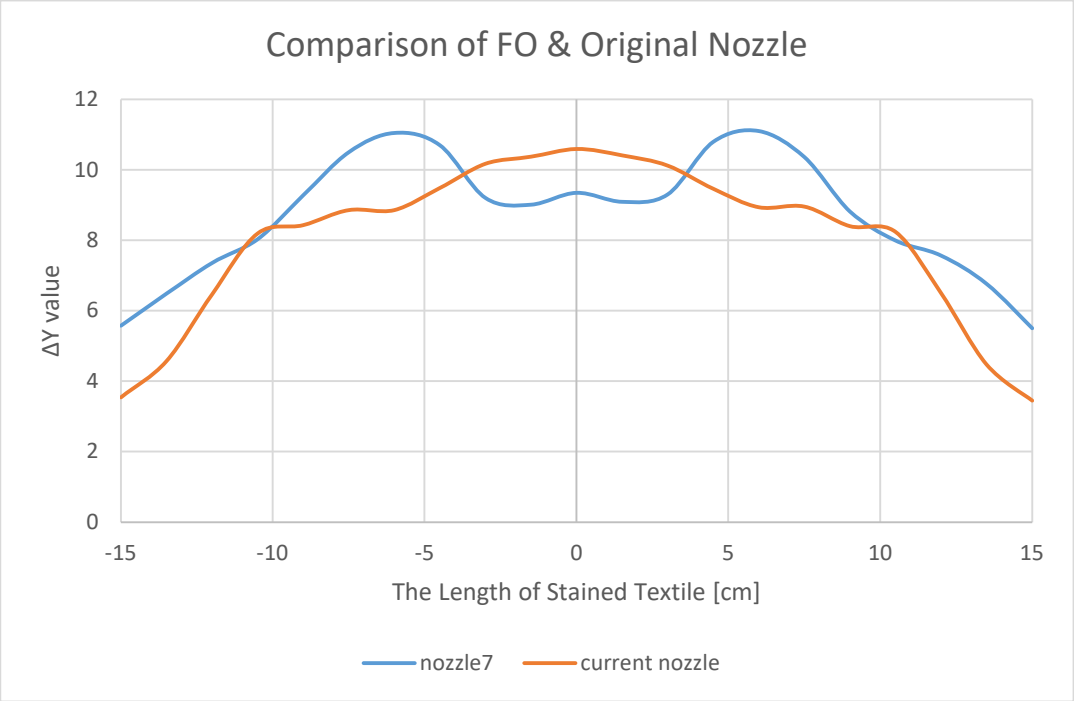


Figure 3.42 Comparison of Fluidic Oscillator Nozzle and Original Nozzle

In the experimental results, the stain removal graphics of the nozzle7, which is the best nozzle in terms of homogeneity and the area under the curve, and the existing nozzle used in the washing machine product, as a result of the experimental studies, are shown in Figure 3.42. It is seen that nozzle7 is better than the original nozzle design in terms of homogeneity and area under the curve. Area under the curve is specific definition for understanding the removing stain capacity, area values under the curve of these nozzles are shown in Table 3.8.

Table 3.8 Comparison of Area Under the Curve for FO & Current Nozzle

Type of Nozzle	*Area Under the Curve [ΔY value x cm]*
Nozzle7	267
Current Nozzle	247

3.8 **Oscillation Frequency Validation**

In the previous titles, transiton time results in analysis results have been examined in detail for each nozzle. In experimental studies, the fps of the camera is 480 fps. The oscillation times in the analysis results are compared with the experimental studies and evaluated for the validation of the test results. The difference between the oscillation times of analysis studies and experimental studies shown in Table 3.9 is less than 5%.

Table 3.9 Validation of Oscillation Time of Analysis and Experimental Results

Type of Nozzle	*Oscillation Time of Analysis Results*	*Oscillation Time of Experimental Results*	*Error Percentage*
Nozzle1	0.128 s	0.128 s	0.2%
Nozzle2	0.174 s	0.171 s	-1.9%
Nozzle3	0.0 s	0.0 s	0%
Nozzle4	0.11 s	0.112 s	1.8%
Nozzle5	0.124 s	0.128 s	3.2%
Nozzle6	0.124 s	0.117 s	-4.8%
Nozzle7	0.128 s	0.133 s	4.4%

CHAPTER 4

ANALYZES OF NOZZLES FOR OPTIMUM DESIGNS WITH THE NEW METHOD

In the previous chapter, it was explained in detail how to find the best nozzle with a CFD analysis for stain removing. As a result of these studies, it was determined that the average velocity graph obtained for a full oscillation at the nozzle outlet was the most effective graph to evaluate stain removal. In order to understand what the velocity graph depends on, the maximum velocity at the nozzle outlet at a particular moment and at a particular point in the y-direction was examined. In addition, the time spent with contact on the side walls at the nozzle outlet during an oscillation and the times elapsed in oscillation were compared for numerical and experimental studies. Finally, the stained textile area was defined as the wall and the shear stress graphs on the wall were analyzed. Shear stresses were used to explain why the stain removal graph was not similar to the velocity graph.

The best nozzle design was determined for each parameter determined. With these observations, the amount of stain removal and uniform stain removal are the two important outputs in optimal nozzle operation. Both outputs are obtained with the information mentioned above.

The numerical and experimental results for the best nozzle solution for each of the w1/w0, w2/w0, and w3/w0 ratio parameters examined in the previous section will be examined under this title. In addition, the results of the w4/w0 ratio were evaluated in the light of the information obtained from the previous section in order to examine the effect of the backflow channels, which are also seen in the literature. In this section, in order to understand the stain removal characteristics of each parameter with the results obtained in the analysis, these ratios within the structural limits were determined and the outputs were obtained. The total area under the

average velocity curves and homogeneous distribution trends at the nozzle outlet were plotted depending on the variation of the parametric ratio. Therefore, the best solution was found by examining these curves.

The selected nozzles were produced, and validation tests were carried out in the experimental setup. Evaluation of test results and comparison with analysis results will be done in the next section.

4.1 The Optimum Nozzle Design for w1/w0 Parameter

In the studies of w1/w0 ratio, the ratios of 1.0, 1.5 and 2.0 were determined in the previous section and analyzed, and their effects were examined in detail with experimental studies. In the literature, it was stated that when this ratio exceeds 2.0, the oscillatory behavior of the flow diminishes. The ratio w1/w0 = 1.0 was determined as the lower limit, assuming that the flow would encounter a sudden obstacle.

The behavior of the nozzle, when w1/w0 ratio is above 2.0, is also examined and compared with that of the nozzles with previously chosen ratios in Figure 4.1.

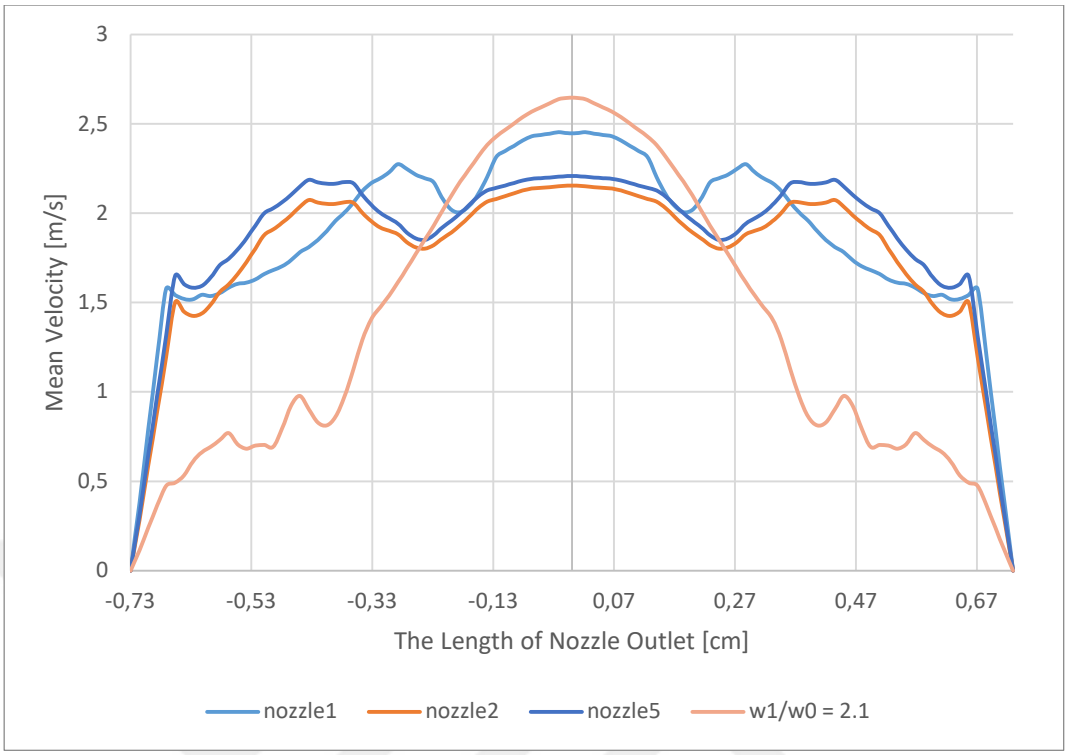


Figure 4.1 The Graph of Mean Velocity Distribution Graph in One Full Oscillation for Nozzle1, Nozzle2, Nozzle5 and w1/w0 = 2.1 Design at Nozzle Outlet

In line with the studies carried out, the ratios w1/w0 = 1 and w1/w0 = 2.6 were taken as the lower and upper limits and flow rate curves for all of these ratios are shown in Figure 4.2. Only w1/w0 = 2.1 nozzle result is shown on the curve because there is no oscillating for more than ratio of w1/w0 = 2.0.

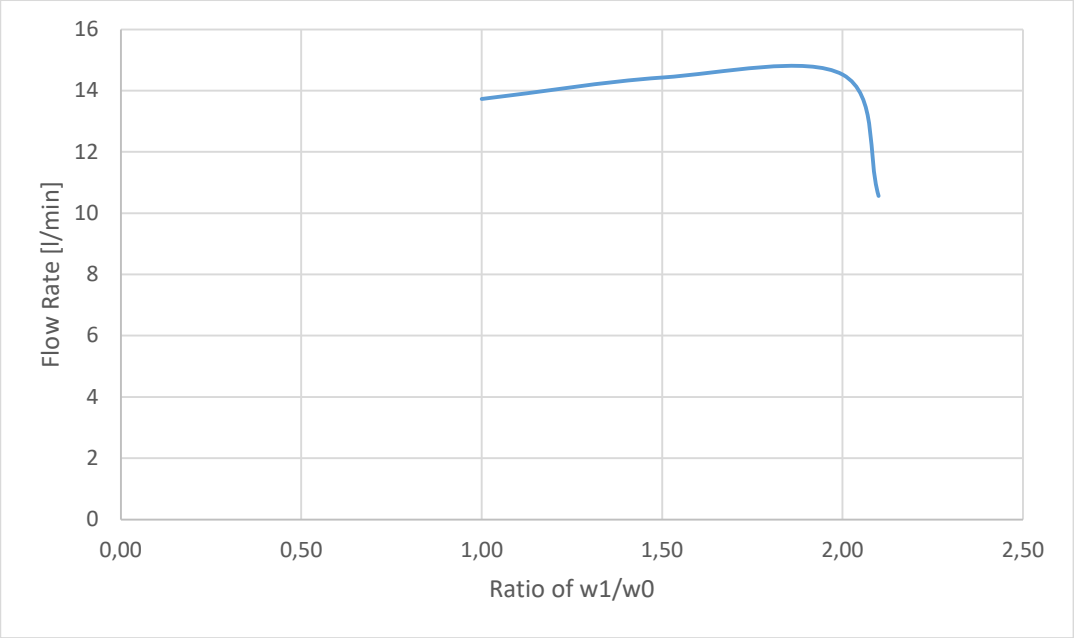


Figure 4.2 The Graph of Flow Rate Depending on Changing Ratio of w1/w0 Parameter

The curve of flow rate due to the w1/w0 ratio change, a linear increase up to the value of 2.0 is observed, then it suddenly decreases and reaches a certain lower value. Considering this graph, the situation where the w1/w0 ratio is 2 seems to be the best solution.

As the second evaluation criteria, the homogeneity of the velocity distribution is examined change in the w1/w0 ratio. For this step, an approximation method was determined by evaluating the values at which the peaks occur in the average velocity graphs, the differences in the middle peak and the peaks on the sides, and finally the shear stress graphs. This approach was determined by examining the distance of the side peaks from the midpoint and the maximum value of the peak formed at the midpoint in the velocity graphs. Flows that do not oscillate and focus on a single point. Therefore, they can be evaluated as the worst distribution when homogeneity is concerned. As a result of these approaches, the homogeneous distribution of the values between 1.0 and 2.6 in the w1/w0 ratio is shown in Figure 4.3. In these distributions, as mentioned before, the oscillation decreases abruptly at ratio of w1/w0 exceeds 2.0.

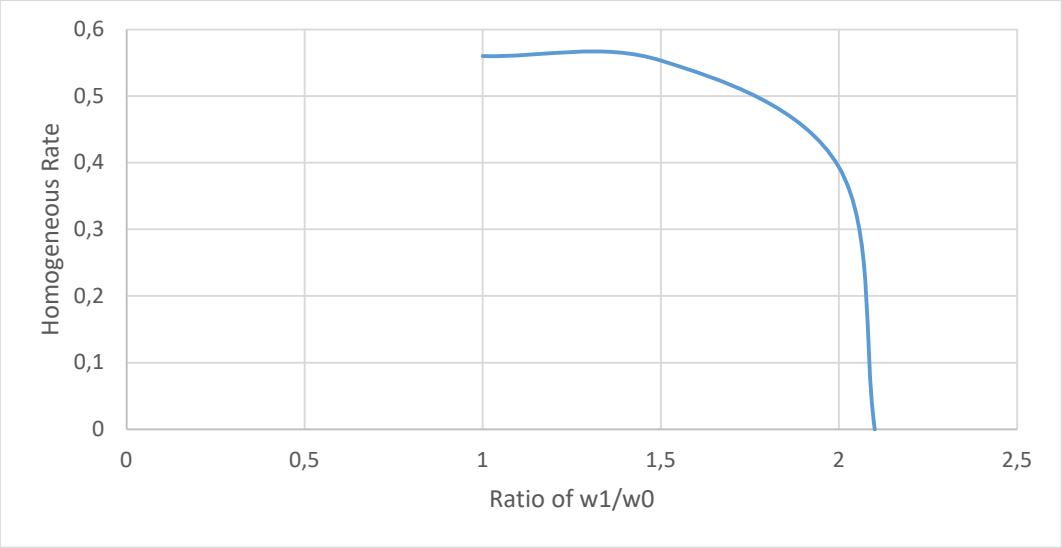


Figure 4.3 The Graph of Homogeneous Distribution Depending on Changing Ratio of w1/w0 Parameter

According to the information obtained from the two approaches, although the design having a w1/w0 ratio of 2.0 is not the best solution in terms of homogeneous distribution, it has been determined as the best nozzle design since it has the highest average velocity value.

4.2 **The Optimum Nozzle Design for w2/w0 Parameter**

To examine the effect of the w2/w0 ratio, ratios of 3.2, 4.06 and 4.8 were analyzed in the previous section and their effects were compared in detail with experimental studies. When this ratio was chosen as 3.2, the flow focused to a point around the center and had very small oscillation. The ratio of 4.8 was preferred because it is structurally very close to the upper limit values for the current design.

In the new numerical studies, the behavior of the w2/w0 ratio is examined as it exceeds 4.8. All the results for w2/w0 changing between 3.2 and 5.4 are plotted in Figure 4.4.

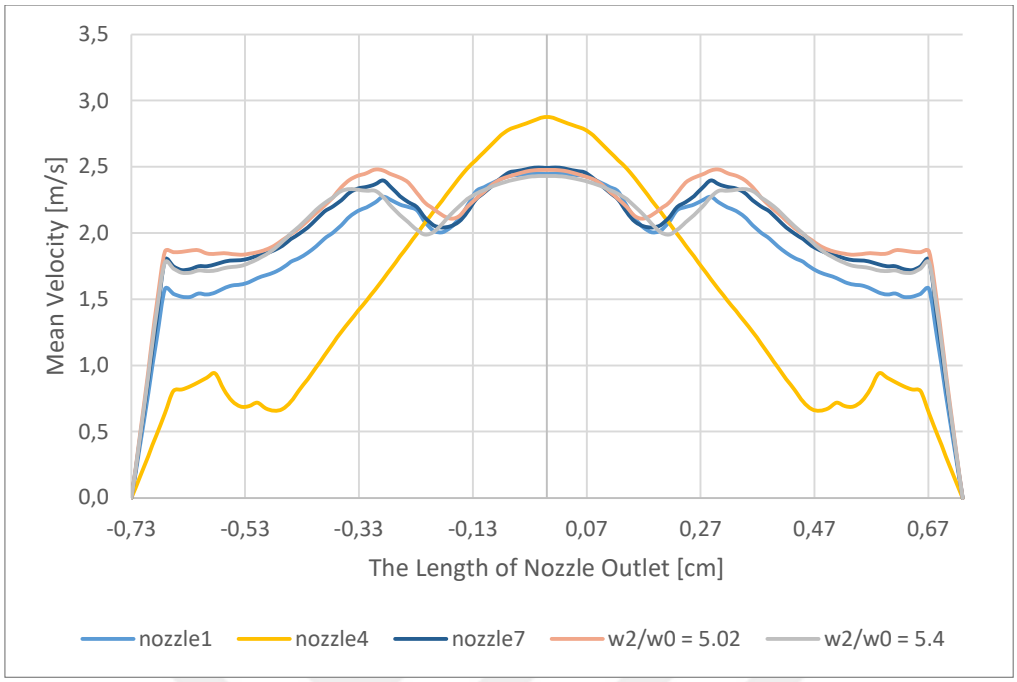


Figure 4.4 The Graph of Mean Velocity Distribution Graph in One Full Oscillation for Nozzle1, Nozzle4, Nozzle7, w2/w0 = 5.02 And w2/w0 = 5.4 Design at Nozzle Outlet

According to the analyzes that was carried out, the ratios of 3.2 and 5.4 were determined as the lower and upper limits of the ratio w2/w0, respectively. The distribution of the flow rate curves for these ratios is shared in Figure 4.5.

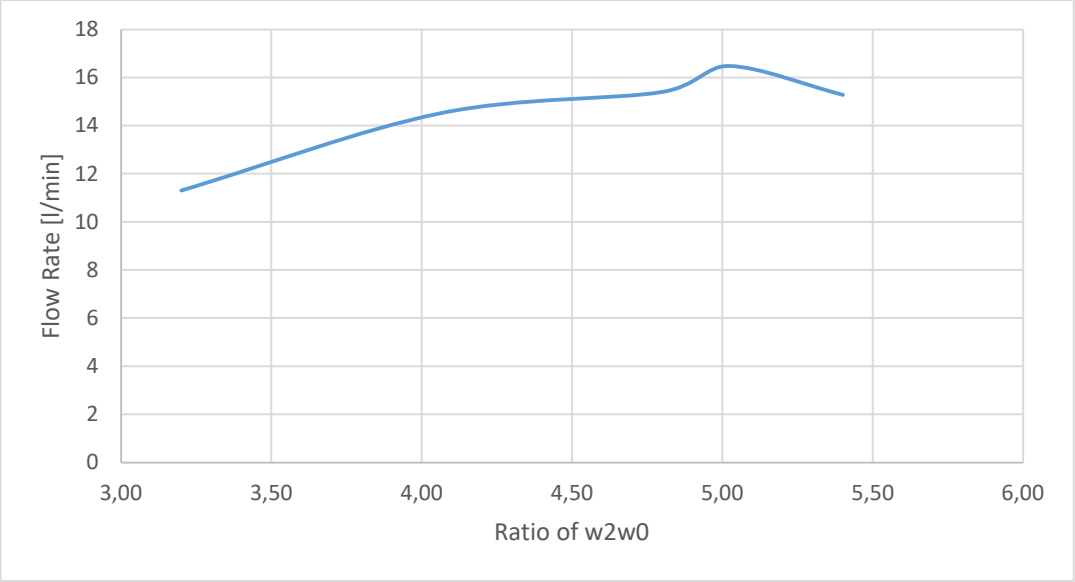


Figure 4.5 The Graph of Flow Rate Distribution Depending on Changing Ratio of w2/w0 Parameter

A careful investigation of Figure 4.5 reveals that the flow rate curve decreases when w2/w0 ratio is below or above 5.02. In this graph, the having w2/w0 ratio of 5.02 seems to be the best solution.

As the second evaluation criteria, it was examined whether there was a homogeneous distribution depending on the change in the w2/w0 ratio. As a result of these approaches, the homogeneous distribution of the ratios of between 4.0 and 5.4 for the w2/w0 ratio is shown in Figure 4.6. The ratio of 3.2 is not shown on the curve because there is no oscillating for this nozzle. When these distributions are investigated, it is seen that the homogeneous distribution decreases as the ratio goes to 3.2 however it is seen that it has a similar distribution above the ratio of 4.0.

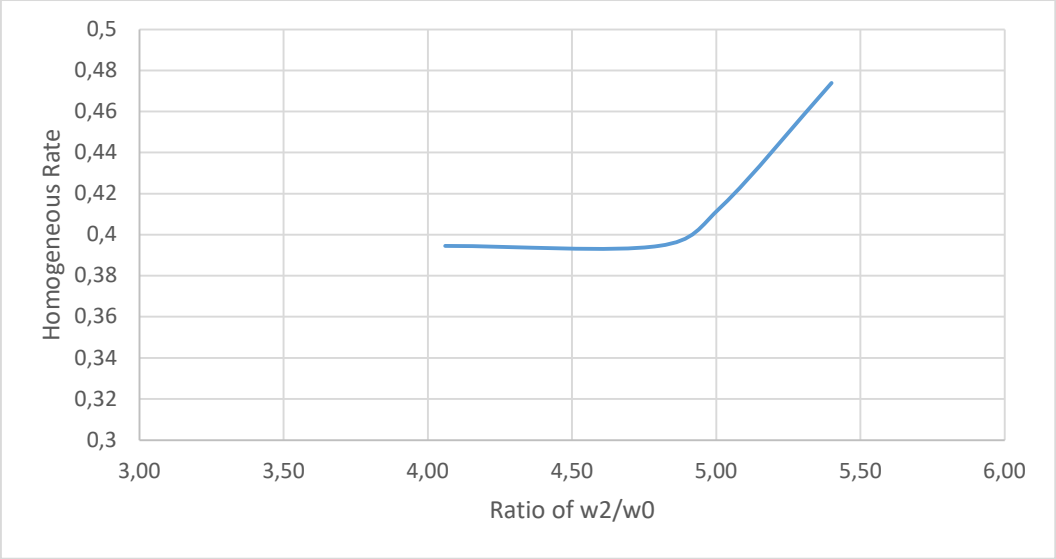


Figure 4.6 The Graph of Homogeneous Distribution Depending on Changing Ratio of w2/w0 Parameter

With the information obtained from these two approaches, although the w2/w0 ratio has many similar solutions in terms of homogeneous distribution, the 5.02 ratio design has been determined as the best nozzle design since it has the highest average velocity value. In the next section, the results of validation tests will be examined comparatively.

4.3 **The Optimum Nozzle Design for w3/w0 Parameter**

To examine the behavior of the w3/w0 ratio, ratios of 1.3, 1.6 and 2.0 were selected in the first step and analyzed to compare with experimental studies. When this ratio was selected as 2.0, the flow was focused at the midpoint and lost its oscillatory behavior. The ratio of 1.6 showed a homogeneous and low flow rate values velocity distribution graph according to all analysis studies, this ratio was chosen to see velocity distribution.

In the new numerical studies, the velocity distribution for w3/w0 ratios below 1.3 are examined and they are presented Figure 4.7 together with the previously selected ratios. It was observed that the ratios between 0.5 and 1.0 had a similar velocity distribution. This kind of behavior was observed, and it was necessary to determine

the anticipated stain removal effect related to this approach. It is seen that two side peaks are formed closer to the center without forming a peak at the midpoint. It is predicted that the effect of shear stress will affect two high peaks near the midpoint which are higher than a single peak at the midpoint.

Considering the shear stress behavior and the average velocity distribution, although the homogeneity of the distribution decreases, it would remove more stains thanks to two peaks which are close to the midpoint. For this reason, the attention is focused to this range of the ratio, and it was determined that the ratio of 0.75 would be the best solution for the w3/w0.

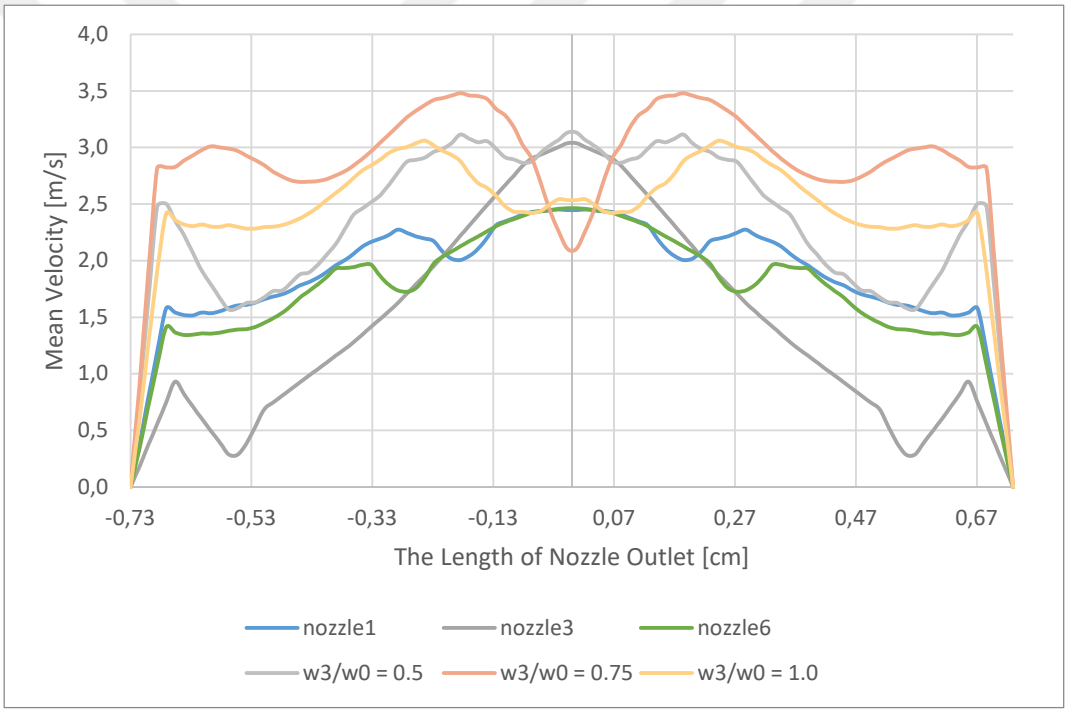


Figure 4.7 The Graph of Mean Velocity Distribution Graph in One Full Oscillation for Nozzle1, Nozzle3, Nozzle6, w3/w0 = 0.5, w3/w0 = 0.75, and w3/w0 = 1.0 Design at Nozzle Outlet

During these studies, the lower and upper limit of this ratio was taken as 0.5 and 2.0, respectively, and the distribution of the flow rate curves for these ratios are shown in Figure 4.8.

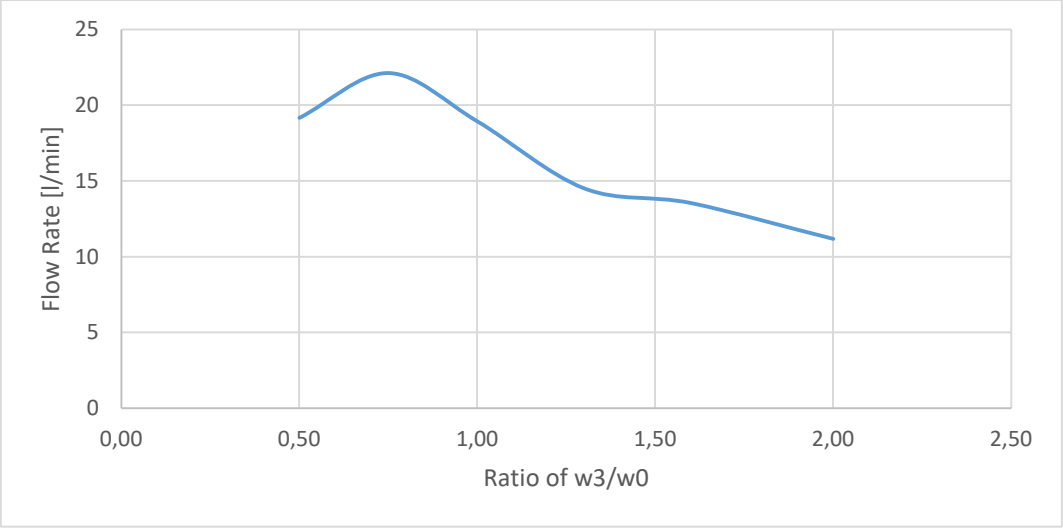


Figure 4.8 The Graph of Flow Rate Distribution Depending on Changing Ratio of w3/w0 Parameter

Looking at the curve of the flow rate graph due to the w3/w0 change, it is seen that the nozzle analysis results ratios between 0.5 and 1 give better results. In terms of this graph, the situation where the ratio of w3/w0 = 0.75 is seen as the best solution.

As the second evaluation criterion, it was examined whether there was a homogeneous distribution depending on the change of w3/w0. For this step, an approximation is made by evaluating the points where the peaks occur in the average velocity graphs, the differences of the peaks at the middle and the sides, and finally the shear stress graphs. As a result of these approaches, the homogeneous distribution of the ratios between 0.5 and 2.0 in the w3/w0 is shown in Figure 4.9. Looking at these distributions, it is seen that the homogeneous distribution decreases as the ratio increases however it shows a behavior contrary to the trend at the ratio of 0.5.

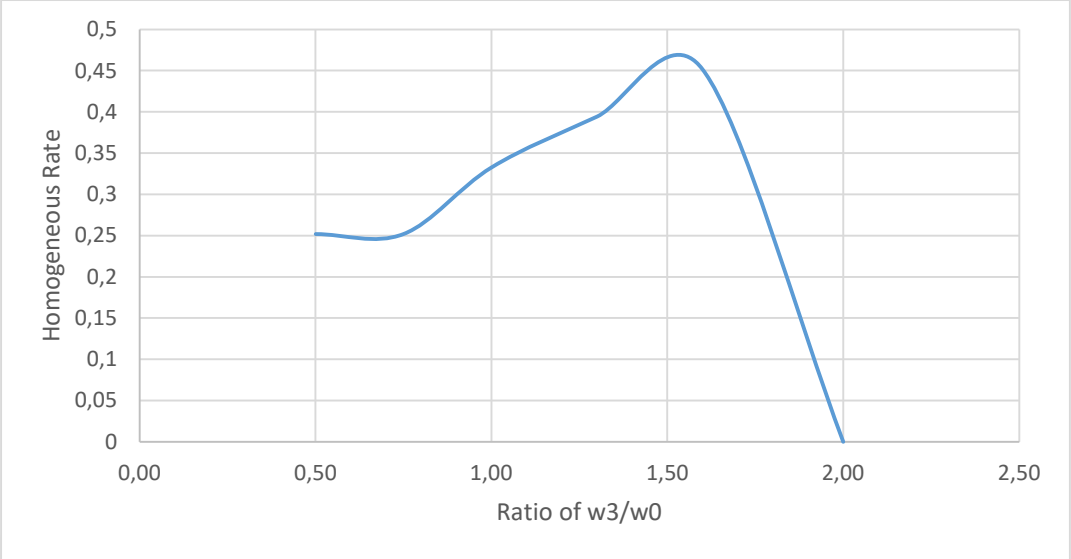


Figure 4.9 The Graph of Homogeneous Distribution Depending on Changing Ratio of w3/w0 Parameter

In line with the information obtained from the two approaches, although the homogeneity distribution was better for w3/w0 ratios between 1.0 and 1.3, the design with an w3/w0 ratio of 0.75 was selected as the best nozzle design since it has the highest average velocity value. As mentioned above, although this flow behavior causes more focused on middle, it is predicted that it can remove too much stain near at the two peaks close to midpoint.

4.4 The Optimum Nozzle Design for w4/w0 Parameter

To examine the effects of the ratio of w4 to w0, a validation study was not carried out in the previous section. Analyzes have been carried out by determining the upper limit of this ratio as 2.0 within the structural. The ratio of w4 to w0 in the nozzle1, which is determined as the reference nozzle, is taken as 1.47.

In the new numerical studies, the behavior of the velocity distribution relative to the in the w4/w0 are shown in Figure 4.10. All results are shared, especially for the detailed examination of the ratios between 0.5 and 3.0 ratios, but the maximum ratio of 2.0 can be selected, even if it is not the best result due to structural limits. Considering the velocity graphs, the ratio of 1.47, which was determined as the

reference ratio, has the lowest average velocity value. It has been observed that the average velocity distribution gives better results when the reference rate is exceeded. In terms of homogeneous distribution, the design with the ratio of 1.0 looks much better however it is disadvantageous in terms of average velocity.

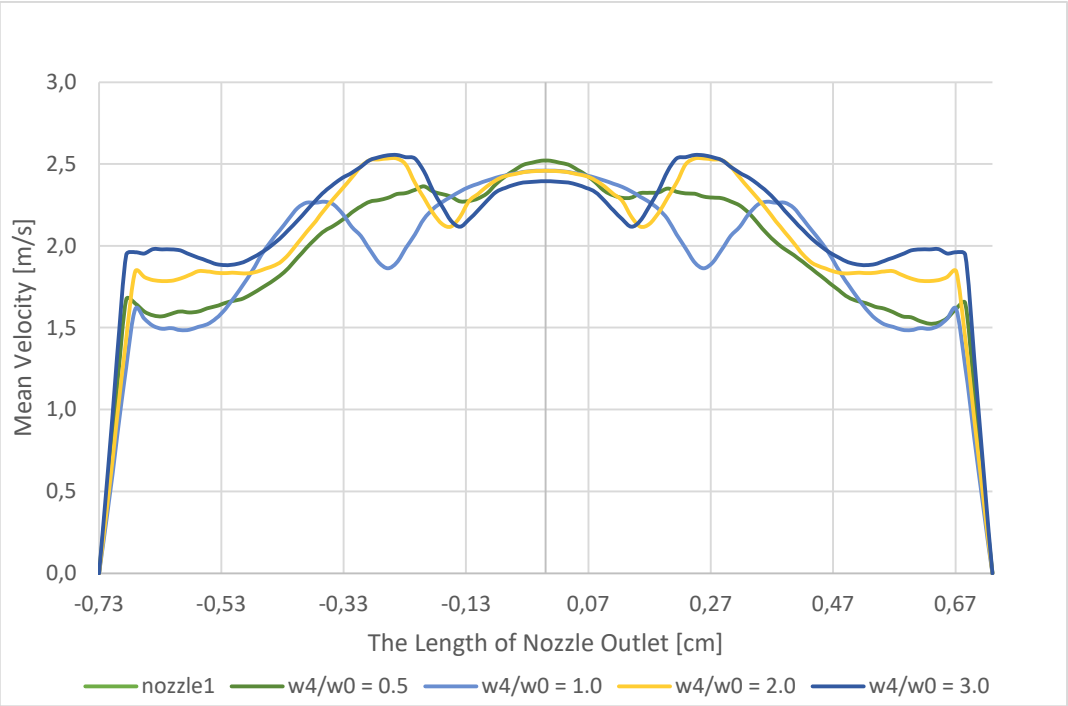


Figure 4.10 The Graph of Mean Velocity Distribution Graph in One Full Oscillation for Nozzle1, w4/w0 = 0.5, w4/w0 = 1.0, w4/w0 = 2.0, and w4/w0 = 3.0 Design at Nozzle Outlet

In the light of the numerical studies, the flow rate curves for the w4/w0 ratios between 0.5 and 3.0 is shared in Figure 4.11.

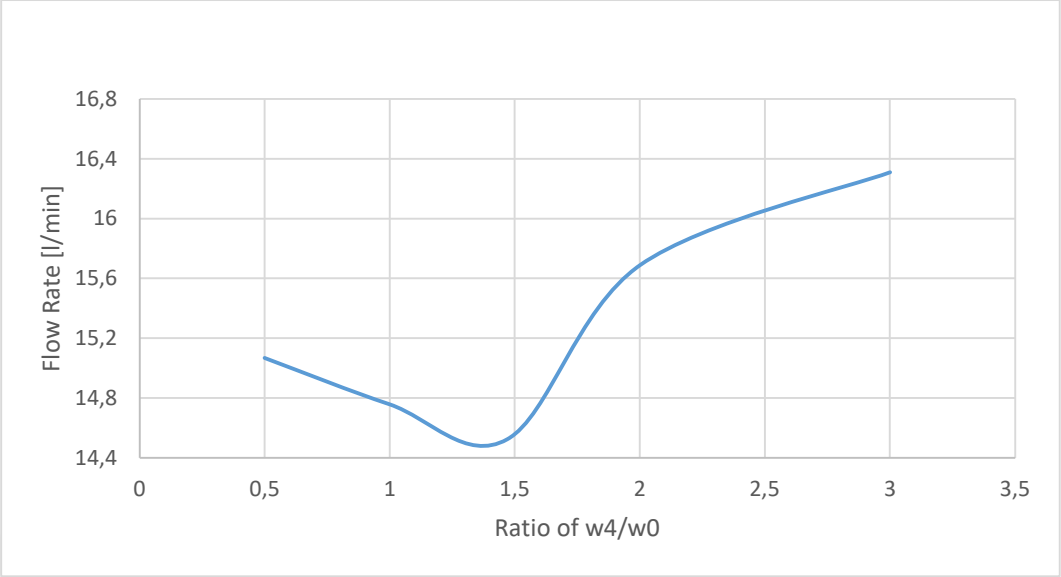


Figure 4.11 The Graph of Flow Rate Distribution Depending on Changing Ratio of w4/w0 Parameter

Considering the flow rate curves as the ratio of w4/w0 changes, it is seen that the nozzles having ratios changing between 2.0 and 3.0 give better results. Due to the structural limits, the ratio of 2.0 was selected as the best solution.

As the second evaluation criteria, it was examined whether a homogeneous distribution exists as the ratio of w4/w0 changes. Using these approaches, the homogeneity of the distribution of for the w4/w0 ratios between 0.5 and 3.0 is shown in Figure 4.12.

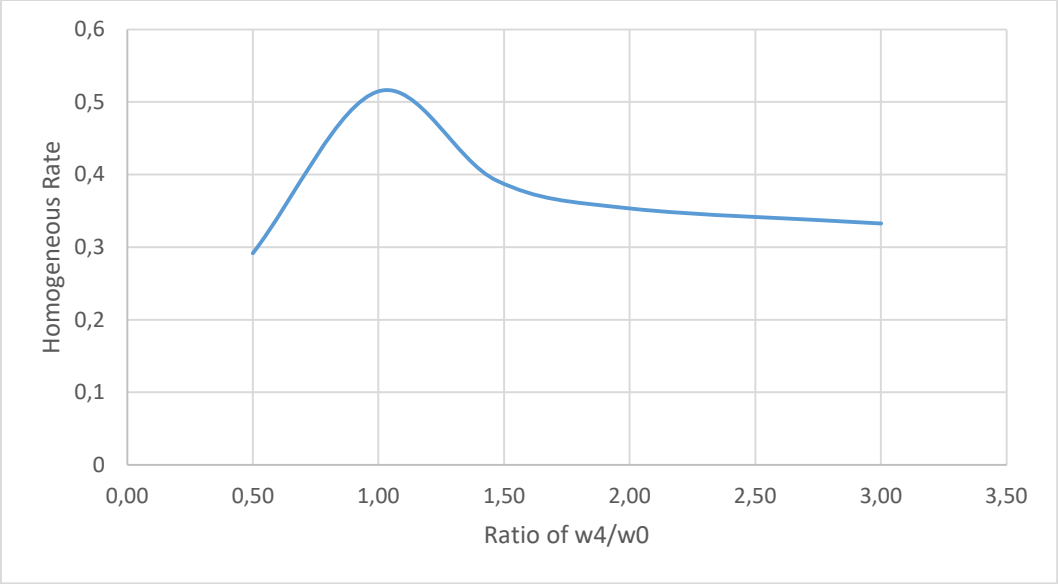


Figure 4.12 The Graph of Homogeneous Distribution Depending on Changing Ratio of w4/w0 Parameter

As a result of the two approaches, it is seen that the w4/w0 ratio of 1.0 is the best design in terms of homogeneous distribution, however the ratio of 2.0 is selected as the best solution when the average velocity value is considered.

CHAPTER 5

EXPERIMENTAL TESTS OF OPTIMUM DESIGNS

The best solutions determined in the previous chapter have been tested for each parameter separately. The results obtained are compared with the studies in the validation study and they will be shown to be the best solution. The best solutions are presented for all four parameters, however the best solution for the w1/w0 is nozzle1 that has been tested before and is determined as the reference nozzle. The w1/w0 parameter has not been examined under this title in detail, but other parameters have been examined in detail.

5.1 The Optimum Nozzle Results for w1/w0 Parameter

2.0 is selected for the w1/w0 ratio as the best solution. The results of this design were examined in detail under the previous headings. Although it does not have the most homogeneous distribution according to the experimental results, nozzle1 has the best stain removal capacity.

5.2 The Optimum Nozzle Results for w2/w0 Parameter

As discussed in the previous chapter, the optimum value of the w2/w0 ratio is determined as 5.02 in an interval changing from 3.2 to 5.4, which is the structural upper limit, for the w2/w0 parameter. The new nozzle is named as nozzle8 and its stain removal graph is shown in Figure 5.1, with the previous nozzles that were designed for this parameter.

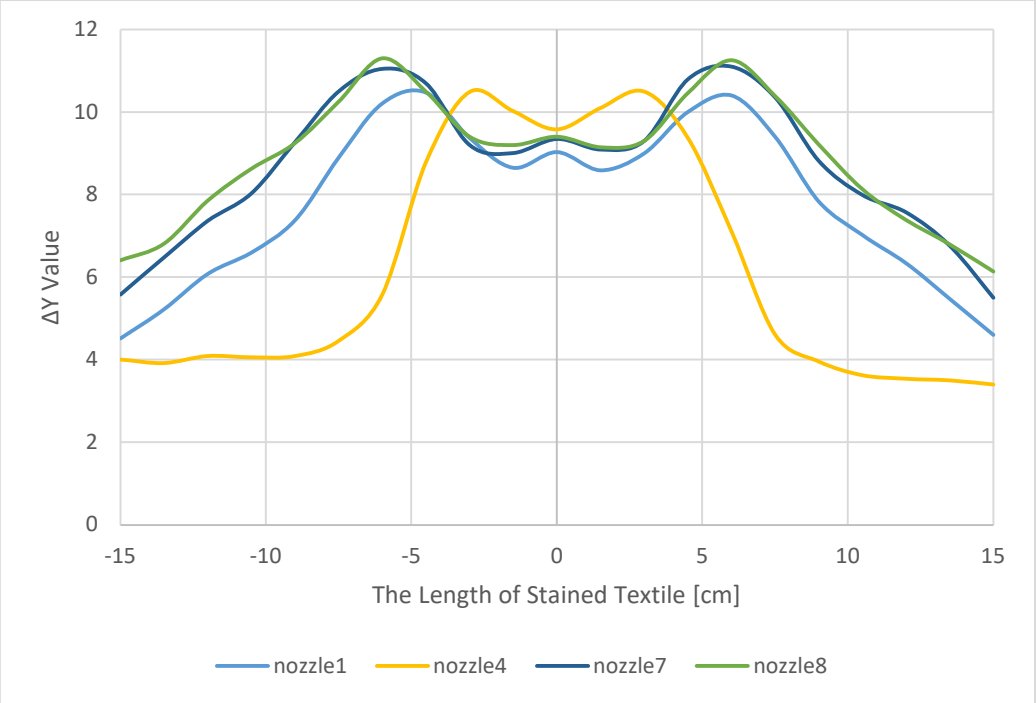


Figure 5.1 The Graph of Experimental Removal Stain Test Results of w2/w0 Parameter for Nozzle1, Nozzle4, Nozzle7 and Nozzle8

When the graph is examined, it is seen that nozzle8, which is designed as the best solution, shows a very similar behavior to that of the design of nozzle7 with a slightly larger area under the velocity curve. Investigating these results reveals that the analyses performed are consistent.

When these results are examined in terms of homogeneous distribution, nozzle8 is seen that they have a similar distribution with nozzle7 and nozzle1 in the analyzes. As a result of experimental studies, it has been seen that the approach is correct for homogeneous distribution.

Areas under the curve for w2/w0 are shown in Table 5.1 for understanding removing stain capacity.

Table 5.1 Areas Under the Curve for w2/w0

Type of Nozzle	*Area Under the Curve [ΔY value x cm]*
Nozzle1	240
Nozzle4	187
Nozzle7	267
Nozzle8	271

5.3 The Optimum Nozzle Results for w3/w0 Parameter

As stated in the previous chapter, the optimum value of the w3/w0 ratio is selected as 0.75 in an interval between ratios of 0.5 to 2.0 ratio for the w3/w0 parameter. The designed new nozzle is named as nozzle9, and the stain removal graph is plotted in Figure 5.2 with the previous nozzles designed for this parameter.

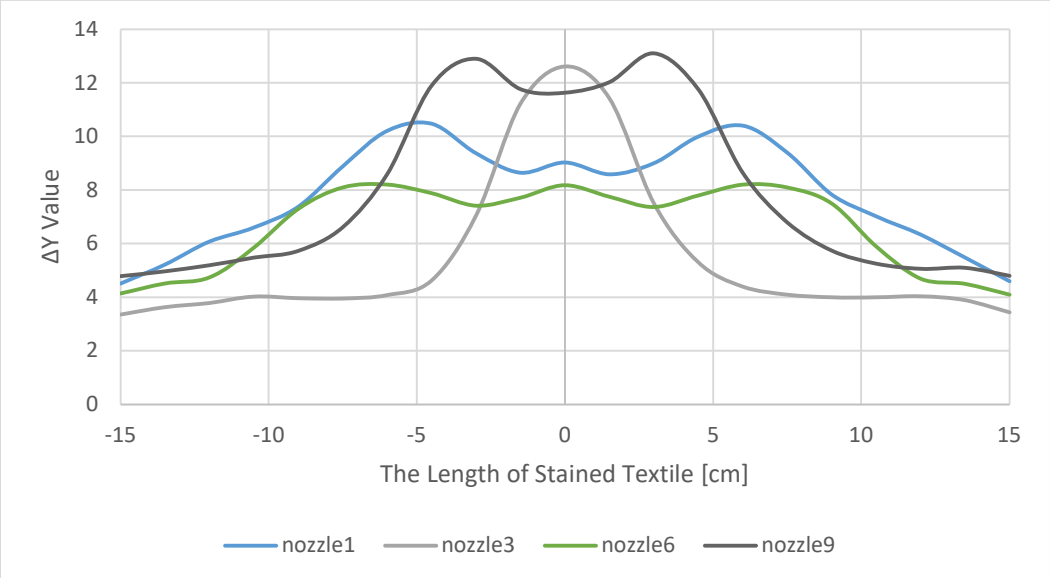


Figure 5.2 The Graph of Experimental Removal Stain Test Results of w3/w0 Parameter for Nozzle1, Nozzle3, Nozzle6 and Nozzle9

When the graph is examined, the nozzle9, which was designed as the best solution, did not make a similar flow movement with any nozzle designed before, but because the two peaks were very high, it was found as the best nozzle design with the highest value in the average velocity graph. Considering this situation, it is seen that the new design consists of two closer peaks in a similar way in the stain removal graph, but it is the best solution in terms of the flow rate or the areas under the velocity curves.

The fact that it is in a disadvantageous position in terms of homogeneous distribution is consistent with the approach determined in the numerical studies however such high stain removal values were not obtained in any other test. For this reason, the nozzle9 design has been validated as the best nozzle solution.

Areas under the curve for w3/w0 are shown in Table 5.2 for understanding removing stain capacity.

Table 5.2 Areas Under the Curve for w3/w0

Type of Nozzle	*Area Under the Curve [ΔY value x cm]*
Nozzle1	240
Nozzle3	166
Nozzle6	203
Nozzle9	244

5.4 **The Optimum Nozzle Results for w4/w0 Parameter**

There has been no previous experimental work for the w4/w0 parameter and has been kept at a constant ratio as 1.47 for all nozzle designs. As a result of the analyzes studies, it was seen that this ratio had the lowest average velocity value. For this

reason, all results of ratios of between 0.5 and 2.0, which was determined as the structural upper limit value, were examined and it was decided that the ratio of 2.0 was the best solution. The newly designed nozzle design is named nozzle10 and its comparison with the reference nozzle is shown in Figure 5.3.

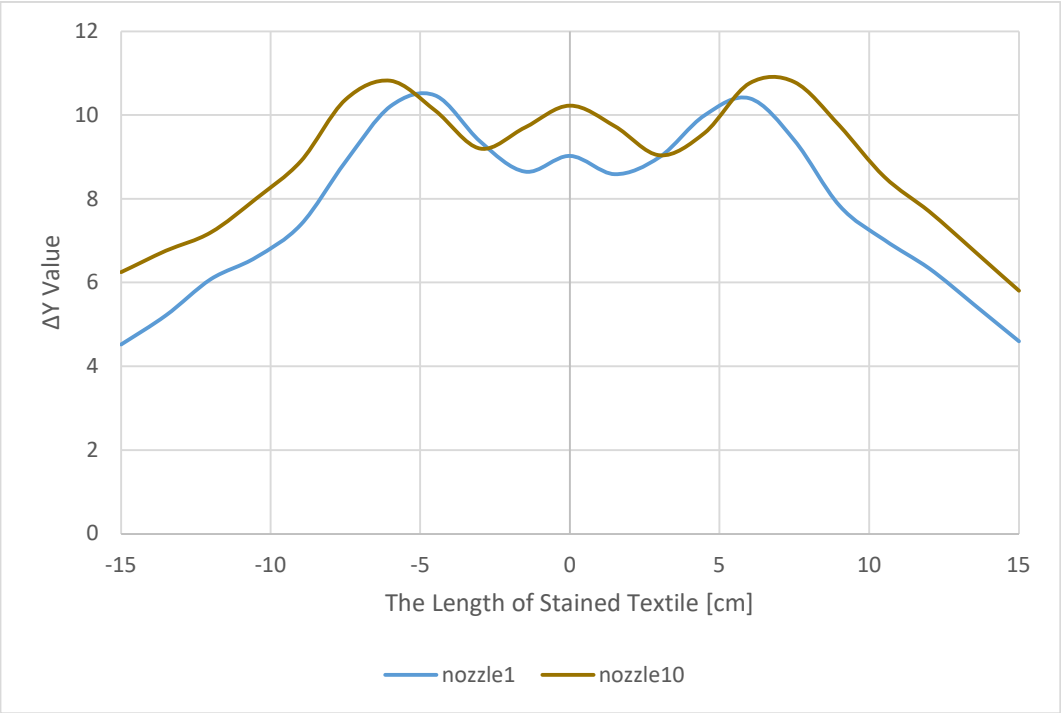


Figure 5.3 The Graph of Experimental Removal Stain Test Results of w4/w0 Parameter for Nozzle1 and Nozzle10

When the graph is investigated, it is seen that nozzle10, which is designed as the best solution, has higher values in all three peaks than the reference nozzle. Looking at the areas under the stain removal curve, it is seen that nozzle10 clearly removes stains better than the reference nozzle design. In the numerical studies, it is seen that the results obtained are consistent with experimental study.

In terms of homogeneous distribution, it is seen that it is more homogeneous compared to the reference nozzle design, nozzle1. It is seen that 2 peaks formed on the sides form peaks at points farther from the midpoint. In addition, it is seen that it makes a more effective stain removal on the peak formed in the middle.

Areas under the curve for w4/w0 are shown in Table 5.3 for understanding removing stain capacity.

Table 5.3 Areas Under the Curve for w4/w0

Type of Nozzle	*Area Under the Curve [ΔY value x cm]*
Nozzle1	240
Nozzle10	269

CHAPTER 6

CONCLUSION

In this thesis, the focus is on the design of the nozzle in the circulation system used in washing machines. One of the most important problems in the current system is that the nozzle designs cannot spray the water a sufficiently wide area. The more the detergent water comes into contact with the laundry, the easier it will be to remove the stain. In this way, energy consumption, water consumption and cycle time will be reduced. In the light of the information obtained within the scope of literature studies, it has been seen that fluid oscillators are used for obtaining oscillating flow in various sectors. An experimental setup was prepared to examine the effect of fluid oscillators on stain removal and the current pump system was used in the experimental setup. Sebum-stained textile, which is the most common type of stain in daily life, was used as the stain type. Flow analyzes of fluid oscillators were carried out with CFD before testing in the experimental setup with the designed nozzle. An approach has been determined to understand how the stain removal behavior in the experimental design will be with CFD studies. This approach is the modeling of the stain removal behavior in experimental studies with the velocity distribution at the nozzle outlet. In these studies, 3 different parameters were determined, and validation tests were carried out to understand this behavior. These parameters were determined as the ratio of the inlet of the nozzle mixing chamber to the nozzle inlet w1/w0, the ratio of the mixing zone width to the nozzle inlet w2/w0 and the ratio of the nozzle outlet throat to the nozzle inlet w3/w0, respectively.

a. The ratios of 1.0, 1.5 and 2.0 for parameter w1/w0 were chosen for validation tests due to different flow behavior. As a result of the tests, when w1/w0 is 2.0, although it creates closer peaks in both the velocity graph and the stain removal tests, the areas under curve are higher in both graphs.

b. The ratios of 3.2, 4.06 and 4.8 for the w2/w0 parameter were determined for validation tests. The reason why the ratio of 3.2 is preferred is that it performs the flow movement in a focused way with narrower oscillations. It has been important for the analysis of narrow oscillating flow in the analysis studies and experimental studies. Although the flow motion of the 4.06 and 4.8 ratio nozzles is similar, the area under the velocity graph of the ratio of 4.8 design is more.
c. The ratios of 1.3, 1.6 and 2.0 for the w3/w0 parameter were determined for the validation study. The behavior of the ratio change in this parameter is very diverse, so three different flow movements are preferred. Since the 1.3 ratio design is determined as the reference ratio, it performs the same action as the previous nozzles. In the ratio of 1.6 design, the fluid spends more time at the midpoint and stain removal is distributed homogeneously. The 2.0 ratio design, on the other hand, sprayed the fluid without creating any oscillations.

As a result of all validation studies, it was decided that the average velocity graph at the nozzle outlet can be used for the stain removal approach. In addition to this information, in order to model stain removal, the part where the stain is located is defined as the wall, and the shear stress graph formed on this wall is used to explain the difference between velocity graphs and stain removal graphs. In addition, knowing the time spent in contact with the wall and the time spent in swing were used to accurately evaluate the velocity graph. With the developed approach method, the best nozzle for each parameter was determined by CFD analysis.

a. The case where W1/w0 = 2.0 was determined as the best solution. Although it does not have the most homogeneous distribution, it is the most advantageous design in terms of the area under the average velocity graph.
b. The best ratio for the w2/w0 parameter was determined as 5.02. Although the most homogeneous solution for this parameter is the 5.4 ratio design, the 5.02 ratio design has the best solution in terms of average velocity graph.

c. The best ratio for the W3/w0 parameter was determined as 0.75. It has been observed that the flow movement varies a lot as the ratios change in this parameter. When the average velocity graph of the 0.75 ratio design is investigated, it is presented as the best solution since it has very high average velocity values although two peaks are very close to each other.
d. Finally, thanks to the developed approach, the ratio of the backflow channel to the nozzle inlet was determined as the w4/w0 parameter. When this parameter is investigated, it is seen that the selected ratio of 1.47 is not the best solution in all the nozzles studied so far. It has been seen that the best design has a 2.0 ratio within the specified range due to the structural limits.

Finally, the best solutions determined were validated by testing in the experimental setup.

By using this approach developed in future studies, different parameters will be examined. Especially when the area to be reached with oscillation changes, analyzes can be performed by changing the angle at the outlet.

REFERENCES

[1] *Deepwave Cleaning Machine*. Jet Cleaning. (2022, June 30). Retrieved December 21, 2022, from https://jet-cleaning.com/en/deepwave/

[2] Kimmel, T., Kunkel, C., Kessler, A. & Nitsch, C. (2017). Influence of Water Circulation in Household Washing Machines on Cleaning Performance. *Tenside Surfactants Detergents*, *54*(2), 125-131. https://doi.org/10.3139/113.110494

[3] *LG Drain & circulation pump-BLDC Motor L LG Global*. LG Global. (n.d.). Retrieved December 21, 2022, from https://www.lg.com/global/business/motor-pump-bldc

[4] Lyu, P., Xu, S., Zhao, Z., & Zhao, X. (2019, December 24). Front-loading washing machine and nozzle of washing machine.

[5] Zhao, Z., Lyu, Pe., Xu, S., & Zhao, X. (2019, August 27). Nozzle, pulsator washing machine, spraying system of pulsator washing machine and outer barrel cover of pulsator washing machine.

[6] Wang, Y., Fan, X., Wang, L., & Zhao, Z. (2021, July 20). Spraying device of roller washing machine and roller washing machine.

[7] Zhao, Z., & Xu, S. (2022, October 12). Micro-bubble spray head and washing device with same.

[8] Tartuferi, M., Del, P. M., Contarini, A., & Russo, M. (2022, August 9). Laundry washing machine equipped with a liquid supply line.

[9] Im, M., Jung H., & Woo K. (2020, December 26). Washing machine and method for controlling the same.

[10] Jung, H., Im, M., Kim, J., Lee, J., & Woo, K. (2021, June 30). Method for controlling washing machine.

[11] Yang, B. Y., Jeon, G. D., Pyo, S. Y., Kim, T. E., & Lee, B. R. (2017, May 31). Bubble generating device and washing machine having the same.

[12] Kasap, F., Mutlu, E., Ilıca, S., Sendinç, T., & Fırat, A. (2020, June 25). Washing machine comprising a sprinkling drum lifter.

[13] Demir, H. V., Kılıç, V. T., Ünal, E., Polat, D., Bayraktar, S., Küçükcoşkun, B., & Ünlüsoy, M. (2018, September 13). A flow-through type induction heater.

[14] Oh, S. Y., Woo, K. C., Kim, J. W., Jeon, S. M., & Kim, N. E. (2005, February 16). Washing machine with vapour generator and water circulation.

[15] Warren, R. W. (1962, January 9). Fluid oscillator.

[16] Stouffer, R. D. (1985, April 2). Liquid Oscillator Device.

[17] Shakouchi, T. (2003). Gas absorption, aeration, by fluidic oscillator operated by gas-liquid two-phase flow. *Volume 2: Symposia, Parts A, B, and C*. https://doi.org/10.1115/fedsm2003-45132

[18] Wang, H., Priestman, G. H., Beck, S. B. M., & Boucher, R. F. (1996). Development of fluidic flowmeters for monitoring crude oil production. *Flow*

Measurement and Instrumentation, *7*(2), 91–98. https://doi.org/10.1016/s0955-5986(97)00009-5

[19] Raman, G., & Raghu, S. (2004). Cavity Resonance Suppression Using Miniature Fluidic Oscillators. *AIAA Journal*, *42*(12), 2608–2612. https://doi.org/10.2514/1.521

[20] Guyot, D., Paschereit, C. O., & Raghu, S. (2009). Active combustion control using a fluidic oscillator for asymmetric fuel flow modulation. *International Journal of Flow Control*, *1*(2), 155–166. https://doi.org/10.1260/175682509788913335

[21] Cerretelli, C., & Kirtley, K. (2006). Boundary Layer Separation Control with Fluidic Oscillators. *Volume 6: Turbomachinery, Parts A and B*. https://doi.org/10.1115/gt2006-90738

[22] Seele, R., Tewes, P., Woszidlo, R., McVeigh, M. A., Lucas, N. J., & Wygnanski, I. J. (2009). Discrete sweeping jets as tools for improving the performance of the V-22. *Journal of Aircraft*, *46*(6), 2098–2106. https://doi.org/10.2514/1.43663

[23] Whalen, E. A., Spoor, M., Vijgen, P. M., Tran, J., Shmilovich, A., Lin, J. C., & Andino, M. (2016). Full-scale flight demonstration of an active flow control enhanced vertical tail. *8th AIAA Flow Control Conference*. https://doi.org/10.2514/6.2016-3927

[24] McDonough, J. R., Law, R., Kraemer, J., & Harvey, A. P. (2017). Effect of geometrical parameters on flow-switching frequencies in 3D printed fluidic oscillators containing different liquids. *Chemical Engineering Research and Design*, *117*, 228–239. https://doi.org/10.1016/j.cherd.2016.10.034

[25] Wen, X., Li, Z., Zhou, L., Yu, C., Muhammad, Z., Liu, Y., Wang, S., & Liu, Y. (2020). Flow Dynamics of a fluidic oscillator with internal geometry variations. *Physics of Fluids*, *32*(7), 075111. https://doi.org/10.1063/5.0012471

[26] Tomac, M. (2020). Effect of the oscillator length on the characteristics of a feedback type fluidic oscillator. *Academic Platform Journal of Engineering and Science*, 432–438. https://doi.org/10.21541/apjes.583500

[27] Bobusch, B. C., Woszidlo, R., Krüger, O., & Paschereit, C. O. (2013). Numerical investigations on geometric parameters affecting the oscillation properties of a fluidic oscillator. *21st AIAA Computational Fluid Dynamics Conference*. https://doi.org/10.2514/6.2013-2709

[28] Jeong, H.-S., & Kim, K.-Y. (2017). Shape optimization of a feedback-channel Fluidic Oscillator. *Engineering Applications of Computational Fluid Mechanics*, *12*(1), 169–181. https://doi.org/10.1080/19942060.2017.1379441

[29] Wu, Y., Yu, S., & Zuo, L. (2019). Large eddy simulation analysis of the heat transfer enhancement using self-oscillating fluidic oscillators. *International Journal of Heat and Mass Transfer*, *131*, 463–471. https://doi.org/10.1016/j.ijheatmasstransfer.2018.11.070

[30] Baghaei, M., & Bergada, J. M. (2020). Fluidic oscillators, the effect of some design modifications. *Applied Sciences*, *10*(6), 2105. https://doi.org/10.3390/app10062105

[31] Hossain, M. A., Agricola, L., Ameri, A., Gregory, J. W., & Bons, J. P. (2018). Sweeping jet impingement heat transfer on a simulated turbine vane leading edge. *Journal of the Global Power and Propulsion Society*, *2*. https://doi.org/10.22261/jgpps.5a7oaz

[32] *Wolf Dynamics - customer-driven flow solutions*. (n.d.). Retrieved April 19, 2023, from http://www.wolfdynamics.com/training/turbulence/OF2021/turbulence_2022 1_OF8_guided_tutorials.pdf